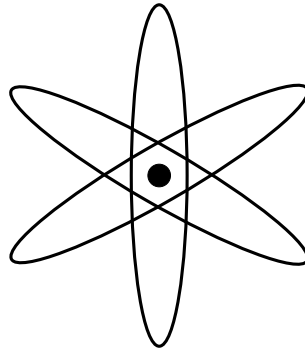


PHYSIK DEPARTMENT



Renormalization Group Evolution in See-Saw Models

Diploma Thesis

by

Michael Andreas Schmidt

December 2004

Thesis written at:

Technische Universität München

Physik-Department T30d

Prof. Dr. Manfred Lindner



Contents

1	Introduction	7
2	Mass Terms	9
2.1	Fermion Masses	9
2.1.1	Dirac Mass Terms	9
2.1.2	Majorana Mass Terms	9
2.1.3	Masses in the Standard Model	10
2.2	Neutrino Mass Terms	10
2.2.1	Extension of the Higgs Sector	11
2.2.2	Introduction of right-handed Neutrinos	11
2.2.3	Smallness of Neutrino Masses	13
3	Renormalization	15
3.1	Power Counting	15
3.2	Regularization	17
3.2.1	UV cutoff	17
3.2.2	Pauli-Villars Regularization	17
3.2.3	Lattice Regularization	18
3.2.4	Dimensional Regularization	18
3.3	Renormalization Schemes	20
3.3.1	On-Shell Scheme	20
3.3.2	Minimal Subtraction Scheme	20
3.3.3	BPHZ Renormalization	21
3.4	Renormalization of Gauge Theories	22
3.5	Renormalization Group	23
3.5.1	Callan-Symanzik Equation	23
3.5.2	Renormalization Group Equations	24
4	Effective Field Theory	27
4.1	Decoupling Theorem	28
4.2	Construction of an EFT from a “full” Theory	28
4.3	Neutrino Mass Operator	29
4.4	See-Saw Mechanism	30
4.4.1	Extensions of the SM	30
4.4.2	Standard See-Saw Mechanism	32
4.4.3	Type-II See-Saw Mechanism	33

4.4.4	Thresholds	33
4.4.5	Parameterization of the See-Saw	34
5	Evolution of the Mixing Parameters and Masses	37
5.1	Extraction of the RGE for the Parameters from the Matrix Equations	37
5.1.1	Evolution of Majorana Masses	37
5.1.2	Evolution of Dirac Masses	38
5.2	Evolution of the left-handed Majorana Neutrino Mass Matrix	39
5.3	Evolution of the charged Lepton Sector	39
5.4	Evolution of the left-handed Leptonic Mixing Parameters	40
5.5	Evolution of the right-handed Neutrino Masses	41
6	RG Evolution in type-I See-Saw Models	43
6.1	Summary of the Evolution in the Effective Theory	43
6.2	General Considerations about the Evolution	43
6.2.1	Different Contributions from P	44
6.2.2	Size of the RG Effect	45
6.3	Evolution of the Angles	45
6.4	Evolution of the Phases	48
6.5	Evolution of the Masses	50
7	Renormalization of SM extended by a Triplet Higgs	53
7.1	Definition of the additional Renormalization Factors	53
7.2	Counterterm Lagrangian	54
7.3	Self Energy Diagrams	54
7.3.1	Self Energy of Higgs Triplet Σ_Δ	54
7.3.2	Self Energy of Doublet Higgs Σ_ϕ	58
7.4	Vertex Corrections	60
7.4.1	Vertex Corrections to $\ell_L \Delta \ell_L$	60
7.4.2	Vertex Corrections to $\nu_R \ell_L \phi$	62
7.4.3	Vertex Corrections to $\phi \Delta \phi$	62
7.4.4	More Loop Corrections to the Higgs Potential	65
7.5	Calculation of the β -Functions	66
7.5.1	β -Function of Y_Δ	68
7.5.2	β -Functions of Λ_6 and the Anomalous Dimension of M_Δ	69
7.5.3	β -Functions of the other Parameters in the Higgs Potential	70
7.5.4	Corrections to other β -Functions	70
7.5.5	β -Function of the Neutrino Mass Matrix	71
8	Numerical Code	73
8.1	MixingParameterTools	73
8.2	REAP	73
8.2.1	RGESolver	74
8.2.2	Implementation of RGESearchTransitions	76
8.2.3	Initial Values and Output Functions	76
9	Summary & Conclusions	77

A	Models	79
A.1	Standard Model (SM)	79
A.2	Standard Parameterization	81
A.3	\mathbb{Z}_2 -symmetric Two Higgs Doublet Model	82
A.4	Minimal Supersymmetric Standard Model	82
A.5	Feynman Rules for the new Vertices involving the Higgs Triplet	83
B	β-Function of a tensorial Quantity	87
C	Mathematics	89
C.1	Diagonalization of Matrices	89
C.1.1	Diagonalization of Hermitian Matrices	89
C.1.2	Singular Value Decomposition	89
C.1.3	Diagonalization of Symmetric Matrices	90
C.2	Group Theory of $SL(2, \mathbb{C})$	90
C.2.1	Lorentz Group	90
C.2.2	Poincaré Group	92
C.3	Useful Formulae in Group Theory	93
C.3.1	Pauli Spin Matrices	93
C.3.2	Dirac Matrices	94
C.3.3	γ -Algebra in d Dimensions	94
C.4	Special Functions	95
C.4.1	Gamma Function	95
C.4.2	Beta Function	96
C.5	Passarino-Veltman Functions	96
C.5.1	The One-Point Function A_0	96
C.5.2	The Two-Point Functions B	96
C.5.3	The Three-Point Functions C	97
C.5.4	The Four-Point Functions D	97
D	Tables	99
	Acknowledgments	103
	Nomenclature	108
	Bibliography	109

Chapter 1

Introduction

In the last few years, there have been large achievements in the field of neutrino physics. In 1998, SuperKamiokande [1] gave the first evidence of neutrino oscillations for atmospheric neutrinos which was independently confirmed by K2K [2]. Four years later, it was proven by the SNO experiment [3] that the solar neutrino deficit measured by the Homestake experiment [4] for the first time is not due to the sun but due to flavor transitions. The data of the Kamland experiment [5] independently determined the solar parameters by measuring the flux of antineutrinos from a reactor. Hence, today, the large mixing angle solution is the only possible solution to neutrino oscillations and there is one maximal mixing angle (θ_{23}) and one large mixing angle (θ_{12}). Thus, the mixing angles in the leptonic sector are large in contrast to the angles in the quark sector. The third angle θ_{13} has not been measured yet, but only an upper limit exists. Moreover, the CP phases are unknown. In the next-generation experiments, the mixing parameters will be measured on a 10 % level [6]. In order to explain the two mass squared differences, at least two neutrinos have to be massive. Actually, there is a third mass squared difference measured by the LSND experiment [7]. This can be most easily explained by sterile neutrinos, but this possibility awaits confirmation and is currently tested. We will neglect the LSND result in what follows. However, there is still no information about the absolute mass scale of neutrino masses. The absolute neutrino mass is only bounded by different experiments from above. The most stringent upper limit of 1 eV on the sum of the neutrino masses is from cosmology, but this bound is highly model-dependent. Other measurements are the measurement of neutrinoless double- β decay in the Heidelberg-Moscow experiment [8] and the model-independent tritium end-point measurement in the Mainz experiment [9]. Part of the group of the Heidelberg-Moscow experiment claimed to have measured neutrinoless double- β decay, but this result is not generally accepted and has to be tested by a number of proposed next-generation experiments. There is also a new tritium end-point experiment called KATRIN [10]. Combined, these experiments can decide the nature of neutrinos: whether they are Dirac or Majorana particles. In addition, the neutrinoless double- β decay experiment will be in principle able to measure the Majorana CP phases, if neutrinos are Majorana particles. Furthermore, the mass hierarchy of the neutrinos is not known. Hence, there are 3 different scenarios depending on the sign of Δm_{atm}^2 : either the neutrino masses have a normal hierarchy, an inverted hierarchy or they are quasi-degenerate. Contrariwise, there have been a lot of attempts to explain the structure of the neutrino mass matrix. The two main issues are the explanation of the smallness of neutrino masses and large mixing angles in contrast to the small angles in the quark sector. Generally, the small

mass is explained by a large hierarchy between the electroweak scale and the scale at which the neutrino mass is generated. Thus, most predictions for the leptonic parameters are valid at some high-energy scale where the symmetry of the model is broken to obtain the symmetry of the Standard Model (SM). This breaking scale is usually close to the Grand Unified Theory (GUT) scale. One specific class of models are see-saw models [11–15] explaining the smallness of the neutrino masses by a heavy particle which is integrated out. Then the scale of the neutrino mass is given by the ratio of the weak scale squared over the mass scale of the heavy particle. In particular, minimal see-saw models are favored nowadays where the heavy particles are right-handed neutrinos in the standard see-saw scenario or a heavy Higgs triplet in type-II see-saw models. They are minimal in the sense, that only another type of particles is introduced into the SM. Recently, the type-II see-saw mechanism has received more attention, because it can naturally explain a quasi-degenerate spectrum of neutrino masses which is difficult in type-I see-saw models. In order to explain the scale of neutrino masses, the masses of the right-handed neutrinos are usually assumed to be lower than the GUT scale in an energy range of $10^{10} - 10^{16}$ GeV. The Higgs triplet in type-II see-saw scenarios resides in the same energy region. However, the parameters in a quantum field theory are not constant, but receive radiative corrections. These radiative corrections induce in the parameters a dependence on the energy scale at which the process is taking place. Hence, processes which take place at high-energies are described by other parameter values than processes in the low-energy regime. Therefore, it is important to relate the predictions of the models at high-energy to the experimental data at low energies. This relation is given by the renormalization group which describes the dependence of the parameters on the energy scale. It turns out that the renormalization group effects on the leptonic parameters are especially large for a quasi-degenerate neutrino mass spectrum.

This diploma thesis is structured in the following way: In the second chapter the possible mass terms of neutrinos are described and some possible minimal extensions of the SM are given which explain neutrino masses. The concept of renormalization is introduced and different renormalization schemes are shortly reviewed in chapter 3. In the following chapter, the notion of effective field theories is illustrated using the example of the see-saw mechanism. The extraction of mixing parameters from the neutrino mass matrix is explained and the evolution of the masses of the right-handed neutrinos is estimated in chapter 5. In chapter 6, the running of the neutrino masses and mixing parameters is discussed in the type-I see-saw scenario, especially the case of a hierarchical pattern in the neutrino Yukawa matrix which is suggested by GUT models. The calculation of the β -functions of the type-II contribution to the neutrino mass is presented in chapter 7. Furthermore, the differences of a type-II see-saw scenario to a type-I see-saw scenario are shortly discussed. Finally, in chapter 8, the numerical code is presented which was developed during this work. After the summary of the main part, the SM Lagrangian is defined and the Feynman rules of the Higgs triplet are presented in App. A. The β -function of a tensorial quantity is given in App. B and some useful formulae which are often needed in renormalization group analysis are compiled in App. C. Finally, App. D contains tables with the RGEs of the mixing parameters. Throughout this thesis, natural units $\hbar = c = 1$ are used. Furthermore, the RL convention is used for Yukawa couplings and the GUT charge normalization is used for the $U(1)_Y$ hypercharge in order to obtain gauge coupling unification at the GUT scale. Part of this work will be published [16].

Chapter 2

Mass Terms

2.1 Fermion Masses

Every term in the Lagrangian has to be a total singlet under the symmetry group. Both, the underlying space-time symmetry (See App. C.2.1) and the internal symmetry group have to be considered in order to decide whether an operator is a total singlet.

There are 2 types of mass terms which are allowed by the underlying space-time symmetry for uncharged¹ spin $\frac{1}{2}$ fermions: Dirac and Majorana mass terms.

2.1.1 Dirac Mass Terms

Let us look more closely at the mass term in the Dirac equation. In the chiral representation of the γ matrices, the left- and right-handed parts of the Dirac spinor separate in the massless case; i.e.: the representation formed by the Dirac spinor will be reducible in left- and right-handed parts if parity is not a symmetry of the theory. The reason is that parity interchanges left- with right-handed fields. The two projection operators onto the left- and right-handed parts are

$$P_{L/R} := \frac{1}{2} (1 \pm \gamma_5) .$$

A Dirac mass term is formed by a product of left- ψ_L and right-handed ψ_R fields which is a singlet under $SL(2, \mathbb{C})$.

$$\begin{aligned} \mathcal{L}_m^{\text{Dirac}} &= -m \bar{\psi} \psi = -m (\bar{\psi}_R + \bar{\psi}_L) (\psi_R + \psi_L) \\ &= -m (\bar{\psi}_R \psi_L + \bar{\psi}_L \psi_R) \end{aligned} \tag{2.1}$$

The barred fields are in the conjugate representation of the gauge group. Thus the product of the barred field with the unbarred field is a singlet under the gauge group and therefore it is a total singlet.

2.1.2 Majorana Mass Terms

There is another possibility to form a singlet under $SL(2, \mathbb{C})$ which corresponds to a mass term. The charge conjugate field $\psi^C := C \bar{\psi}^T = i\gamma^2 \psi^*$ ($C = i\gamma^2 \gamma^0$) has opposite handedness,

¹Charged particles can not have a Majorana mass term, because the Majorana mass term is not a singlet under the $U(1)$ -symmetry corresponding to the charge.

i.e. a left-handed field is transformed to a right-handed field by charge conjugation (See App. C.2.1) and vice versa. Thus the product is a singlet under $SL(2, \mathbb{C})$. Furthermore, the charge conjugate field is in the conjugate representation of the gauge group. Hence the barred charge conjugate field is in the same irreducible representation (irrep) as the field. Therefore,

$$\mathcal{L}_{m,L}^{\text{Majorana}} = -m_L \overline{\psi_L^C} \psi_L + \text{h.c.} \quad (2.2)$$

will also be a mass term, if the product contains a gauge group singlet. In electroweak interactions ($SU(2)_L \times U(1)_Y$), the particle has to be a singlet under $U(1)_Y$. Thus no Majorana mass terms are allowed in the standard model (SM). The Majorana mass term is symmetric, i.e. $m^T = m$, since $\overline{\psi_L^C} \psi_L$ is invariant under $\psi_L \leftrightarrow \psi_L^C$. In addition, Majorana masses violate lepton number conservation, which is an accidental symmetry of the SM, by a factor of 2, since they mix particles with their antiparticles.

2.1.3 Masses in the Standard Model

The Standard Model (SM) forbids explicit mass terms for fermions, because the left-handed fields are in a different representation of the gauge group as the right-handed fields. In particular, left-handed fields are $SU(2)_L$ -doublets and right-handed fields are singlets. Thus it is not possible to form a total singlet out of the product of left- and right-handed fields alone. Therefore all fermions of the standard model would be massless without spontaneous symmetry breaking. The introduction of a scalar boson – the Higgs boson – leads to interaction terms of two fermions with the Higgs boson, which is called Yukawa interaction

$$\mathcal{L}_{\text{Yuk}} = -Y_{fg} \overline{e_R^f} \ell_L^g \cdot \phi + \text{h.c.} \quad (2.3)$$

If the ground state of the Higgs potential is not invariant under the symmetry group, the symmetry will be spontaneously broken and the Higgs acquires a vacuum expectation value (vev) which leads to a Dirac mass term for the fermions.

$$\mathcal{L}_{\text{mass}} = -Y_{fg} \overline{e_R^f} v e_L^g + \dots + \text{h.c.} \quad (2.4)$$

However, neutrino masses are forbidden in the SM, since there is no right-handed neutrino to form a Dirac mass term or other particles to form a Majorana mass term.

2.2 Neutrino Mass Terms

There are several extensions of the SM which predict neutrino masses. First, we shall discuss a bottom-up approach [17] which shows, how the SM can be extended to contain neutrino masses. Then some examples are given which produce the different possibilities of neutrino mass terms in their low-energy limit.

Effective neutrino masses can be generated in several different ways. By looking at the Kronecker products of the irreps of the left-handed lepton doublet $\ell_L \sim (\mathbf{2}, -\frac{1}{2})^2$ and the

²The representation of a particle is a combination of an irrep of $SU(2)_L$ and an irrep of $U(1)_Y$, which can be characterized by 2 numbers. The dimension of the irrep of $SU(2)_L$ is the first number and the hypercharge Y the second one.

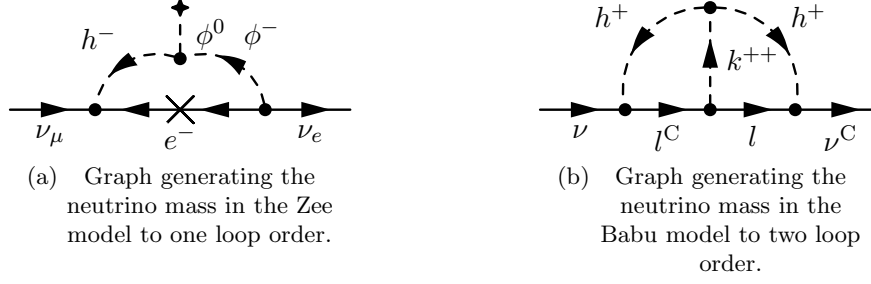


Figure 2.1: Models generating the neutrino mass radiatively.

right-handed neutrino singlets $\nu_R \sim (1, 0)$, the following products are possible

$$\overline{\ell}_L \nu_R \sim \left(2, -\frac{1}{2}\right) \otimes (1, 0) = \left(2, -\frac{1}{2}\right) \quad (2.5a)$$

$$\overline{\ell}_L^C \ell_L \sim \left(2, -\frac{1}{2}\right) \otimes \left(2, -\frac{1}{2}\right) = (1, -1) \oplus (3, -1) \quad (2.5b)$$

$$\overline{\nu}_R^C \nu_R \sim (1, 0) \otimes (1, 0) = (1, 0) \quad (2.5c)$$

Thus there are two essentially different possibilities to extend the SM in order to generate neutrino masses: an extension of the Higgs sector or the introduction of right-handed neutrinos.

2.2.1 Extension of the Higgs Sector

Eq. (2.5b) suggests to add either a Higgs singlet or a Higgs triplet. The Higgs singlet s^+ must be charged ($Q = 1$) to generate a neutrino mass term. Thus the vacuum is charged, when it acquires a vev which is not desirable.

In the case of the Higgs triplet, the Higgs can acquire a vev which corresponds to an uncharged vacuum, since the hypercharge is -1 . This results in $Q - T_3 = Y = -1$ and T_3 in the triplet is 0 or ± 1 . However, the triplet contributes to other mass terms, too. Especially, the W and Z boson masses are changed. Hence the $\rho = \frac{M_W^2}{M_Z^2 \cos^2 \theta_W}$ parameter which is sensitive to changes in the Higgs sector also changes and deviates from 1 at tree level. The value of ρ , however, is strongly restricted by experiments to $0.9998^{+0.0008}_{-0.0005}$ [18].

Another possibility is that the Higgs particles do not acquire vevs, but the neutrino mass is generated radiatively. This ensures small neutrino masses, because the mass is proportional to the loop. Loop diagrams yield small values due to the loop factor of $\frac{1}{8\pi^2}$ from the integration over the loop momentum on the one hand and the proportionality to some power of a small coupling on the other hand. One example is the Zee model [19] in which a Higgs singlet is introduced to generate the neutrino mass to one loop order (See Fig. 2.1(a)). Another possibility is the Babu model [20], where 2 charged Higgs singlets h^+ and k^{++} are introduced generating the neutrino mass at 2 loop level (See Fig. 2.1(b)).

2.2.2 Introduction of right-handed Neutrinos

The introduction of right-handed neutrinos provides the possibility of a Dirac mass term for neutrinos as well as a Majorana mass term for the right-handed neutrinos, if lepton number

is violated. There will be no Majorana mass term for the left-handed neutrinos, since an extension of the Higgs sector is needed to produce it. Majorana mass terms can be forbidden by the introduction of a gauged B-L symmetry which leads to Dirac neutrinos, but Yukawa couplings have to be small to explain the small mass of neutrinos. In the case of Majorana neutrinos, the smallness of the masses can be explained by the standard see-saw mechanism which is treated in Sec. 4.4. In the case of one family³, the mass terms for the neutrinos in the SM are given by

$$-m_D \overline{\nu_R} \nu_L - \frac{1}{2} M \overline{\nu_R} \nu_R^C + \text{h.c.} . \quad (2.6)$$

Thus the masses of the left- and right-handed neutrinos can be cast in one 2×2 matrix.

$$-\frac{1}{2} \overline{(\nu_L, \nu_R^C)^C} \begin{pmatrix} 0 & m_D \\ m_D & M \end{pmatrix} \begin{pmatrix} \nu_L \\ \nu_R^C \end{pmatrix} + \text{h.c.} , \quad (2.7)$$

where $m_D = Y_\nu \langle \phi \rangle$ is the Dirac mass term of the neutrinos. There is one small eigenvalue which is approximately given by the see-saw formula

$$m_\nu = -m_D M^{-1} m_D , \quad (2.8)$$

and one large eigenvalue which is approximately given by M . There are variants of the see-saw mechanism, too. One example is the double see-saw mechanism [21] where the scale of the neutrino mass generation is lowered by the introduction of another right-handed neutrino which does not have a Majorana mass term. This leads to the following mass matrix

$$\begin{pmatrix} 0 & m_D & 0 \\ m_D & 0 & M \\ 0 & M & \mu \end{pmatrix} \quad (2.9)$$

which will lead to one small and 2 large mass eigenvalues if $\mu \ll M$. The light mass eigenvalue is given by $m_\nu \sim m_D M^{-1} \mu M^{-1} m_D$. Thus the mass of the neutrino is doubly suppressed by the large mass M . Hence the mass scale M can be considerably lower than in the type-I see-saw case.

Finally, the Higgs sector can be enhanced in addition to the introduction of right-handed neutrinos. The introduction of a Higgs triplet can be motivated from left-right (LR) symmetric models like the Pati-Salam model [22]

$$\text{SU}(4)_{\text{PS}} \otimes \text{SU}(2)_L \otimes \text{SU}(2)_R \xrightarrow{\langle \phi_{B-L} \rangle} \text{SU}(3)_c \otimes \text{SU}(2)_L \otimes \text{U}(1)_Y \xrightarrow{\langle \phi_{\text{ew}} \rangle} \text{SU}(3)_c \otimes \text{U}(1)_{\text{em}} \quad (2.10)$$

which contains a triplet Higgs to generate masses. In the context of LR-symmetry, Higgs triplets have a mass which is of the order of the LR-breaking scale. They can generate a naturally small effective Majorana mass term for the left-handed neutrinos via the type-II see-saw mechanism [23–26]. The Pati-Salam model can be embedded in $\text{SO}(10)$, E_6 and other GUT models. Thus Higgs triplets appear naturally in the context of GUTs.

³This can be easily generalized to 3 families.

2.2.3 Smallness of Neutrino Masses

The smallness of the neutrino mass can be explained by a large hierarchy in the particle spectrum in a given GUT model or by a Planck scale effect [26] where the suppression is implied by the Planck scale. Then the masses of the neutrinos which are generated at the high-scale, e.g. by integrating out a particle, are small. This is possible for Majorana neutrinos, e.g. see-saw scenarios [11–15] as well as for Dirac neutrinos [21, 27–29]. On the other hand, the smallness might be due to a bulk effect in the context of models with extra dimensions, e.g. the SM particles live on a brane, but the right-handed neutrino can propagate in the bulk. Thus the Yukawa coupling of the neutrinos are suppressed by the size of the extra dimension compared to the Yukawa couplings of the other fermions [30]. There are a lot of possibilities to construct models with extra dimensions, especially models with large extra dimensions are favored, since the compactification scale is very low.

In the following, we assume, that neutrinos are Majorana particles and the smallness of their mass is explained by the type-II see-saw mechanism.

Chapter 3

Renormalization

In perturbative quantum field theory there are divergent Feynman diagrams. These ultra-violet divergencies are not physical and have to be removed to obtain physical predictions¹. They are removed by introducing counterterms which cancel the UV divergencies. These counterterms are polynomial in the external momenta and masses [33, 34]. Thus the locality of the theory is maintained. The systematic determination of the counterterms is achieved by the renormalization program [35–37].

By the renormalization program, the theories are classifiable in 3 categories:

- super-renormalizable theories which only have a finite number of divergent diagrams.
- renormalizable theories which have an infinite number of divergent theories, but need only finitely many counterterms.
- non-renormalizable theories which have infinitely many divergent diagrams and need infinitely many counterterms.

The type of a theory is determined by power counting.

3.1 Power Counting

Each Feynman diagram has a superficial degree of divergence D which is governed by its vertices and external lines, i.e. the integral behaves as

$$\int^{\infty} k^{D-1} dk . \quad (3.1)$$

Thus diagrams with negative overall degree of divergence will be super-renormalizable, if the subdivergencies are removed, diagrams with $D \leq 0$ are renormalizable and diagrams with $D > 0$ are non-renormalizable by power-counting. There are 3 different types of contributions to the degree of divergence. Propagators contribute with

$$\sum_f I_f(2s_f - 2) , \quad (3.2)$$

¹There are infrared divergencies, too. However, they will disappear, if the emission of an arbitrary number of low-energy massless particles is added, since these can not be measured by a detector, e.g. the emission of soft photons [31, 32].

where I_f is the number of internal lines and $s_f = A + B$ characterizes the type of the particle which is propagating. (A, B) denotes the Lorentz representation (See Sec. C.2.1) of the particle. Thus scalars $(0, 0)$ have $s_f = 0$. Majorana fermions $(\frac{1}{2}, 0)$ or $(0, \frac{1}{2})$ and Dirac fermions $(\frac{1}{2}, 0) \oplus (0, \frac{1}{2})$ have $s_f = \frac{1}{2}$. Every derivative introduces one additional momentum factor into the integrand. Thus the total contribution from derivatives is

$$\sum_i N_i d_i , \quad (3.3)$$

where N_i is the number of vertices and d_i is the number of derivatives at vertex i . Finally, every loop contributes a factor of 4 because of the integration over the loop momentum. The number of loops equals the number of independent internal momenta. Every internal line contributes one momentum, but the momentum-conserving δ -distribution at each vertex decreases the number of independent loop momenta by 1. Thus the contribution from the loops is

$$4 \cdot \#\text{loops} = 4 \left(\sum_f I_f - \left(\sum_i N_i - 1 \right) \right) . \quad (3.4)$$

Combining all these contributions, the degree of divergence of a diagram with loops is

$$\begin{aligned} D &= \sum_f I_f (2s_f - 2) + \sum_i N_i d_i + 4 \left(\sum_f I_f - \left(\sum_i N_i - 1 \right) \right) \\ &= 4 - \sum_f E_f (1 + s_f) - \sum_i N_i \Delta_i , \end{aligned} \quad (3.5)$$

where $\Delta_i = 4 - d_i - \sum_f n_{if} (1 + s_f)$ is the mass dimension of the coupling constant of the vertex i , n_{if} is the number of lines of particle type f connected to vertex i . In order to derive the last equality, the topological relation

$$2I_f + E_f = \sum_i N_i n_{if} \quad (3.6)$$

between internal lines I_f , external lines E_f and vertices N_i was used. This relation states that internal lines are connected to two vertices in contrast to external lines.

There is an upper bound on the superficial degree of divergence in theories which have only vertices with $\Delta_i \geq 0$:

$$D \leq 4 - \sum_f E_f (1 + s_f) . \quad (3.7)$$

Thus these theories need only finitely many counterterms and are renormalizable. If all couplings of a theory satisfy $\Delta_i > 0$, there are only finitely many divergent diagrams and the theory is super-renormalizable. Otherwise, the theory is non-renormalizable. There are some exceptions to power counting.

- Tree level diagrams are finite, but power counting determines the superficial degree of divergence to be $D = 0$.
- Symmetries can reduce the degree of divergence of a diagram.

- However, anomalies, i.e. classical symmetries which are not symmetries on the quantum level, introduce additional terms to the Lagrangian which are forbidden by the symmetries. Thus in order to show renormalizability of a theory, it has to be proven that there are no anomalies.
- A diagram can have an negative overall degree of divergence, but there might be subdivergencies. Subdivergencies can be treated by the Bogoliubov-Parasiuk-Hepp-Zimmermann (BPHZ) formalism (See Sec. 3.3.3).

The notion of renormalizability used above is in the power counting sense which is defined by Dyson's criterion [38], that a renormalizable Lagrangian density should not contain operators of dimension higher than 4. This is a sufficient but not necessary condition, that all divergencies are canceled by a finite number of terms. Renormalizability in the modern sense [39] just demands the cancellation of divergencies without imposing the restriction of a finite number of counterterms. Hence, there might be infinitely many terms in the bare Lagrangian.

3.2 Regularization

Before renormalization, the theory has to be regularized. Obviously, the renormalization should not depend on the regularization technique. If they were, the result would be meaningless, since it could be changed by simply choosing a different regularization scheme.

3.2.1 UV cutoff

The simplest regularization prescription is to introduce an UV cutoff Λ . This method takes into account that the divergence stems from high momenta:

$$\int_0^\infty dq \rightarrow \int_0^\Lambda dq. \quad (3.8)$$

As there are no infinite momenta, this results in finite diagrams, i.e. even if there is some power of momentum in the numerator, the result will be finite. However, the UV cutoff violates gauge invariance and therefore the gauge invariance of the renormalized theory has to be explicitly proven afterwards. Thus a symmetry preserving regularization prescription is more convenient.

3.2.2 Pauli-Villars Regularization

In the Pauli-Villars regularization method the propagator of particles S_F is replaced by a different propagator rendering the diagrams finite. For a simple scalar theory the propagator becomes

$$S_F^{\text{PV}}(p, m; M) = \frac{i}{p^2 - m^2 + i\varepsilon} - \frac{i}{p^2 - M^2 + i\varepsilon} = \frac{i}{p^2 - m^2 + i\varepsilon} \frac{m^2 - M^2}{p^2 - M^2 + i\varepsilon}, \quad (3.9)$$

where M is large and has the dimension of a mass. For $M \rightarrow \infty$, this regulated propagator reduces to the original propagator. The Pauli-Villars regularization is gauge invariant and can be understood physically. The propagator has an additional pole at $p^2 = M^2$. This pole corresponds to an additional particle of mass M canceling the divergence. After the

divergence is subtracted, the mass of the introduced particle is taken to infinity. Thus this additional particle decouples and is basically removed. Sometimes the Pauli-Villars regulated propagator may look more complicated, since one additional particle is not enough to cancel the divergencies.

3.2.3 Lattice Regularization

Another possible regularization technique is the discretization of space-time, since the divergencies stem from high momenta or equivalently small distances. Thus the discretization removes all contributions from distances smaller than the lattice spacing. After the subtraction of the divergency, the lattice spacing is taken to zero. For a lattice of finite volume, as they are used in numerical calculations, there is also an IR cutoff. The problem in lattice regularization is, that Poincaré invariance is explicitly broken. Therefore it has to be proven, that the renormalized theory is Poincaré-invariant.


3.2.4 Dimensional Regularization

Dimensional regularization [40–42] provides a gauge- and Poincaré invariant regularization method. The theory is analytically continued to $d = 4 - \epsilon$ dimensions. The divergent integrals become finite and after renormalization the limit $d \rightarrow 4$ is taken. If the renormalization scheme is gauge-invariant and Poincaré invariant, the renormalized theory also preserves these symmetries. As the mass dimension of couplings depends on the dimension of space-time, the couplings are multiplied by an arbitrary parameter μ , which has the dimension of mass. The arbitrariness of this parameter leads to the renormalization group (See Sec. 3.5). Problems will arise in dimensional regularization, if expressions like $\text{tr}(\gamma_5 \gamma^\mu \gamma^\nu \gamma^\xi \gamma^\eta)$ show up. These are due to intrinsic 4 dimensional quantities like $\gamma_5 = i\gamma^0 \gamma^1 \gamma^2 \gamma^3$ and $\epsilon_{\mu\nu\kappa\lambda}$ which can not be consistently generalized to d dimensions. Hence, the usual relations defined in 4 dimensions lead to contradictions. However, the γ -algebra can be changed [42] in such a way, that all expressions are defined consistently², but as long as these expressions do not show up, naive dimensional regularization can be used, i.e. the usual γ -algebra which is much easier to use in calculations.

The dimensional regularization is explained by an explicit calculation of the wave function renormalization in ϕ^4 theory. The bare Lagrangian is given by

$$\mathcal{L} = \frac{1}{2} \partial_\mu \phi_B \partial^\mu \phi_B - \frac{m_B^2}{2} \phi^2 - \frac{\lambda_B}{4!} \phi_B^4. \quad (3.10)$$

Therefore the degree of divergence is $D = 4 - E$ where E is the number of external legs and the only divergent n -point functions are the two-point and the four-point function. The 2 point function is

$$\Gamma^{(2)} = \text{---} + \text{---} \text{---} \text{---} + \dots, \quad (3.11)$$


²Details are given in App. C.3.3.

which is divergent with degree of divergence $D = 2$. Evaluating the Feynman diagram yields

$$\frac{1}{2}\lambda \int \frac{d^4p}{(2\pi)^4} \frac{1}{p^2 - m^2 + i\varepsilon} , \quad (3.12)$$

where $\frac{1}{2}$ is a symmetry factor appearing, because the diagram is invariant under the exchange of the two legs of the loop. The continuation to d dimensions results in

$$\frac{1}{2}\lambda\mu^\epsilon \int \frac{d^dp}{(2\pi)^d} \frac{1}{p^2 - m^2 + i\varepsilon} , \quad (3.13)$$

As the coupling λ should remain dimensionless, it is rescaled

$$\lambda \rightarrow \lambda\mu^\epsilon , \quad (3.14)$$

where the mass dimension of μ equals $[\mu] = 1$. Then, the integral can be solved by transforming it to the known form of Passarino-Veltman functions (See App. C.5) or equivalently the integral can be Wick rotated to Euclidean space-time ($x_0 \rightarrow ix_4$) and solved by the choice of a convenient coordinate system, as it is done in this case:

$$-i\frac{\lambda\mu^\epsilon}{2} \int \frac{d^dp}{(2\pi)^d} \frac{1}{p^2 + m^2} \quad (3.15)$$

Introducing spherical coordinates, the integral reduces to an one dimensional integral

$$-i\frac{\lambda\mu^\epsilon}{2} (2\pi)^d \frac{2\pi^{\frac{d}{2}}}{\Gamma(\frac{d}{2})} \int_0^\infty dp \frac{p^{d-1}}{p^2 + m^2} , \quad (3.16)$$

where the formula for the volume of a d dimensional sphere $\int d\Omega_d = \frac{2\pi^{\frac{d}{2}}}{\Gamma(\frac{d}{2})}$ was used. This integral can be solved by the Euler Beta function (See Sec. C.4.2):

$$-i\frac{\lambda}{32\pi^2} \left(\frac{4\pi\mu}{m}\right)^\epsilon m^2 \Gamma\left(-1 + \frac{\epsilon}{2}\right) . \quad (3.17)$$

The result for the four-point function can be similarly obtained. It is the sum of 3 divergent diagrams

$$\Gamma^{(4)} = \text{diagram 1} + \text{diagram 2} + \text{diagram 3} + \text{diagram 4} , \quad (3.18)$$

which sum up to

$$\frac{i\lambda^2}{32\pi^2} \mu^\epsilon \Gamma\left(\frac{\epsilon}{2}\right) \sum_{l=s,t,u} F(l, m, \mu) , \quad (3.19)$$

where $F(s, m, \mu) = \int_0^1 dz \left(\frac{sz(1-z) - m^2}{4\pi\mu^2} \right)^{\frac{\epsilon}{2}}$.

The way of subtracting the divergence depends on the renormalization scheme.

3.3 Renormalization Schemes

In order to renormalize a diagram, the divergent part and possibly finite terms are subtracted from the diagram and absorbed in the coupling constants. There are different renormalization schemes, because the diagram can be matched to the experimental value at any arbitrary scale. The result is the same for all schemes.

3.3.1 On-Shell Scheme

In this scheme the divergence is subtracted such that the particles are on-shell, i.e. the pole of the propagator of the particles is at the physical mass. Hence, the renormalization condition is that the mass in the renormalized propagator

$$G^{(2)} = \frac{iZ}{p^2 - m^2 - \Sigma_r + i\varepsilon} , \quad (3.20)$$

equals the physical mass m_{ph} , i.e.

$$m_{\text{ph}}^2 = m^2 + \Sigma_r . \quad (3.21)$$

This fixes the mass counterterm. Furthermore the wave function renormalization is fixed by the condition that the residue at the pole $p^2 = m_{\text{ph}}^2$ is unity, i.e.

$$Z = 1 . \quad (3.22)$$

Hence the subtraction can be physically motivated.

3.3.2 Minimal Subtraction Scheme

In the minimal subtraction (MS) scheme, only the divergent part of the integral is subtracted. In general, it is used together with dimensional regularization. In order to subtract the divergent part, the Feynman diagram is expanded in $\epsilon = 4 - d$. Then the term proportional to ϵ^{-1} is subtracted. The result generally depends on the renormalization scale μ which has been introduced in dimensional regularization. This dependence of the MS scheme on the renormalization scale μ can be interpreted as an one-parameter family of renormalization schemes. Thus there is not one MS scheme, but there is an one-parameter family of MS schemes. In calculations, the parameter μ is set to the energy scale at which the process is taking place, in order to cancel the logarithms which appear in the result.

In general, the result of the diagram is expanded in the parameter governing the regularization. This is ϵ in the case of dimensional regularization. Expanding the Γ function in the example given in Sec. 3.2.4 yields

$$-\frac{i\lambda}{32\pi^2}m^2 \left[\frac{2}{\epsilon} + 1 - \gamma_E + 2 \ln \left(\frac{4\pi\mu}{m} \right) + \mathcal{O}(\epsilon) \right] = \frac{i\lambda}{16\pi^2}m^2 \frac{1}{\epsilon} + \text{finite} \quad (3.23)$$

for the two-point function and

$$\frac{i3\lambda^2\mu^\epsilon}{16\pi^2\epsilon} + \text{finite} \quad (3.24)$$

for the four-point function to 1 loop order. The divergent part is absorbed into the renormalized couplings and masses:

$$\lambda = Z_\lambda \lambda_B = \left(1 + Z_\lambda^{(1)}\right) \lambda_B \quad (3.25a)$$

$$m^2 = m_B^2 + \delta m^2 \quad (3.25b)$$

$$\phi = \sqrt{Z_\phi} \phi_B . \quad (3.25c)$$

Thus the counterterms are

$$Z_\phi = 1 , \quad (3.26a)$$

$$\delta m^2 = - \frac{\lambda}{16\pi^2} m^2 \frac{1}{\epsilon} , \quad (3.26b)$$

$$\text{and } Z_\lambda^{(1)} = - \frac{3\lambda}{16\pi^2 \epsilon} \mu^\epsilon . \quad (3.26c)$$

There are variations of the MS scheme, as it is described above. In the modified minimal subtraction scheme ($\overline{\text{MS}}$) scheme, the finite terms which do not depend on the external momentum and naturally appear in dimensional regularization, $-\gamma_E + \ln(4\pi)$, are subtracted in addition to the divergent term.

It will also be possible to have a mixture of the on-shell and the MS scheme, if they are applied for different counterterms. Often the divergency from the tadpole diagrams is renormalized by imposing the condition that the vacuum expectation value of the fields vanish. Thus there is no linear term in the theory.

3.3.3 BPHZ Renormalization

The Bogoliubov-Parasiuk-Hepp-Zimmermann (BPHZ) [43–45] scheme does not need a regularization, because it directly works with the integrand. At first, all subdivergencies are renormalized recursively. Then the remaining overall divergency is renormalized. This works by defining the graph $\bar{R}(G)$ which is the graph G with all subdivergencies renormalized. Then the renormalized graph $R(G)$ is defined as

$$R(G) = \bar{R}(G) + C(\bar{R}(G)) , \quad (3.27)$$

where C is the operation which generates an appropriate counterterm, when it is applied to a graph. C vanishes for convergent graphs. In the original paper, a zero-momentum subtraction scheme has been used. In this scheme, the counterterm of a diagram with degree of divergence D is given by the first $D + 1$ terms in the expansion of the diagram in terms of the external momenta. Although this scheme is mathematically elegant, because it does not need a UV regulator, it is problematic in massless theories, since the counterterms are IR divergent. However, C can be any renormalization scheme.

The counterterm for a connected one-particle-irreducible (OPI)³ graph is the counterterm which is determined by the chosen renormalization scheme. The counterterm for a disconnected graph is simply the product of the counterterms of the connected components

$$C(\gamma_1 \cup \gamma_2) = C(\gamma_1)C(\gamma_2) . \quad (3.28)$$

³An OPI graph can not be divided in two disconnected graphs by cutting one internal line.

Therefore the problem of renormalizing a graph is split in the renormalization of the overall divergency and the renormalization of subdivergencies. The graph with all subdivergencies renormalized can be obtained from the unrenormalized graph $U(G)$ by

$$\bar{R}(G) = U(G) + \sum_{\gamma \subsetneq G} C(\gamma) , \quad (3.29)$$

i.e. the counterterm for any divergent proper subgraph is added. This prescription can be applied recursively to the subgraphs. As Zimmermann pointed out [46, 47], the sum of the integrand of the unrenormalized graph and all counterterms is equivalent to the unrenormalized graph where all parameters (couplings, masses, wave functions, ...) have been replaced by their renormalized version. Thus the integral is finite and there are no divergencies left which need to be regularized. This recursive scheme for renormalization can be cast in one formula.

Forest Formula

The forest formula summarizes the result of the BPHZ scheme. A forest is a possible set of boxes which surround the graph and/or its subgraphs in such a way that the boxes might be nested but do not overlap. Then the renormalized graph can be expressed as a sum over all forests.

$$R(G) = \sum_{U \in \mathcal{F}(G)} \prod_{\gamma \in U} C_\gamma(G) , \quad (3.30)$$

where $\mathcal{F}(G)$ is the set of all forests of G and $C_\gamma(G)$ is the graph G with the subgraph γ of G replaced by its counterterm. For a proof of the forest formula, see either the book of Collins on Renormalization [35] or the original paper of Zimmermann [45]. The forest formula shows the mathematical structure which is underlying the renormalization procedure⁴. In the following, the MS scheme and dimensional regularization are used.

3.4 Renormalization of Gauge Theories

In general, symmetries which exist on a classical level do not necessarily exist in the quantized theory. This ‘violation’ of a symmetry is called an anomaly. In particular, gauge invariance will have to be proven, if the renormalization prescription is not gauge invariant or if a gauge has been fixed before the renormalization which is necessary to quantize the theory. However, there still remains a symmetry, the Becchi-Rouet-Stora (BRS) symmetry [49]. It relates the fields with the ghost fields from the quantization procedure by

$$\delta\psi = it_\alpha \theta \psi \omega^\alpha \quad (3.31a)$$

$$\delta A_{\alpha\mu} = \theta D_\mu \omega_\alpha \quad (3.31b)$$

$$\delta\omega_\alpha = -\frac{1}{2}\theta f_{\alpha\beta\gamma} \omega_\beta \omega_\gamma \quad (3.31c)$$

$$\delta\omega_\alpha^* = -\theta h_\alpha \quad (3.31d)$$

$$\delta h_\alpha = 0 , \quad (3.31e)$$

⁴In fact, the mathematical structure of renormalization is a Hopf algebra which is formed by the forests, i.e. the algebra of rooted trees. [48]

where t_α is a generator of the gauge group, D_μ is the covariant derivative, $f_{\alpha\beta\gamma}$ are the structure constants, ω_α and ω_α^* are the ghost and anti-ghost field, respectively which are introduced as virtual particles in the quantization procedure. They have the wrong spin-statistics connection, because they are anti-commuting despite of their scalar nature. h_α is an auxiliary field which does not propagate and θ is a fermionic variable. Thus the BRS-operator is fermionic and this symmetry is a supersymmetry, since it relates bosons and fermions. Furthermore, it is nilpotent, i.e. $\delta_{\text{BRS}}^2 = 1$. In order to prove renormalizability of a gauge theory, it must be shown that the BRS symmetry is still respected after the renormalization. This was proven by using Slavnov-Taylor identities [50, 51] to constrain the renormalized action, such that the renormalized action is BRS-invariant [49, 52–54]. They reflect the classical gauge symmetry in the quantum field theory context where a gauge has been chosen.

3.5 Renormalization Group

The renormalization group (RG) describes the invariance of physical observables under the change of the renormalization prescription. Thus the theory itself does not change under the renormalization group, but only the renormalized couplings and masses. In the $\overline{\text{MS}}$ scheme the renormalization group becomes obvious, since the counterterms depend on the renormalization scale μ . Different values of μ correspond to different renormalization prescriptions and the variation of the parameter μ is described by the renormalization group. Moreover, in the $\overline{\text{MS}}$ scheme the evolution of the coupling constants and masses can be predicted and, hence, the parameters of a theory in the high-energy regime can be related to the parameters in the low-energy limit. This dependence on the energy scale has already been measured for the electromagnetic fine structure constant $\alpha_{\text{em}} = \frac{e^2}{4\pi}$. On the one hand, α_{em} was determined to be

$$\alpha_{\text{em}}^{-1}(181.94 \text{ GeV}) = 126.2_{-3.2}^{+3.5} \quad (3.32)$$

at LEP in the OPAL experiment at a center of mass energy of 181.94 GeV [55]. On the other hand, it was measured at very low energies in the quantum Hall effect [18] to be given by

$$\alpha_{\text{em}}^{-1}(0 \text{ GeV}) = 137.035999911(46) . \quad (3.33)$$

These two measurements contradict each other without considering the renormalization group evolution which reconciles the two values. This dependence on the renormalization scale μ is described by the Callan-Symanzik equation which expresses the change of renormalized Green's functions under the renormalization group.

3.5.1 Callan-Symanzik Equation

As bare quantities do not depend on the renormalization scale μ , the derivative of bare quantities with respect to the renormalization scale μ has to vanish:

$$\left. \frac{d}{d\mu} G_{\text{B}}^{(n)} \right|_{\text{bare}} = 0 , \quad (3.34)$$

where $G_{\text{B}}^{(n)} = \langle 0 | \mathcal{T} \phi_{\text{B}}(x_1) \dots \phi_{\text{B}}(x_n) | 0 \rangle$ is the bare n -point Green's function. From this observation, the Callan-Symanzik equation [56, 57] is derived. It is simply Eq. (3.34) which is

expressed in renormalized quantities. For a theory with a scalar field ϕ with mass m and a gauge field A_μ coupling to the scalar with coupling strength g and gauge fixing parameter ξ , the Callan-Symanzik equation is given by

$$\left[\mu \frac{\partial}{\partial \mu} + \beta \frac{\partial}{\partial g} - \gamma_m m \frac{\partial}{\partial m} - \delta_\xi \xi \frac{\partial}{\partial \xi} + \frac{n}{2} \gamma \right] G^{(n)}(p_i, g, m, \xi; \mu, \epsilon) = 0. \quad (3.35)$$

γ and γ_m are referred to as anomalous dimensions of the wave function and mass, respectively, and β is called β -function. It is a quasi-linear first-order partial differential equation (PDE) describing the variation of the renormalized Green's functions under a change of μ . These PDEs can be solved by the method of characteristic curves which transforms the PDE in a system of ordinary differential equations (ODE) for the coefficients of the derivatives. The obtained ODEs are called the renormalization group equations (RGE). This example of a Callan-Symanzik equation is easily translated to arbitrary quantum field theories which have fermionic degrees of freedom and more fields.

3.5.2 Renormalization Group Equations

The renormalization group equations corresponding to Eq.(3.35)

$$\beta := \mu \frac{dg}{d\mu} \quad (3.36a)$$

$$\gamma_m := -\frac{1}{m} \mu \frac{dm}{d\mu} \quad (3.36b)$$

$$\gamma := \frac{1}{Z_\phi} \mu \frac{dZ_\phi}{d\mu} \quad (3.36c)$$

$$\delta_\xi := -\frac{1}{\xi} \mu \frac{d\xi}{d\mu} \quad (3.36d)$$

can be obtained from the corresponding counterterms by expressing the renormalized quantities in terms of their counterterms and bare quantities. In the case of ϕ^4 theory, the β -function of λ is

$$\beta_\lambda = \mu \frac{d(Z_\lambda \lambda_B)}{d\mu} = -\frac{3}{16\pi^2} \lambda^2 \mu^\epsilon \xrightarrow{\epsilon \rightarrow 0} -\frac{3}{16\pi^2} \lambda^2 \quad (3.37)$$

and the anomalous dimension of the mass is given by

$$\gamma_m = -\frac{1}{2m^2} \mu \frac{d(m_B^2 + \delta m^2)}{d\mu} = \frac{\lambda}{32\pi^2} \left(\frac{4\pi\mu}{m} \right)^\epsilon \xrightarrow{\epsilon \rightarrow 0} \frac{\lambda}{32\pi^2}. \quad (3.38)$$

The anomalous dimension of the wave function vanishes, because the wave function does not get renormalized. After the coupling constant and the mass have been fixed at one value of μ , they are determined at all scales, because this set differential equations is a first-order ODE which needs only one initial value. As it was already pointed out, the dependence of the couplings and masses on the energy scale has already been measured in the case of electromagnetic interactions. The experimental data shows the increase of the coupling constant with increasing energy. This is a general property of Abelian gauge symmetries, because the gauge bosons are not charged and therefore they do not couple among each other. In non-Abelian gauge theories, the evolution of the gauge coupling g depends on

the particle content of the theory. The β -function for the gauge coupling of an arbitrary non-Abelian theory is given by

$$\beta_g = \frac{g^3}{16\pi^2} \left[-\frac{11}{3} C_2(\text{Ad}) + \frac{4}{3} \sum_i C_2(F_i) + \frac{1}{3} \sum_i C_2(S_i) \right], \quad (3.39)$$

where C_2 is the quadratic Casimir invariant of the gauge group which is defined for a representation A as

$$C_2(A) = \text{tr}(T^a(A)T^a(A)) \quad (3.40)$$

Ad denotes the adjoint representation and F_i and S_i designate the representations of the fermions and scalars of type i , respectively. In particular, the strong coupling in a model with n_F fermions

$$\beta_{g_3} = -\frac{g_3^3}{16\pi^2} \left(11 - \frac{2}{3} n_F \right) \quad (3.41)$$

becomes weaker at high energies and tends to zero which is known as asymptotic freedom. This year's Nobel prize was awarded for the discovery of asymptotic freedom to Gross, Politzer and Wilczek [58]. In this section the β -function of a quantity which can be multiplicatively renormalized has been shown. In general, the parameters of a theory are tensors which have to be renormalized additively. The β -function of a tensorial quantity can be obtained in a similar way [59–61]. The general formula is given in App. B.

Chapter 4

Effective Field Theories

The concept of Effective Field Theories (EFT) provides a framework to systematically look only at the relevant degrees of freedom. All other degrees of freedom which are off-shell are integrated out. Hence, heavy particles which can not become on-shell at the energy scale considered are integrated out. The process of integrating out can be understood in several ways. In the context of Feynman Path integrals, it results in evaluating the path integral over the degrees of freedom which do not resonate. By looking at Feynman diagrams, the process of integrating out shows up as the deletion of all lines of heavy particles. This leads to new interaction vertices, since lines are contracted. More precisely, the transition to an EFT is the expansion of the full theory in the inverse of a dimensionful parameter Λ characterizing the off-shell degrees of freedom. This expansion is characterized by power counting, since all processes are weighted by the power of the inverse mass scale Λ .

$$\mathcal{L} = \mathcal{L}^{(0)} + \mathcal{L}^{(1)} + \mathcal{L}^{(2)} + \dots, \quad (4.1)$$

where $\mathcal{L}^{(n+1)}$ is suppressed by Λ against $\mathcal{L}^{(n)}$. The 0th order part $\mathcal{L}^{(0)}$ is not suppressed by Λ and will have to be renormalizable, if \mathcal{L} is renormalizable. Otherwise, there would be non-renormalizable diagrams in the “full” theory, since $\mathcal{L}^{(0)}$ is contained in the Lagrangian of the “full” theory. Therefore an EFT can be as precise as it is needed, because higher-order terms can be systematically considered to improve the precision. This systematic approach is guaranteed by the “Power counting” of the EFT. Basically, there are two cases when EFTs are interesting.

- *Top-Down approach:* On the one hand, EFTs are necessary to solve problems which are too complicated in the full theory, because too many degrees of freedom have to be considered (e.g. the H-atom is solved more easily in relativistic Quantum Mechanics than in the Standard Model.). It might be even impossible to solve the problem perturbatively in the full theory whereas it is solvable in the EFT perturbatively.
- *Bottom-Up approach:* On the other hand, the full theory might be unknown. Then an EFT can give important hints to find the full theory. At least, it allows to solve problems in the low-energy regime (e.g. Fermi Theory was known before Glashow-Salam-Weinberg (GSW) theory of electroweak interactions.). Thus the concept of EFTs is a tool to see signs of new physics.

Another example, in which EFTs are useful, is the calculation of processes in which several energy scales are relevant. The problem is that large logarithms from the renormalization

procedure have to be summed up, but the renormalization scale can not be comparable to both scales. Using an EFT, the heavy degrees of freedom can be integrated out and only one energy scale is remaining. Then all large logarithms have been removed.

In order to be a well defined EFT, the low-energy effective theory must decouple from the high-energy degrees of freedom.

4.1 Decoupling Theorem

Decoupling means that all Feynman graphs containing a propagator for a field whose mass M is greater than the external momenta of that graph, are suppressed by a power of the external momenta p over the heavy mass M . Thus the Green's functions in the effective theory equal the Green's functions of the full theory up to corrections $\mathcal{O}(p/M)$ and therefore the heavy particles are unobservable until close to their threshold. The couplings and masses of the low-energy effective theory have no a-priori value to which the measurements can be compared. Symanzik [62] and later Appelquist and Carazzone [63] showed that the low-energy effective theory does indeed decouple from the high-energy degrees of freedom and it is a renormalizable theory in the limit of $M \rightarrow \infty$. However, there are exceptions to this decoupling theorem. One famous example is Fermi theory which is the effective low-energy theory of electroweak theory. In the Fermi theory without the Four-Fermi interaction, the low-energy symmetries forbid interactions like β -decay and therefore β -decay is only generated by the Four-Fermi interaction. This deviation from zero is detectable at low energies and the heavy degrees of freedom do not completely decouple from the low-energy effective theory, but they induce new non-renormalizable interactions. Therefore Fermi theory is still a good EFT, but the non-renormalizable first-order effects are essential. This is a general phenomenon in EFTs: the EFT contains more symmetries than the full theory and interactions are forbidden which are allowed in the full theory. Another example are chiral gauge theories and the decoupling of chiral fermions. In the SM, the top quark is much heavier than the other quarks and therefore it can be integrated out at low energies. However, the mass of the top quark is generated by the Higgs mechanism. Thus the limit $m_t \rightarrow \infty$ corresponds to the limit $y_t \rightarrow \infty$, i.e. the coupling of the top quark to the Higgs becomes strong and therefore the top quark does not decouple. The last example is the gauge hierarchy problem which will be a problem, if the SM is embedded in a GUT. It can be summed up in the question, why there are so strong hierarchies and why they are stable against radiative corrections. The question of stability against radiative corrections is due to the quadratic corrections which the mass of scalar particles receives. Fermions, on the other hand, receive only logarithmic corrections. Thus the corrections to the scalar mass are considerably larger than corrections to fermion masses and therefore scalar masses are expected to be lifted to the scale where the particles with the highest mass which they couple to reside. Hence, the heavy particles do not necessarily decouple from the Higgs sector.

4.2 Construction of an EFT from a “full” Theory

The construction of an EFT can be summed up in the following steps:

- The relevant degrees of freedom have to be identified.
- All off-shell degrees of freedom are integrated out.

- Identify the expansion parameter, like the mass of the W boson in Fermi Theory in order to establish the power counting.
- Then the terms in the EFT action can be ordered in powers of the expansion parameter. The zeroth order term will be a renormalizable Lagrangian, if the “full” theory is renormalizable.
- The parameters of the EFT have to be matched to the parameters of the “full” theory. The matching conditions are obtained by requiring that measurable quantities in both theories agree at the matching scale. The parameters will be matched at tree level, if 1-loop renormalization group running is used. However, if the renormalization group equations are calculated in n loop, (n-1)-loop matching will be needed. Then the parameters of the EFT have to be evolved down to the low energy regime from the matching scale.
- Finally the parameters of the EFT have to be run down to the regime at which the process is taking place.

4.3 Neutrino Mass Operator

Now, the concept of EFTs will be applied to neutrino masses, in particular within the bottom-up approach. The SM does not contain a neutrino mass term, but it was shown in oscillation experiments [64] that at least two neutrinos are massive. Therefore the SM is not a “full” theory describing everything, but it is the 0th order of an EFT.

$$\mathcal{L}^{(0)} = \mathcal{L}_{\text{SM}} \quad (4.2)$$

It is renormalizable, because the SM is renormalizable [40–42], as it is expected for the 0th order part of an EFT. The next step is the introduction of higher dimensional operators. There is only one operator of dimension 5 which is compatible with the SM gauge group $\text{SU}(3)_C \times \text{SU}(2)_L \times \text{U}(1)_Y$ and can be constructed with SM fields [65]:

$$\mathcal{L}^{(1)} \sim \frac{1}{4} \kappa_{fg} \overline{\ell_{La}^f} \epsilon_{ab} \phi_b (\ell_{Lc}^g)^C \epsilon_{cd} \phi_d . \quad (4.3)$$

It describes the coupling of two left-handed doublets to two Higgs doublets. After electroweak symmetry breaking, this operator generates a Majorana mass term for the left-handed neutrino ν_L . One might argue, that the same construction should work for other particles, but since the other particles are charged, the resulting mass term is not a singlet under $\text{U}(1)_{\text{em}}$. Thus this is the only dimension 5 operator.

$$\begin{array}{ccc}
 \begin{array}{c} \text{Diagram 1: } \ell_{La}^f \text{ and } \ell_{Lc}^g \text{ lines with } \phi_b, \phi_d \text{ Higgs lines and a } \kappa \text{ box.} \\ -\frac{1}{4} \kappa_{fg} \overline{\ell_{La}^f} \epsilon_{ab} \phi_b \cdot (\ell_{Lc}^g)^C \epsilon_{cd} \phi_d \end{array} & \xrightarrow{\phi \rightarrow \langle \phi \rangle + \phi'} & \begin{array}{c} \text{Diagram 2: } \nu_L^f \text{ and } \nu_L^g \text{ lines with } v, v \text{ Majorana lines and a } \kappa \text{ box.} \\ -\frac{v^2}{4} \kappa_{fg} \overline{\nu_L^f} (\nu_L^g)^C \end{array} \\
 \end{array} \quad (4.4)$$

Therefore, this operator generates a Majorana mass term for ν_L .

$$\mathcal{L}_{\nu\text{mass}} = -\frac{1}{8}\kappa_{fg}(\epsilon_{ab}\epsilon_{cd} + \epsilon_{ad}\epsilon_{bc})\overline{l_{La}^f}\phi_b(l_{Lc}^g)^C\phi_d \quad (4.5)$$

The coefficient in front of the dimension 5 operator has dimension -1 . In particular, it can be written as a fraction of a dimensionless coupling over a mass scale Λ which can serve as expansion parameter to control the power counting. As this is the only dimension 5 operator, other new physics effects are suppressed by another power of Λ .

Since the SM has survived all precision tests so far and explains all measurement in good agreement except for neutrino masses, the SM plus this effective neutrino mass operator have to be the low-energy limit of every reasonable theory predicting Majorana neutrino masses. One possible UV completion of this EFT is the introduction of right-handed neutrinos or a Higgs triplet which generate the effective neutrino mass operator via the see-saw mechanism.

4.4 See-Saw Mechanism

It is possible to generate small neutrino masses via the see-saw mechanism [11–15] in accordance with phenomenology. There are two variants of the see-saw mechanism, the standard or type-I and the type-II see-saw mechanism. However, before introducing the see-saw mechanism, the extensions of the Standard Model (SM) are stated which are relevant for the see-saw mechanism. The SM Lagrangian and its particle content are given in App. A.1.

4.4.1 Extensions of the SM

Extension of SM by right-handed Neutrinos

One conservative extension of the SM is the introduction of another irrep, i.e. another particle. As the total singlet is the only fundamental irrep not contained in the SM, the introduction of a total singlet¹, i.e. a right-handed neutrino, is suggestive. It allows the following new terms in the Lagrangian.

$$\mathcal{L}_{\nu_R} = \overline{\nu_R}\not{D}\nu_R - (Y_\nu)_{ij}\overline{\nu_R}^i\ell_L^j\phi^C - \frac{1}{2}M_{ij}\overline{\nu_R}^i\nu_R^j + \text{h.c.} \quad (4.6)$$

The Majorana mass term is possible in the SM for right-handed neutrinos only, because they are total singlets. Thus neutrinos will naturally be Majorana particles unless there is an additional symmetry which forbids Majorana mass terms. One such symmetry is lepton number conservation, but it is only an accidental symmetry in the SM.

Extension of SM by a Higgs Triplet

The SM can also be extended by a charged Higgs triplet¹ $\Delta \sim (\mathbf{3}, \mathbf{1})$.

$$\Delta = \frac{\sigma^i}{\sqrt{2}}\Delta_i = \begin{pmatrix} \Delta^+/\sqrt{2} & \Delta^{++} \\ \Delta^0 & -\Delta^+/\sqrt{2} \end{pmatrix} \quad (4.7)$$

This extension leads to several additional terms in the Lagrangian which can be obtained from the decomposition of the product representations of $\text{SU}(2)_L$ which is given in Tab. 4.1.

¹It is also possible to extend the MSSM or the 2HDM by right-handed neutrinos or a Higgs triplet.

	1	2	3	4	5
1	1	2	3	4	5
2	.	1 \oplus 3	2 \oplus 4	3 \oplus 5	4 \oplus 6
3	.	.	1 \oplus 3 \oplus 5	2 \oplus 4 \oplus 6	3 \oplus 5 \oplus 7
4	.	.	.	1 \oplus 3 \oplus 5 \oplus 7	2 \oplus 4 \oplus 6 \oplus 8
5	1 \oplus 3 \oplus 5 \oplus 7 \oplus 9

Table 4.1: Product representations of irreps of SU(2). $A \otimes B = \sum_i C_i$ where A and B are the representation given in the first column and row, respectively.

All possible SU(2)_L-singlets, which can be formed by a Higgs triplet and a Higgs doublet and are compatible with the U(1)_Y and Lorentz group structure, have to be included in the Higgs potential [65]. In addition, there is a new Yukawa coupling of the left-handed lepton doublets to the triplet Higgs. Therefore the Lagrangian is given by

$$\mathcal{L} = \mathcal{L}_{\text{kin}} + \mathcal{L}_{\Delta^4} + \mathcal{L}_{\phi^2 \Delta^2} + \mathcal{L}_{\phi \Delta \phi} + \mathcal{L}_{\ell_L \Delta \ell_L} , \quad (4.8)$$

where the terms are given by

$$\mathcal{L}_{\text{kin}} = \text{tr} \left[(D_\mu \Delta)^\dagger D^\mu \Delta \right] - M_\Delta^2 \text{tr} \left(\Delta^\dagger \Delta \right) \quad (4.9a)$$

$$\mathcal{L}_{\Delta^4} = -\frac{\Lambda_1}{2} \left(\text{tr} \Delta^\dagger \Delta \right)^2 - \frac{\Lambda_2}{2} \left[\left(\text{tr} \Delta^\dagger \Delta \right)^2 - \text{tr} \left(\Delta^\dagger \Delta \Delta^\dagger \Delta \right) \right] \quad (4.9b)$$

$$\mathcal{L}_{\phi^2 \Delta^2} = -\Lambda_4 \phi^\dagger \phi \text{tr} \left(\Delta^\dagger \Delta \right) - \Lambda_5 \phi^\dagger \left[\Delta^\dagger, \Delta \right] \phi \quad (4.9c)$$

$$\mathcal{L}_{\phi \Delta \phi} = -\frac{\Lambda_6}{\sqrt{2}} \phi^T i \sigma_2 \Delta^\dagger \phi + \text{h.c.} \quad (4.9d)$$

$$\mathcal{L}_{\ell_L \Delta \ell_L} = -\frac{1}{\sqrt{2}} (Y_\Delta)_{fg} \ell_L^{Tf} i \sigma_2 \Delta \ell_L^g + \text{h.c.} . \quad (4.9e)$$

The Yukawa coupling between the Higgs triplet and the lepton doublets is described by a symmetric matrix Y_Δ . The Feynman rules corresponding to \mathcal{L} are given in App. A.5.

As it can be seen in Tab. 4.1, there is a third singlet in the product representation of 4 SU(2)_L triplets² in addition to the terms given in \mathcal{L}_{Δ^4} . It is formally given by

$$\mathcal{L}_{\Lambda_3} = -\frac{\Lambda_3}{2} \left(\Delta^\dagger \otimes \Delta \right)_5 \cdot \left(\Delta^\dagger \otimes \Delta \right)_5 , \quad (4.10)$$

where the subscript **5** indicates, that the 5 dimensional irrep is extracted from the Kronecker product of the two triplets which corresponds to a 3×3 matrix. The irrep **5** is embedded in the Kronecker product as the subspace of traceless symmetric matrices. Furthermore, the SU(2)_L structure of the 3 terms is different which can be seen from the Clebsch-Gordan series. Thus this term has to be added in principle. However, Λ_3 is assumed to vanish in this work. As it turns out that it can not be generated radiatively³, it will remain zero. The effect of Λ_3 and the reason, why it is not generated radiatively, has to be studied in a later work.

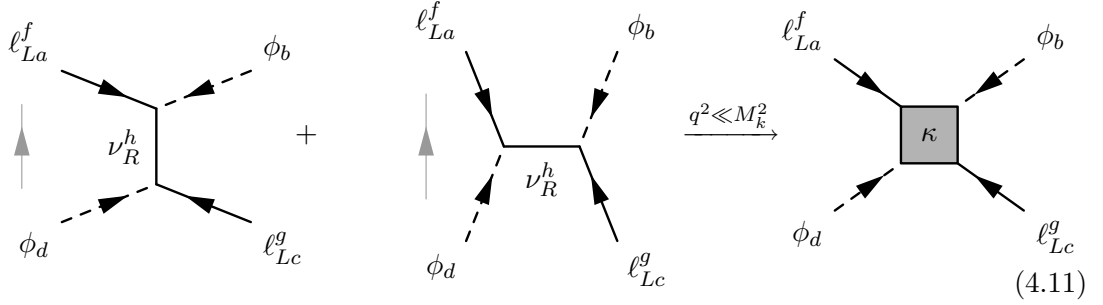
²In general, every product representation of 4 identical irreps **n** of SU(2)_L contains n singlets.

³See the result of the calculation in Sec. 7.4.4.

4.4.2 Standard See-Saw Mechanism

The standard/type-I see-saw mechanism is implemented in the framework of the SM extended by heavy right-handed neutrinos ($M = \mathcal{O}(10^{10} - 10^{16})$ GeV). This is the mass scale needed to explain neutrino masses smaller than 1 eV. In addition, the right-handed neutrinos can explain the baryon asymmetry of the universe via the leptogenesis mechanism [66,67]. In leptogenesis, the baryon asymmetry is explained by an out-of-equilibrium decay of right-handed neutrinos. This produces a lepton asymmetry which is transformed in a baryon asymmetry via sphaleron processes.

However, the current experiments are taking place at much lower energies. Thus right-handed neutrinos do not contribute to physical processes anymore. The see-saw mechanism states that they are integrated out at their mass scale and this leads to an effective operator describing the masses of the light neutrinos.



In terms of formulas, we have

$$\begin{aligned}
 & \left[-i (Y_\nu^T)_{fh} \epsilon_{ab} P_L \right] \frac{i \not{q} + i M_h}{q^2 - M_h^2 + i\epsilon} \left[-i (Y_\nu)_{hg} \epsilon_{cd}^T P_L \right] \\
 & + \left[-i (Y_\nu^T)_{fh} \epsilon_{ad} P_L \right] \frac{i \not{q} + i M_h}{q^2 - M_h^2 + i\epsilon} \left[-i (Y_\nu)_{hg} \epsilon_{cb}^T P_L \right] \\
 & \xrightarrow{q^2 \ll M_h^2} i (Y_\nu^T)_{fh} M_h^{-1} (Y_\nu)_{hg} (\epsilon_{ab} \epsilon_{cd} + \epsilon_{ad} \epsilon_{cb}) P_L . \quad (4.12)
 \end{aligned}$$

Thus the matching condition is given by

$$\kappa = 2 Y_\nu^T M^{-1} Y_\nu \quad (4.13)$$

at tree-level. As the Majorana mass of the right-handed neutrinos is assumed to be of the order of $(10^{10} - 10^{16})$ GeV and the Yukawa couplings are of the order of one, the left-handed neutrinos have a mass of $\frac{v^2}{M} \leq 1$ eV.

4.4.3 Type-II See-Saw Mechanism

In the type-II see-saw scenario, there is a Higgs triplet in addition to the right-handed neutrinos which also contributes to the effective mass matrix of the light neutrinos.

$$\left[(Y_\Delta)_{fg} (\sigma_2 \sigma_k)_{ac} \right] \frac{i}{q^2 - M_\Delta^2} [\Lambda_6 (\sigma_2 \sigma_k)_{db}] \xrightarrow{q^2 \ll M_\Delta^2} -i \frac{\Lambda_6}{M_\Delta^2} (Y_\Delta)_{fg} (\epsilon_{ab} \epsilon_{cd} + \epsilon_{ad} \epsilon_{cb}) \quad (4.14)$$

Hence, the tree-level matching condition is given by

$$\kappa = -2 \frac{Y_\Delta \Lambda_6}{M_\Delta^2}. \quad (4.15)$$

In the high-energy region of this theory, the neutrino mass matrix can be described by a 6×6 mass matrix (See Sec. 2.2.2) which has a non-vanishing entry in the upper-left 3×3 block in contrast to the matrix in Sec. 2.2.2. The upper-left block is given by the type-II contribution of the see-saw mechanism. A quasi-degenerate spectrum can be obtained naturally in the type II see-saw framework, since the triplet contribution can set the overall mass scale and the contribution of the right-handed neutrinos which is likely to be hierarchical through the hierarchy in the Yukawa matrices, determines the splitting of the masses or can be neglected altogether.

4.4.4 Thresholds

In general, the right-handed neutrinos are non-degenerate. Even if a symmetry at the GUT scale demands degeneracy of the masses, the renormalization group running will generate a splitting of the neutrino masses after the symmetry is broken. Thus, in general, there are several thresholds, at which the right-handed neutrinos are integrated out. This leads to interesting running effects which is illustrated in Fig. 4.1

In this figure, the evolution of the leptonic mixing angles is shown in a type-I see-saw scenario. The different grayish regions correspond to different EFTs. At each border, one right-handed neutrino is integrated out and the renormalization group equations change. This leads to kinks in the curves at the thresholds. Of course, the same happens at the thresholds of other particles, like the Higgs triplet. The parameters of each EFT are given in the upper part of the plot. $\overset{(n)}{M}$ is the $n \times n$ Majorana mass matrix of the right-handed neutrinos, $\overset{(n)}{Y}_\nu$ is the $n \times 3$ neutrino Yukawa matrix and $\overset{(n)}{\kappa}$ is the 3×3 effective light neutrino mass matrix. Between the thresholds, the neutrino mass matrix has two contributions. One contribution is the effective neutrino mass operator and the other is due to the right-handed neutrinos. In general, the both contributions are not simultaneously diagonalizable.

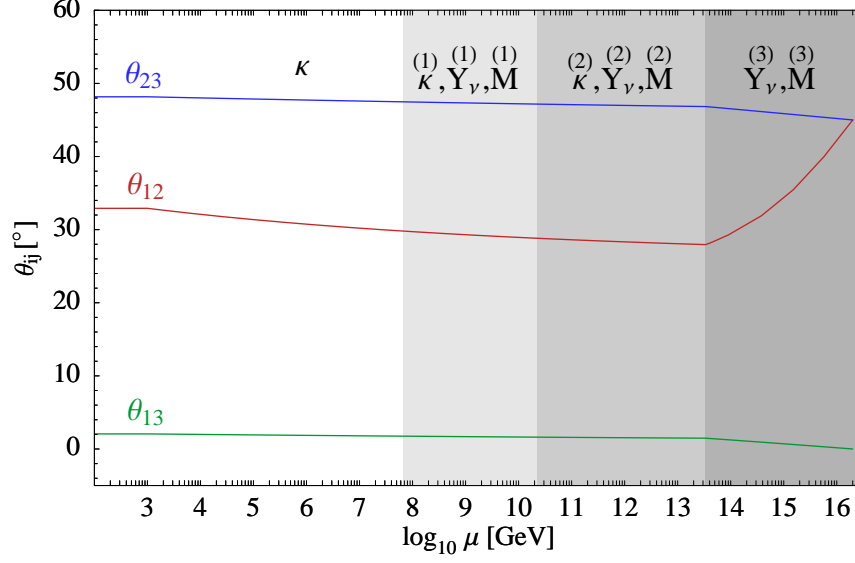


Figure 4.1: Transitions between several effective theories illustrating the evolution of the leptonic mixing angles in the case of non-degenerate right-handed neutrinos

Parameter	Best-fit	Allowed range (3σ CL)
θ_{12} [$^\circ$]	33.2	$28.7 \dots 38.1$
θ_{23} [$^\circ$]	45.0	$35.7 \dots 55.6$
θ_{13} [$^\circ$]	0.000	≤ 12.5
Δm_{21}^2 [10^{-5} eV^2]	8.1	$7.2 \dots 9.1$
$ \Delta m_{31}^2 $ [10^{-3} eV^2]	2.2	$1.4 \dots 3.3$
m_e [MeV]	$0.510998918 \pm 0.000000044$	
m_μ [MeV]	$105.6583692 \pm 0.0000094$	
m_τ [MeV]	$1776.99^{+0.29}_{-0.26}$	

Table 4.2: Experimental data in the leptonic sector taken from the Particle Data Group [18] and global fits to neutrino oscillations [64].

4.4.5 Parameterization of the See-Saw

There are several different parameterizations of the see-saw [68–70]. Today only 12 parameters are in principle accessible, since processes involving the other parameters are suppressed by the mass of the right-handed neutrinos. These 12 parameters are the masses of the charged leptons and of the neutrinos and the mixing angles and CP phases of the (P)MNS (Pontecorvo-Maki-Nakagawa-Sakata) matrix. However, only the masses of the charged leptons, the mass squared differences of the neutrinos and the angles θ_{12} and θ_{23} have already been measured. There is an upper bound on the CHOOZ angle θ_{13} only (See Tab. 4.2). The number of parameters which is needed for a given model in the leptonic Yukawa sector can be easily calculated [69]. First the parameters of the Yukawa and mass matrices are counted. Then the number of parameters of the symmetry group which is broken by the Yukawa matrices is subtracted.

$$Y_{\text{phys}} = Y - N_G + N_{G'} , \quad (4.16)$$

where Y_{phys} is the number of physical parameters in the Yukawa sector, Y is the number of parameters characterizing the Yukawa matrices and N_G and $N_{G'}$ are the number of generators of the symmetry group for vanishing Yukawa interactions and the generators of the subgroup which is unbroken by the Yukawa interactions, respectively. In the following, the number of physical parameters in the type-II see-saw model is determined as an example.

The starting point is the SM with n flavors extended by m right-handed neutrinos and one Higgs triplet. The kinetic part of the Lagrangian is given by

$$\mathcal{L}_{\text{kin}} = \overline{l}_L \not{D} l_L + \overline{e}_R \not{D} e_R + \overline{\nu}_R \not{D} \nu_R + \text{tr} \left[(D_\mu \Delta)^\dagger D^\mu \Delta \right]. \quad (4.17)$$

It is invariant under the following flavor symmetry transformation

$$l_L \rightarrow V_l l_L \quad (4.18a)$$

$$e_R \rightarrow V_e e_R \quad (4.18b)$$

$$\nu_R \rightarrow V_\nu \nu_R, \quad (4.18c)$$

where V_l and V_e are unitary $n \times n$ matrices and V_ν is a unitary $m \times m$ matrix in flavor space. Hence, the symmetry group is $U(n)_l \otimes U(n)_e \otimes U(m)_\nu$. However, this flavor symmetry is broken by the Yukawa couplings and the Majorana mass matrix. The part of the Lagrangian which is relevant for this symmetry breaking, is given by

$$\begin{aligned} \mathcal{L}_{\text{mass}} = & -\frac{1}{2} (Y_e)_{ij} \overline{l}_{Lj} \phi e_{Ri} - \frac{1}{2} (Y_\nu)_{ij} \overline{l}_{Lj}^\alpha \epsilon_{\alpha\beta} \phi^\beta \nu_{Ri} - \frac{1}{2} M_{ij} \overline{\nu}_R^C i \nu_{Rj} \\ & - \frac{1}{\sqrt{2}} (Y_\Delta)_{ij} \overline{l}_L^{Ti} i \sigma_2 \Delta \ell_L^j, \end{aligned} \quad (4.19)$$

where Y_e is the $n \times n$ Yukawa matrix for charged leptons, Y_ν is the $m \times n$ neutrino Yukawa matrix, M is the $m \times m$ Majorana mass matrix of the right-handed neutrinos and Y_Δ is the $n \times n$ Yukawa matrix for the leptonic left-handed doublet coupling to the Higgs triplet. As these matrices are not flavor diagonal, they clearly break the symmetry. However, the complete Lagrangian will be invariant under this symmetry, if the Yukawa matrices Y_e , Y_ν and Y_Δ and also M transform according to

$$(Y_e, Y_\nu, Y_\Delta, M) \rightarrow (Y'_e, Y'_\nu, Y'_\Delta, M') = \left(V_e Y_e V_l^\dagger, V_\nu Y_\nu V_l^\dagger, V_l^* Y_\Delta V_l^\dagger, V_\nu^* M V_\nu^\dagger \right). \quad (4.20)$$

As the lepton number is not conserved, all flavor symmetries are broken by the Yukawa matrices and there are

$$n^2 + nm + \frac{n(n+1)}{2} + \frac{m(m+1)}{2} - 2 \frac{n(n-1)}{2} - \frac{m(m-1)}{2} = \frac{n(n+3)}{2} + m(n+1) \quad (4.21a)$$

physical moduli and

$$n^2 + \frac{n(n+1)}{2} + \frac{m(m+1)}{2} - 2 \frac{n(n+1)}{2} - \frac{m(m+1)}{2} = \frac{n(2m+n-1)}{2} \quad (4.21b)$$

physical phases⁴. In the case of the SM extended by 3 right-handed neutrinos, there are 21 moduli and 12 phases. The same can be done as well for other extensions of the SM. The number of the parameters of different EFTs are summarized in Tab. 4.3.

⁴ Y_e is a general complex matrix. Thus it is characterized by n^2 moduli and n^2 phases. Y_Δ is described by $\frac{n(n+1)}{2}$ moduli and $\frac{n(n+1)}{2}$ phases, because it is symmetric. Unitary matrices are characterized by $\frac{n(n-1)}{2}$ moduli and $\frac{n(n+1)}{2}$ phases.

couplings	$\#\nu_R$	mod.	ph.
(Y_ν, M)	3	15	9
(Y_ν, Y_Δ, M)	3	21	12
(Y_ν, κ, M)	3	21	12
(Y_ν, κ, M)	2	17	9
(Y_ν, κ, M)	1	13	6
(κ)	n.a.	9	3

Table 4.3: Number of parameters in different see-saw models and parameterization. All models contain the charged lepton Yukawa matrix Y_e besides the given couplings. ‘mod.’ means moduli and ‘ph.’ means phases.

One parameterization is obtained by choosing Y_e and M to be diagonal. Then Y_ν and Y_Δ are described by the product of a diagonal matrix with two unitary matrices.

$$Y_\nu = U_R \text{diag}(y_1, \dots, y_n) U_L^\dagger \quad (4.22)$$

$$Y_\Delta = V^* \text{diag}(z_1, \dots, z_n) V^\dagger \quad (4.23)$$

U_L and U_R can be described by 3 angles and 3 phases each and V can be described by 3 angles and 6 phases.

The parameterization used in this thesis is the low-energy parameterization which is valid in the effective theory. The relevant parameters are the masses of the charged leptons and neutrinos and in addition the 3 angles and 3 CP phases in the MNS matrix. In the type-I see-saw scenario, the twisting matrix U_L between $Y_e^\dagger Y_e$ and $Y_\nu^\dagger Y_\nu$ is used in the discussion of the running in Sec. 6 in addition. The twisting matrix is the matrix which diagonalizes $Y_\nu^\dagger Y_\nu$ in the basis where $Y_e^\dagger Y_e$ is diagonal. Hence it is defined as

$$Y_e^\dagger Y_e = \text{diag} \quad U_L^\dagger Y_\nu^\dagger Y_\nu U_L = \text{diag} \quad (4.24)$$

Moreover, the twisting matrix U_L^Δ between $Y_e^\dagger Y_e$ and $Y_\Delta^\dagger Y_\Delta$ is used in the type-II see-saw scenario.

Chapter 5

Evolution of the Mixing Parameters and Masses

There are two different approaches to solve the renormalization group equations for the leptonic mixing parameters. On the one hand, the evolution of the mass matrices can be solved and then they are diagonalized to extract the mixing parameters. This approach is used in the numerical code [71,72]. On the other hand, the mass matrices can be diagonalized at first and then solved. The latter approach is used to derive the analytic formulae for the mixing parameters [73–77]. The neutrinos acquire their mass after electroweak symmetry breaking, but we can consider the ‘would-be’ neutrino mass above the electroweak symmetry breaking in order to compare it to the prediction of GUT models. At first, the extraction of the RGEs of the mixing parameters from the RGEs of the mass matrices is described and then it is applied to the left-handed neutrino mass matrix and the right-handed neutrino masses.

5.1 Extraction of the RGE for the Parameters from the Matrix Equations

5.1.1 Evolution of Majorana Masses

Majorana masses matrices M are symmetric. Thus the evolution of Majorana matrices is equivalent to the evolution of symmetric matrices. The β -functions are proportional to the matrix itself to 1 loop order, because the masses can be renormalized multiplicatively [59–61]. Therefore the most general form of the β -function is given by

$$16\pi^2\beta_M = P^T M + MP + \alpha M , \quad (5.1)$$

where $P = P(t)$ is an arbitrary matrix and $\alpha = \alpha(t)$ is an arbitrary complex number and the parameter t is defined as $t = \ln \mu$. However, if there are more contributions to the Majorana mass matrix, the different contributions will in general have different RGEs. Therefore, this analysis only applies to one contribution. From this equation, the evolution of the masses and mixing parameters has been derived in the papers [73–76]. At first, this equation can be turned in an equation depending on the mixing matrix U and the mass matrix in the mass basis D

$$U^T M U = \text{diag}(M_1, \dots, M_n) =: D . \quad (5.2)$$

Inserting Eq. (5.2) in Eq. (5.1) yields

$$\dot{D} = \frac{1}{16\pi^2} \left(\alpha D + P'^T D + D P' \right) - T^* D + D T, \quad (5.3)$$

where $P' := U_\nu^\dagger P U_\nu$, $T := U_\nu^\dagger \dot{U}_\nu$ and the anti-hermiticity of T was used. This matrix equation corresponds to a set of 12 equations which govern the evolution of the 3 eigenvalues and the 9 mixing parameters. The real part of the diagonal entries results in

$$\dot{M}_i = \frac{1}{16\pi^2} \left(\text{Re } \alpha + 2 \text{Re } P'_{ii} \right) M_i, \quad (5.4)$$

which are the differential equations describing the evolution of the mass eigenvalues. The 9 mixing parameters are described by the 3 equations for the imaginary diagonal entries

$$\text{Im } T_{ii} = -\frac{1}{32\pi^2} \left(\text{Im } \alpha + 2 \text{Im } P'_{ii} \right) M_i \quad (5.5)$$

and the 6 equations of the off-diagonal entries ($i \neq j$) read:

$$\text{Re } T_{ij} = -\frac{1}{16\pi^2} \frac{M_i + M_j}{M_i - M_j} \text{Re } P'_{ij} \quad (5.6)$$

$$\text{Im } T_{ij} = \frac{1}{16\pi^2} \frac{M_i - M_j}{M_i + M_j} \text{Im } P'_{ij} \quad (5.7)$$

5.1.2 Evolution of Dirac Masses

The derivation for a Dirac mass matrix is analogous. The most general form of the β -function of a hermitian matrix, which preserves the hermiticity and is proportional to the hermitian matrix itself, is given by

$$\beta_H = F^\dagger H + H F + \tilde{\alpha} H, \quad (5.8)$$

where $F = F(t)$ is an arbitrary matrix and $\tilde{\alpha} = \tilde{\alpha}(t)$ is an arbitrary complex number. Again the matrix H can be decomposed in a diagonal matrix with the eigenvalues of H on the diagonal and an unitary matrix describing the transformation of the given basis to the mass basis.

$$U_H^\dagger H U_H = \text{diag}(h_1, \dots, h_n) =: D_H \quad (5.9)$$

Inserting (5.9) in (5.8) yields

$$\dot{D}_H = \frac{1}{16\pi^2} \left(F'^\dagger D_H + D_H F' + \tilde{\alpha} D_H \right) - X D_H + D_H X, \quad (5.10)$$

where $F' = U_H^\dagger F U_H$ and $X = U_H^\dagger \dot{U}_H$. The matrix equation defines the off-diagonal entries of X and the eigenvalues of H as

$$\dot{h}_i = \frac{1}{16\pi^2} \left(2 \text{Re } F'_{ii} + \tilde{\alpha} \right) h_i \quad (5.11)$$

$$X_{ij} = \frac{1}{16\pi^2} \frac{h_j + h_i}{h_j - h_i} F'_{ij}. \quad (5.12)$$

In addition, $\text{Im } \tilde{\alpha} = 0$ has to be satisfied¹. The diagonal entries of X remain undefined. However, they only influence the unphysical phases appearing in the diagonalization of Y_e which can be absorbed in a redefinition of the fields [16, 74].

¹This is automatically satisfied in the SM, MSSM and 2HDM.

5.2 Evolution of the left-handed Majorana Neutrino Mass Matrix

As it was already noted earlier, the neutrino mass matrix is described by

$$m_\nu \stackrel{(4.4)}{=} -\frac{v^2}{4}\kappa \quad (5.13)$$

below the see-saw scales. Above and in between the see-saw scales, it is given by a combination of the effective neutrino mass operator and the see-saw formula

$$m_\nu = -\frac{v^2}{4} (\kappa + 2Y_\nu^T M^{-1} Y_\nu) . \quad (5.14)$$

Above the see-saw scales, the dimension 5 operator κ vanishes in the type-I see-saw scenario, since the only source for the neutrino mass is the contribution of the right-handed neutrinos via the type-I see-saw mechanism. However, κ will be non-zero in type-II scenarios, if the Higgs triplet is heavier than the heaviest right-handed neutrino. Thus, there are two contributions to the mass matrix which have to be treated separately. In the MSSM, the both terms have the same RGE due to the non-renormalization theorem in supersymmetric theories, but in the SM and 2HDM, the two contributions have a different flavor-diagonal contribution. This results in a changed evolution of all² parameters. This effect can even give the dominant contribution [78]. The β function for m_ν can be derived from the β functions of κ , Y_ν . In the SM, MSSM and 2HDM, the matrix P^3 , which shows up in Sec. 5.1.1, can be parameterized by

$$P := C_e Y_e^\dagger Y_e + C_\nu Y_\nu^\dagger Y_\nu \quad (5.15)$$

and α is given by

$$\alpha := \alpha_1 g_1^2 + \alpha_2 g_2^2 + \alpha_u \text{tr} Y_u^\dagger Y_u + \alpha_d \text{tr} Y_d^\dagger Y_d + \alpha_e \text{tr} Y_e^\dagger Y_e + \alpha_\nu \text{tr} Y_\nu^\dagger Y_\nu + \alpha_\lambda \lambda . \quad (5.16)$$

The coefficients in the definition of P and α in Eqs. (5.15) and (5.16) are given in Tab. 5.1.

5.3 Evolution of the charged Lepton Sector

The derivation for the evolution of the parameters in the charged lepton part is analogous. The relevant quantity is $Y_e^\dagger Y_e$ which describes the contribution to the MNS matrix and the masses of the charged leptons. The matrix F and $\tilde{\alpha}$ are defined in a similar manner to P and α and read:

$$F := D_e Y_e^\dagger Y_e + D_\nu Y_\nu^\dagger Y_\nu \quad (5.17a)$$

$$\tilde{\alpha} := \tilde{\alpha}_1 g_1^2 + \tilde{\alpha}_2 g_2^2 + \tilde{\alpha}_u \text{tr} Y_u^\dagger Y_u + \tilde{\alpha}_d \text{tr} Y_d^\dagger Y_d + \tilde{\alpha}_e \text{tr} Y_e^\dagger Y_e + \tilde{\alpha}_\nu \text{tr} Y_\nu^\dagger Y_\nu + \tilde{\alpha}_\lambda \lambda \quad (5.17b)$$

The matrix is given by $U_H = U_e$ and the coefficients of F and $\tilde{\alpha}$ are given in Tab. 5.2

²Let A and B be two arbitrary symmetric matrices. If $U^T(A+B)U$ is diagonal, $U^T(aA+bB)U$ will be in general not diagonal. In general, it will be only diagonal, if there is common scaling ($a=b$) [16].

³In the type-I see-saw, this is the most general form to 1 loop order, since the only flavor-non-diagonal contribution comes from the coupling to the charged leptons via the Yukawa term. All other contributions are flavor-diagonal. In type-II see-saw models, there is an additional contribution from the coupling of the left-handed lepton doublet to the Higgs triplet.

Model	contrib.	C_e	C_ν	α_1	α_2	α_u	α_d	α_e	α_ν	λ
SM	κ	$-\frac{3}{2}$	$\frac{1}{2}$	0	-3	6	6	2	2	1
SM	$2Y_\nu^T M^{-1} Y_\nu$	$-\frac{3}{2}$	$\frac{1}{2}$	$-\frac{9}{10}$	$-\frac{9}{2}$	6	6	2	2	0
MSSM	κ	1	1	$-\frac{6}{5}$	-6	6	0	0	2	0
MSSM	$2Y_\nu^T M^{-1} Y_\nu$	1	1	$-\frac{6}{5}$	-6	6	0	0	2	0

Table 5.1: Coefficients for the evolution of the neutrino mass. In the case of the effective theory, $C_\nu = 0$ and $\alpha_\nu = 0$.

Model	D_e	D_ν	$\tilde{\alpha}_1$	$\tilde{\alpha}_2$	$\tilde{\alpha}_u$	$\tilde{\alpha}_d$	$\tilde{\alpha}_e$	$\tilde{\alpha}_\nu$	λ
SM	$-\frac{3}{2}$	$-\frac{3}{2}$	$-\frac{9}{2}$	$-\frac{9}{2}$	6	6	2	2	0
MSSM	3	1	$-\frac{18}{5}$	-6	0	6	2	0	0

Table 5.2: Coefficients for the evolution of the charged leptons. In the case of the effective theory, $D_\nu = 0$ and $\tilde{\alpha}_\nu = 0$.

5.4 Evolution of the left-handed Leptonic Mixing Parameters

The evolution of the MNS matrix $U = U_e^\dagger U_\nu$ is described by

$$U^\dagger \dot{U} = \dot{U}_e^\dagger U_\nu + U_e^\dagger \dot{U}_\nu = T - U^\dagger X U . \quad (5.18)$$

So far, no basis was specified. The equations are valid in every chosen basis. However, the calculation considerably simplifies in the basis where $Y_e^\dagger Y_e$ is diagonal, because the matrices T and X can be calculated in terms of the mixing parameters describing the MNS matrix. As the charged leptons are strongly hierarchical, the contribution of the charged lepton part is negligible compared to the contribution of the neutrinos for the evolution of the mixing angles and phases. However, in the case of a hierarchical neutrino mass spectrum, both contributions are of the same order. In the following, we neglect the contribution from the charged leptons, i.e. we set $X=0$. The contributions are treated in [16]. In this basis, P can be expressed by the eigenvalues of $Y_e^\dagger Y_e$ and $Y_\nu^\dagger Y_\nu$ in addition to the mixing parameters describing the twisting matrix U_L .

$$P = C_e \text{diag} (y_e^2, y_\mu^2, y_\tau^2) + C_\nu U_L \text{diag} (y_1^2, y_2^2, y_3^2) U_L^\dagger \quad (5.19)$$

This shows that the renormalization group equations of the mixing parameters are basis-independent despite the fact that they are derived in a specific basis. As it can be seen in Eq. (5.19), the phases in the off-diagonal entries of P can be traded against the unphysical phases. Indeed, the unphysical phases do not decouple from the physical phases in the renormalization group equations. Thus, they will become non-zero, even if they vanish at the GUT scale and they will contribute to the running of the physical parameters. Thus the ‘unphysical’ phases are not unphysical. The analytic formulae are given in the basis where all unphysical phases vanish. The same considerations apply for F . Thus the resulting equations are still basis-independent, despite the calculation in the basis where $Y_e^\dagger Y_e$ is diagonal.

The differential equations governing the parameters which are given in the tables in App. D, are expanded in the small CHOOZ angle θ_{13} and the limits $y_e \rightarrow 0, y_\mu \rightarrow 0$ are taken.

5.5 Evolution of the right-handed Neutrino Masses

The same technique can also be used for the right-handed neutrino sector, because the two matrices describing the right-handed neutrinos are the right-handed Majorana mass matrix M and the hermitian matrix $Y_\nu Y_\nu^\dagger$.

The matrix P in Sec. 5.1.1 equals $C_r Y_\nu Y_\nu^\dagger$ where $C_r = 2$ for the MSSM and $C_r = 1$ for the SM and 2HDM, and α vanishes for the right-handed neutrinos. Thus the running of the right-handed neutrino masses is described by

$$\dot{M}_i = \frac{2}{16\pi^2} \text{Re}(P_{ii}) M_i, \quad (5.20)$$

where P is given in the mass basis of the right-handed neutrinos. It can be seen, that there are no large renormalization group effects for the right-handed neutrino masses, because the Yukawa couplings are of the order of one. Thus the running can be estimated to

$$\frac{\dot{M}_i}{M_i} = \frac{C_r}{8\pi^2} \sum_j |(Y_\nu)_{ij}|^2 \approx 0.007 C_r \mathcal{O}(1) \ll 1. \quad (5.21)$$

The RGE for M_i is solved analytically by

$$M_i(t) = M_i(t_0) e^{\frac{C_r}{8\pi^2} \int_{t_0}^t dt' \sum_j |(Y_\nu(t'))_{ij}|^2}, \quad (5.22)$$

where $M_i(t_0) \leq e^{t_0} = \mu_0$, in order that the equation is reasonable, i.e. the mass of the right-handed neutrinos is lighter than μ_0 and they can still become on-shell. From this equation, the threshold M_i^t where the right-handed neutrinos are integrated out⁴, can be calculated by requiring $M_i(M_i^t) = M_i^t$. This yields

$$M_i^t = M_i(\mu_0) \left(\frac{M_i^t}{\mu_0} \right)^{\frac{C_r}{8\pi^2} \sum_j |(Y_\nu(\tilde{\mu}))_{ij}|^2}, \quad (5.23)$$

where the mean value theorem for integrals was used which determines $\tilde{\mu}$ and $M_i^t \leq \tilde{\mu} \leq \mu_0$. Solving Eq. (5.23) for M_i^t yields

$$M_i^t = M_i(\mu_0)^{\frac{1}{1-\xi}} \mu_0^{\frac{\xi}{\xi-1}} \xrightarrow{\xi \ll 1} M_i(\mu_0) \left(\frac{M_i(\mu_0)}{\mu_0} \right)^\xi \quad (5.24)$$

for $\xi \neq 1$ where ξ is defined as $\frac{C_r}{8\pi^2} \sum_j |(Y_\nu(\tilde{\mu}))_{ij}|^2$. In the case of $\xi = 1$, Eq. (5.23) is solved by $M_i^t = \mu_0$. For degenerate right-handed neutrino masses, the degeneracy will only persist, if the neutrino Yukawa couplings satisfy

$$\sum_j |(Y_\nu(t))_{ij}|^2 = \sum_j |(Y_\nu(t))_{1j}|^2 \quad \forall i \forall t. \quad (5.25)$$

⁴Possible threshold corrections are neglected.

However, in general, the degeneracy is lifted. In particular, if there is a strong hierarchy in Y_ν as it is suggested by GUT models, $(Y_\nu)_{33} \gg (Y_\nu)_{22} \gg (Y_\nu)_{11}$, the mass M_3 runs strongest. If it is further assumed, that $\sum_j |(Y_\nu)_{ij}|^2$ does not run very fast, ξ can be approximated by $\frac{C_r y_i^2}{8\pi^2}$, the value at the GUT scale, and the thresholds of the right-handed neutrinos is given by

$$M_i^t = M(\Lambda_{\text{GUT}}) \left(\frac{M(\Lambda_{\text{GUT}})}{\Lambda_{\text{GUT}}} \right)^{\frac{C_r y_i^2}{8\pi^2}}. \quad (5.26)$$

Therefore the right-handed neutrinos have an inverted hierarchy

$$M_3 < M_2 < M_1 \quad (5.27)$$

and the splitting of the thresholds of the right-handed neutrinos which are degenerate at the GUT scale, is given by

$$M_i^t - M_j^t = M \left[\left(\frac{M}{\Lambda_{\text{GUT}}} \right)^{\frac{C_r y_i^2}{8\pi^2}} - \left(\frac{M}{\Lambda_{\text{GUT}}} \right)^{\frac{C_r y_j^2}{8\pi^2}} \right]. \quad (5.28)$$

Thus a stronger hierarchy in Y_ν yields a larger splitting of the right-handed neutrino masses. Recently, resonant leptogenesis [16, 79] has been discussed where this splitting is of the order of the decay width of the right-handed neutrinos. This results in an enhancement of the lepton asymmetry. In the resonant leptogenesis scenario, the renormalization group effects are important, because even small changes in the right-handed neutrino mass can violate the resonance condition.

Chapter 6

RG Evolution in type-I See-Saw Models

6.1 Summary of the Evolution in the Effective Theory

The running of the mixing parameters can be described by simple analytic formulae [75] which show the same analytic structure

$$\mu \frac{d\theta_{ij}}{d\mu}, \mu \frac{d\delta}{d\mu}, \mu \frac{d\varphi_i}{d\mu} \propto \sum_k \frac{f_k(\text{masses}, \delta, \varphi_1, \varphi_2)}{m_j^2 - m_i^2} \times F_k^{(ij)}(\text{Yukawa couplings}, \theta_{12}, \theta_{13}, \theta_{23}) . \quad (6.1)$$

In contrast to the quark sector, there will be strong running in the leptonic sector, if the neutrino masses are quasi-degenerate. This is due to the mass squared differences in the denominator of each term. Another reason for the strong running are the large mixing angles of the MNS matrix, because the slope of the angles is proportional to the sine of the angle. This results in a fixed point for zero mixing. In the MSSM, the running is also enhanced by a large value of $\tan \beta$, since the evolution is proportional to y_τ^2 . Non-zero phases generally damp the running and the phase difference will tend to decrease, if the parameters are run down from a high scale. θ_{12} increases for $\theta_{13} = 0$ while running the parameters down. These results which are valid in the effective theory below the see-saw scales change above the lightest right-handed neutrino.

6.2 General Considerations about the Evolution

The same structure as in Eq. (6.1) also holds above and in between the see-saw scales, but the formulae become more complicated, because $P = C_\nu Y_\nu^\dagger Y_\nu + C_e Y_e^\dagger Y_e$ is not diagonal. Therefore, off-diagonal entries contribute to the running and the evolution gets more interesting, but often there are only a few dominant contributions from the different matrix elements of P . Moreover, the contribution from $Y_\nu^\dagger Y_\nu$ does not strongly depend on $\tan \beta$ in the MSSM, because the neutrino mass is proportional to $\sin^2 \beta = \frac{\tan^2 \beta}{1 + \tan^2 \beta}$. Hence, the contribution from $Y_\nu^\dagger Y_\nu$ dominates for small $\tan \beta$. In between the see-saw scales, the neutrino mass matrix consists of 2 contributions which, in general, differently transform under the renormalization group which was stated in Sec. 5.2. The following discussion applies for one contribution, as it is the case above the see-saw scales and in the MSSM between the see-saw scales, too. In the case of 2 contribution, there will be additional effects if the terms are of the same order.

6.2.1 Different Contributions from P

The matrix P can be written in a basis independent way:

$$P = C_e \text{diag}(y_e^2, y_\mu^2, y_\tau^2) + C_\nu U_L \text{diag}(y_1^2, y_2^2, y_3^2) U_L^\dagger. \quad (5.19)$$

Furthermore, this equation can be rewritten in a way, that the dominant parts are obvious. The charged lepton masses show a strong hierarchy and it is suggested by GUT models that the eigenvalues of $Y_\nu^\dagger Y_\nu$ are hierarchical, too.

$$P = C_e y_\tau^2 \left[\text{diag}(0, 0, 1) + \text{diag} \left(\frac{y_e^2}{y_\tau^2}, \frac{y_\mu^2}{y_\tau^2}, 0 \right) \right] + C_\nu y_3^2 \left[(U_{Li3} U_{Lj3}^*)_{i,j=1,2,3} + U_L \text{diag} \left(\frac{y_1^2}{y_3^2}, \frac{y_2^2}{y_3^2}, 0 \right) U_L^\dagger \right] \quad (6.2)$$

The first term for the charged lepton part and the neutrino part, respectively, dominate and the remaining two terms can be neglected for almost all cases. In this approximation, the main contribution is from the term proportional to P_{33} . However, a large twisting can generate other large entries, too. The Majorana phases φ_1 and φ_2 do not contribute in this approximation. The contribution from $Y_\nu^\dagger Y_\nu$ depends on the twist between $Y_e^\dagger Y_e$ and $Y_\nu^\dagger Y_\nu$. For $Y_\nu \sim Y_u$, the twisting matrix is $U_L = V_{\text{CKM}}^\dagger$. Thus U_L is close to the identity matrix. Another possibility is $Y_\nu \sim Y_e$, then there is no twist and $U_L = \mathbb{1}_{3 \times 3}$. Therefore, it is reasonable to assume, that U_L is the identity matrix, because in either case, the angles are small, i.e. U_L is close to the identity. In this approximation, P simplifies further to

$$P = (C_e y_\tau^2 + C_\nu y_3^2) \text{diag}(0, 0, 1). \quad (6.3)$$

Thus the only additional effect above the see-saw scales is the enhancement of the running. The renormalization group equations for the parameters which do not show large RG effects, can be approximated analytically. Special care has to be taken for the evolution of θ_{12} and Δm_{sol}^2 , since their running does not yield a simple rescaling.

In the case of quasi-degenerate eigenvalues of $Y_\nu^\dagger Y_\nu$, the evolution of the mixing parameters is proportional to the parameter characterizing the deviation from degeneracy. This is due to the fact, that real flavor-diagonal parts only contribute to the evolution of the masses.

$$P = C_e y_\tau^2 \left[\text{diag}(0, 0, 1) + \text{diag} \left(\frac{y_e^2}{y_\tau^2}, \frac{y_\mu^2}{y_\tau^2}, 0 \right) \right] + C_\nu y_3^2 \left[\mathbb{1} + U_L \text{diag} \left(\frac{y_1^2 - y_3^2}{y_3^2}, \frac{y_2^2 - y_3^2}{y_3^2}, 0 \right) U_L^\dagger \right] \quad (6.4)$$

Hence, there is no contribution from the neutrino Yukawa couplings to the evolution of the mixing parameters in the approximation of a degenerate spectrum and it is the same as below the see-saw scales besides the contribution to the running of the mass eigenvalues. A complete degeneracy of the neutrino Yukawa couplings means, that the contribution of the right-handed neutrinos is flavor-diagonal and therefore, there is no evolution of the mixing parameters.

	$\dot{\theta}_{12}$			$\dot{\theta}_{13}$			$\dot{\theta}_{23}$		
	d.	n.h.	i.h.	d.	n.h.	i.h.	d.	n.h.	i.h.
P_{11}	$\frac{m^2}{\Delta m_{\text{sol}}^2}$	1	ζ^{-1}	$\mathcal{O}(\theta_{13})$	$\mathcal{O}(\theta_{13})$	$\mathcal{O}(\theta_{13})$	$\mathcal{O}(\theta_{13})$	$\mathcal{O}(\theta_{13})$	$\mathcal{O}(\theta_{13})$
P_{22}	$\frac{m^2}{\Delta m_{\text{sol}}^2}$	1	ζ^{-1}	$\frac{m^2}{\Delta m_{\text{atm}}^2}$	$\sqrt{\zeta}$	$\mathcal{O}(\theta_{13})$	$\frac{m^2}{\Delta m_{\text{atm}}^2}$	1	1
P_{33}	$\frac{m^2}{\Delta m_{\text{sol}}^2}$	1	ζ^{-1}	$\frac{m^2}{\Delta m_{\text{atm}}^2}$	$\sqrt{\zeta}$	$\mathcal{O}(\theta_{13})$	$\frac{m^2}{\Delta m_{\text{atm}}^2}$	1	1
$\text{Re } P_{21}$	$\frac{m^2}{\Delta m_{\text{sol}}^2}$	1	ζ^{-1}	$\frac{m^2}{\Delta m_{\text{atm}}^2}$	1	1	$\frac{m^2}{\Delta m_{\text{atm}}^2}$	$\sqrt{\zeta}$	$\mathcal{O}(\theta_{13})$
$\text{Re } P_{31}$	$\frac{m^2}{\Delta m_{\text{sol}}^2}$	1	ζ^{-1}	$\frac{m^2}{\Delta m_{\text{atm}}^2}$	1	1	$\frac{m^2}{\Delta m_{\text{atm}}^2}$	$\sqrt{\zeta}$	$\mathcal{O}(\theta_{13})$
$\text{Re } P_{32}$	$\frac{m^2}{\Delta m_{\text{sol}}^2}$	1	ζ^{-1}	$\frac{m^2}{\Delta m_{\text{atm}}^2}$	$\sqrt{\zeta}$	$\mathcal{O}(\theta_{13})$	$\frac{m^2}{\Delta m_{\text{atm}}^2}$	1	1
$\text{Im } P_{21}$	$\frac{m^2}{\Delta m_{\text{sol}}^2}$	$\mathcal{O}(\theta_{13})$	ζ^{-1}	$\frac{m^2}{\Delta m_{\text{atm}}^2}$	1	1	$\frac{m^2}{\Delta m_{\text{atm}}^2}$	$\sqrt{\zeta}$	$\mathcal{O}(\theta_{13})$
$\text{Im } P_{31}$	$\frac{m^2}{\Delta m_{\text{sol}}^2}$	$\mathcal{O}(\theta_{13})$	ζ^{-1}	$\frac{m^2}{\Delta m_{\text{atm}}^2}$	1	1	$\frac{m^2}{\Delta m_{\text{atm}}^2}$	$\sqrt{\zeta}$	$\mathcal{O}(\theta_{13})$
$\text{Im } P_{32}$	$\mathcal{O}(\theta_{13})$	$\mathcal{O}(\theta_{13})$	$\mathcal{O}(\theta_{13})$	$\frac{m^2}{\Delta m_{\text{atm}}^2}$	$\sqrt{\zeta}$	$\mathcal{O}(\theta_{13})$	$\frac{m^2}{\Delta m_{\text{atm}}^2}$	$\sqrt{\zeta}$	$\mathcal{O}(\theta_{13})$

Table 6.1: Generic enhancement and suppression factors for the evolution of the angles, yielding an estimate of the size of the RG effect. The table entries correspond to the terms in the mixing parameter RGEs with the coefficient given by the first column. A ‘1’ indicates that there is no generic enhancement or suppression. ‘d.’ stands for a degenerate neutrino mass spectrum, i.e. $\Delta m_{\text{atm}}^2 \ll m_1^2 \sim m_2^2 \sim m_3^2 \sim m^2$. ‘n.h.’ denotes a normally hierarchical spectrum, i.e. $m_1 \ll m_2 \ll m_3$, and ‘i.h.’ means an inverted hierarchy, i.e. $m_3 \ll m_1 \lesssim m_2$.

6.2.2 Size of the RG Effect

The equations for the angles and phases have the same general form as below the see-saw scales:

$$\mu \frac{d\theta_{ij}}{d\mu}, \mu \frac{d\delta}{d\mu}, \mu \frac{d\varphi_i}{d\mu} \propto \sum_k \frac{f_k(\text{masses}, \delta, \varphi_1, \varphi_2)}{m_j^2 - m_i^2} \times F_k^{(ij)}(\text{Yukawa couplings}, \theta_{12}, \theta_{13}, \theta_{23}). \quad (6.5)$$

Thus, the maximum of the contribution is governed by a function of the masses and phases over the mass squared difference corresponding to the involved neutrinos. However, as there are more contributions above the see-saw scales, the different contributions may cancel. The coefficients which determine the size are abbreviated and summarized in Tab. D.1.

As the maximum of the coefficient is mainly determined by the mass squared difference in the denominator, the coefficients \mathcal{Q}_{12}^\pm , \mathcal{S}_{12} , \mathcal{C}_{13}^{12} and \mathcal{C}_{23}^{12} are generically larger. Non-zero phases can damp the running for \mathcal{Q}_{ij}^\pm , \mathcal{A}_{ij}^\pm and \mathcal{D}_2 and increase the running for \mathcal{S}_{ij} , \mathcal{B}_{ij}^\pm , \mathcal{C}_{ij}^{kl} and \mathcal{D}_1 . Below the see-saw scales, the Majorana phases generally damp the running.

6.3 Evolution of the Angles

The evolution of θ_{12} will be strongly affected by the renormalization group unless there are cancellations between the different dominant contributions because of the proportionality to \mathcal{Q}_{12}^+ and \mathcal{S}_{12} , respectively, which are generically large. The contributions of the real parts of P are proportional to \mathcal{Q}_{12}^+ and thus they are damped for large Majorana phase differences. On the other hand, the contributions of the imaginary parts are proportional to \mathcal{S}_{12} and

thus they are enlarged by an increasing phase difference. The term proportional to $\text{Im } P_{32}$ is an exception, since it is proportional to $\sin \theta_{13}$. In the case of a strong normal hierarchy, there is no enhancement. However, in the case of a moderate normal hierarchy ($\Delta m_{\text{sol}}^2 < m_1^2 \ll \Delta m_{\text{atm}}^2$), the RG effect is proportional to $\frac{m_1^2}{\Delta m_{\text{sol}}^2}$, as it is for an inverted hierarchy where the evolution of θ_{12} is generically enhanced by ζ^{-1} which is the ratio of the mass squared differences $\zeta = \frac{\Delta m_{\text{sol}}^2}{\Delta m_{\text{atm}}^2}$. Thus, there is a large RG effect for a degenerate spectrum and an inverted hierarchy and a small effect for a normal hierarchy. The radiative generation of θ_{12} is possible by the terms proportional to P_{21} and P_{31} whereby the generation by P_{31} is only possible if $\theta_{23} > 0$.

Recently, the observation of the relation

$$\theta_{12} + \theta_c = \frac{\pi}{4} \quad (6.6)$$

in the experimental data was discussed [80–83]. However, this quark-lepton complementarity (QLC) relation is expected to be a symmetry at the scale of quark-lepton unification which is at the scale of $\mathcal{O}(10^{13} - 10^{15})$ GeV in the Pati-Salam model [22] or at the GUT scale ($\mathcal{O}(10^{16})$ GeV). Thus it must be expected, that the QLC relation is changed by the renormalization group [82], especially, because the RG effect on θ_{12} is generically large. If this symmetry is realized, it will impose constraints on the parameters influencing the RG evolution, in order to suppress the RG effect that the symmetry is compatible with the experimental data. Conditions for a small RG effect on θ_{12} can be read off from Tab. D.2. Especially, the term proportional to P_{33} is relevant, because it describes the evolution in the effective theory. These conditions are a hierarchical mass spectrum of the neutrinos, opposite CP parity of the masses m_1 and m_2 and a small value of $\tan \beta$ in the MSSM. This is illustrated in Figs. 6.1(a), 6.1(b) and 6.1(c) which show the region in parameter space compatible with QLC realized at the GUT scale for diagonal Y_ν with a normal hierarchy. The angles are fixed and the other parameters are varied in the given ranges. In the plots, the region which is compatible with QLC is the enveloping of the dots. In Fig. 6.1(a), the dependence on $\tan \beta$ and the absolute neutrino mass scale are shown. Small values of $\tan \beta$ and a strong hierarchy are compatible with QLC. For quasi-degenerate neutrino masses, the RG effect on θ_{12} is too large that QLC can be realized, unless $\tan \beta$ is small. In Fig. 6.1(b), the dependence on the Majorana phase difference is shown. An opposite CP parity of the masses damps the running. Hence, the parameter region compatible with QLC shows a bulge near a Majorana phase difference of π . In Fig. 6.1(c), the dependence on the RG effect above the lightest right-handed neutrino is illustrated. Large neutrino Yukawa couplings enhance the running of θ_{12} in the same way as large values of $\tan \beta$. Hence, QLC can not be realized for large neutrino Yukawa couplings and quasi-degenerate neutrino masses. The QLC relation is not affected by the hierarchy in Y_ν , because the contribution from the neutrino Yukawa couplings to the evolution of the mixing parameters cancels in the degenerate case. In particular, the QLC relation can be realized in the limit of vanishing m_1 for almost all parameter values, because the RG change of θ_{12} can be estimated to $\Delta \theta_{12} \leq \frac{1}{64\pi^2} \ln \frac{\Lambda_{\text{GUT}}}{\Lambda_{\text{EW}}} \approx 0.023$. Thus, experiments would have to determine θ_{12} with an accuracy better than 0.5% to test the QLC relation.

The running of θ_{23} is generically smaller as the running of θ_{12} , because all contributions are proportional to some linear combination of either \mathcal{Q}_{13}^+ and \mathcal{Q}_{23}^+ or \mathcal{S}_{13} and \mathcal{S}_{23} , i.e. proportional to $\frac{m^2}{\Delta m_{\text{atm}}^2}$. The main contributions to the running come from P_{22} , P_{33} and P_{32} . The contributions of the terms proportional to P_{21} and P_{31} are smaller, since they are proportional

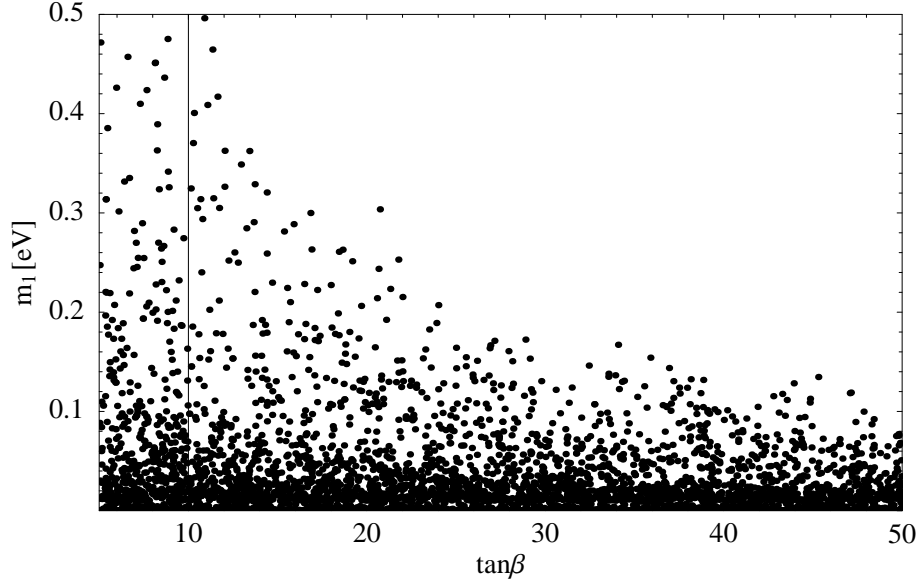
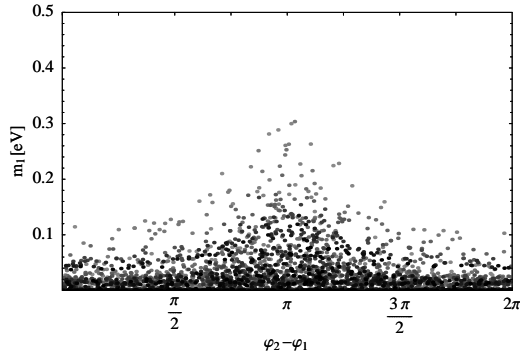
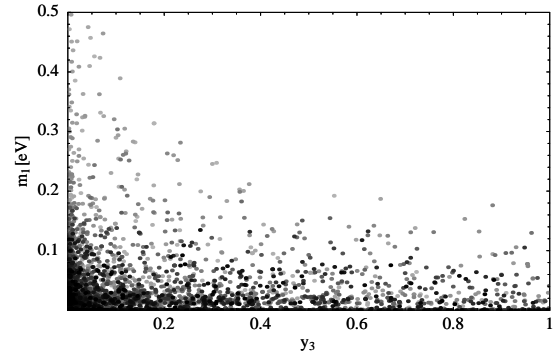
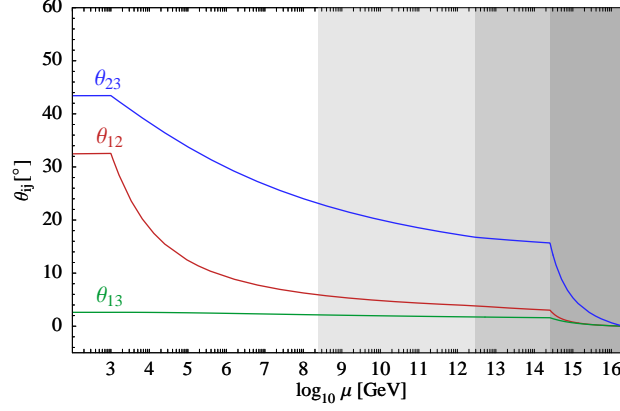
(a) Dependence of the QLC relation on $\tan \beta$.(b) Dependence of the QLC relation on the Majorana phase difference. The different gray levels of the dots correspond to different values of $\tan \beta \in (15, 50)$. Darker dots correspond to larger values of $\tan \beta$.(c) Dependence of the QLC on the strength of the neutrino Yukawa couplings. The different gray levels of the dots correspond to different values of $\tan \beta \in (5, 50)$. Darker dots correspond to larger values of $\tan \beta$.

Figure 6.1: Scatters plot indicating the parameter region which is compatible with QLC. All plots show the dependence on the neutrino mass hierarchy which is described by the lightest neutrino mass. The parameters at the GUT scale are: $\theta_{12} + \theta_e = \frac{\pi}{4}$, $\theta_{13} = 0$, $\theta_{23} = \frac{\pi}{4}$, $\delta, \varphi_i \in [0, 2\pi)$, $m_1 \in [10^{-10}, 0.5]$ eV, $\Delta m_{\text{sol}}^2 \in [5 \cdot 10^{-5}, 5 \cdot 10^{-4}]$ eV², $\Delta m_{\text{atm}}^2 \in [1.5 \cdot 10^{-3}, 6 \cdot 10^{-3}]$ eV², $y_3 \in [10^{-3}, 1]$, $\frac{y_2}{y_3} = \frac{y_1}{y_2} \in [10^{-2}, 1]$ and $\tan \beta \in [5, 50]$.

Figure 6.2: This is an example for the evolution from zero mixing to the LMA solution. The initial values are given by: $m_1 = 0.1 \text{ eV}$, $\Delta m_{\text{atm}}^2 = 1.33 \cdot 10^{-3} \text{ eV}^2$, $\Delta m_{\text{sol}}^2 = 1.05 \cdot 10^{-4} \text{ eV}^2$ and $\tan \beta = 5$.



to the difference of two almost equal coefficients. In the case of a strong normal hierarchy, there is no enhancement, as well as in the case of an inverted hierarchy. This can be seen in Tab. 6.1. Only in the case of a degenerate spectrum, a large RG effect can be expected. It is possible to generate θ_{23} radiatively by non-zero P_{32} and P_{31} entries, too. The contributions from P_{31} will only be possible, if $\theta_{12} > 0$ and the imaginary parts require non-zero phases. There are no large RG effects on θ_{13} , because the running is proportional to $\frac{m^2}{\Delta m_{\text{atm}}^2}$, too. The main contributions to θ_{13} are from the off-diagonal terms P_{21} and P_{31} , because all other terms are proportional to differences of the abbreviations which are defined in Tab. 6.3. Only for a degenerate spectrum, there are sizable RG effects. Contrariwise, the generic enhancement factors are close to unity. The radiative generation of θ_{13} is possible.

Zero mixing is a fixed point below the see-saw scales [75], because the evolution of the mixing angles is proportional to the sine of the specific angle. However, above and between the see-saw scales, there are off-diagonal entries in P whose contribution are non-zero for zero mixing. Hence, zero mixing is not a fixed point any longer. This is illustrated in Fig. 6.2. However, this is just an example that zero mixing is not a fixed point above the see-saw scales, because the choice of the neutrino Yukawa matrix Y_ν is rather special:

$$Y_\nu = \begin{pmatrix} 0.001 & 0.0001 & -0.01 \\ 0.0001 & 0.1 & 0.01 \\ -0.01 & 0.1 & 1 \end{pmatrix}. \quad (6.7)$$

The enhancement factors of the contributions proportional to P_{ij} are given in Tab. 6.1.

6.4 Evolution of the Phases

The CP phases show a fast running in general. The corresponding generic enhancement and suppression factors are given in Tab. 6.2. As for the RGE of the Dirac phase δ , there is always a term proportional to θ_{13}^{-1} which is further enhanced for a degenerate spectrum. This implies that the running of δ is in general significant for small θ_{13} , irrespectively of the hierarchy¹. For $\theta_{13} = 0$, δ and $\dot{\delta}$ are undefined. However, it is possible to define an analytic

¹Note, however, that in measurable quantities δ appears always in combination with $\sin \theta_{13}$, so that the RG change of predictions for experiments may not be significant.

	$\dot{\varphi}_i$			$\dot{\delta}$		
	d.	n.h.	i.h.	d.	n.h.	i.h.
P_{11}	$\frac{m^2}{\Delta m_{\text{sol}}^2}$	$\mathcal{O}(\theta_{13})$	ζ^{-1}	$\frac{m^2}{\Delta m_{\text{sol}}^2}$	$\sqrt{\zeta}$	ζ^{-1}
P_{22}	$\frac{m^2}{\Delta m_{\text{sol}}^2}$	$\sqrt{\zeta}$	ζ^{-1}	$\frac{m^2}{\Delta m_{\text{atm}}^2}\theta_{13}^{-1} + \frac{m^2}{\Delta m_{\text{sol}}^2}$	$\sqrt{\zeta}\theta_{13}^{-1}$	ζ^{-1}
P_{33}	$\frac{m^2}{\Delta m_{\text{sol}}^2}$	$\sqrt{\zeta}$	ζ^{-1}	$\frac{m^2}{\Delta m_{\text{atm}}^2}\theta_{13}^{-1} + \frac{m^2}{\Delta m_{\text{sol}}^2}$	$\sqrt{\zeta}\theta_{13}^{-1}$	ζ^{-1}
$\text{Re } P_{21}$	$\frac{m^2}{\Delta m_{\text{sol}}^2}$	$\sqrt{\zeta}$	ζ^{-1}	$\frac{m^2}{\Delta m_{\text{atm}}^2}\theta_{13}^{-1} + \frac{m^2}{\Delta m_{\text{sol}}^2}$	θ_{13}^{-1}	$\theta_{13}^{-1} + \zeta^{-1}$
$\text{Re } P_{31}$	$\frac{m^2}{\Delta m_{\text{sol}}^2}$	$\sqrt{\zeta}$	ζ^{-1}	$\frac{m^2}{\Delta m_{\text{atm}}^2}\theta_{13}^{-1} + \frac{m^2}{\Delta m_{\text{sol}}^2}$	θ_{13}^{-1}	$\theta_{13}^{-1} + \zeta^{-1}$
$\text{Re } P_{32}$	$\frac{m^2}{\Delta m_{\text{sol}}^2}$	$\sqrt{\zeta}$	ζ^{-1}	$\frac{m^2}{\Delta m_{\text{atm}}^2}\theta_{13}^{-1} + \frac{m^2}{\Delta m_{\text{sol}}^2}$	$\sqrt{\zeta}\theta_{13}^{-1}$	ζ^{-1}
$\text{Im } P_{21}$	$\frac{m^2}{\Delta m_{\text{sol}}^2}$	1	ζ^{-1}	$\frac{m^2}{\Delta m_{\text{atm}}^2}\theta_{13}^{-1} + \frac{m^2}{\Delta m_{\text{sol}}^2}$	θ_{13}^{-1}	$\theta_{13}^{-1} + \zeta^{-1}$
$\text{Im } P_{31}$	$\frac{m^2}{\Delta m_{\text{sol}}^2}$	1	ζ^{-1}	$\frac{m^2}{\Delta m_{\text{atm}}^2}\theta_{13}^{-1} + \frac{m^2}{\Delta m_{\text{sol}}^2}$	θ_{13}^{-1}	$\theta_{13}^{-1} + \zeta^{-1}$
$\text{Im } P_{32}$	$\frac{m^2}{\Delta m_{\text{atm}}^2}$	1	1	$\frac{m^2}{\Delta m_{\text{atm}}^2}\theta_{13}^{-1} + \frac{m^2}{\Delta m_{\text{atm}}^2}$	$\sqrt{\zeta}\theta_{13}^{-1}$	ζ^{-1}

Table 6.2: Generic enhancement and suppression factors for the evolution of the CP phases, yielding an estimate of the size of the RG effect. The table entries correspond to the terms in the mixing parameter RGEs with the coefficient given by the first column. A ‘1’ indicates that there is no generic enhancement or suppression. ‘d.’ denotes a degenerate neutrino mass spectrum, i.e. $\Delta m_{\text{atm}}^2 \ll m_1^2 \sim m_2^2 \sim m_3^2 \sim m^2$. ‘n.h.’ denotes a normally hierarchical mass spectrum, i.e. $m_1 \ll m_2 \ll m_3$, and ‘i.h.’ means an inverted hierarchy, i.e. $m_3 \ll m_1 \lesssim m_2$.

continuation yielding a smooth evolution [75]. In addition, for the degenerate or inverted hierarchical spectrum, the running of δ gets enhanced by terms proportional to $m^2/\Delta m_{\text{sol}}^2$ or ζ^{-1} , respectively. The coefficients of P_{fg} in $\dot{\delta}$ are given in Tab. D.3, from where one obtains the RGE as $\dot{\delta} = \theta_{13}^{-1}\dot{\delta}^{(-1)} + \dot{\delta}^{(0)} + \mathcal{O}(\theta_{13})$.

The situation is similar for the Majorana phases. By the same reasoning as for the running of the solar angle, the generic RG effects are large for degenerate masses and for an inverted hierarchy, while they are suppressed for a strong normal hierarchy. The coefficients of P_{fg} in $\dot{\varphi}_i$ are given in Tab. D.4.

The evolution of the Majorana phase difference is governed by a simple equation which can be read off from Tab. 6.3. It indicates strong running, since the slope is still inversely proportional to Δm_{sol}^2 . However, in the case of equal Majorana phases, only the imaginary entries in P and terms proportional to θ_{13} contribute to the running. Besides, the contribution proportional to the real parts is suppressed for large solar mixing.

If $Y_\nu^\dagger Y_\nu$ is close to the identity matrix, its contribution to the running is very small, since the terms proportional to the diagonal entries cancel approximately. Then, only the contribution from $Y_e^\dagger Y_e$ remains, so that the evolution above the see-saw scales is essentially the same as below. However, many GUT models suggest a hierarchical structure for Y_ν like for the other Yukawa matrices. Then the main contribution will be due to P_{33} and the next-to-leading contribution will be from $\text{Re } P_{32}$, if the twisting matrix between $Y_e^\dagger Y_e$ and $Y_\nu^\dagger Y_\nu$ is close to the identity. Thus, the phase difference tends to decrease while running down², as it is the

²More accurately, it runs away from π and towards either 0 or 2π , i.e. $|\varphi_1 - \varphi_2|$ decreases for $|\varphi_1 - \varphi_2| < \pi$ and increases for $|\varphi_1 - \varphi_2| > \pi$.

	$16\pi^2 (\dot{\varphi}_1 - \dot{\varphi}_2)$
P_{11}	$-4\mathcal{S}_{12} \cos 2\theta_{12}$
P_{22}	$4\mathcal{S}_{12}c_{23}^2 \cos 2\theta_{12}$
P_{33}	$4\mathcal{S}_{12}s_{23}^2 \cos 2\theta_{12}$
$\text{Re } P_{21}$	$-8\mathcal{S}_{12}c_{23} \cos 2\theta_{12} \cot 2\theta_{12}$
$\text{Re } P_{31}$	$8\mathcal{S}_{12}s_{23} \cos 2\theta_{12} \cot 2\theta_{12}$
$\text{Re } P_{32}$	$-4\mathcal{S}_{12} \cos 2\theta_{12} \sin 2\theta_{23}$
$\text{Im } P_{21}$	$-4\mathcal{Q}_{12}^- c_{23} \cot 2\theta_{12}$
$\text{Im } P_{31}$	$4\mathcal{Q}_{12}^- s_{23} \cot 2\theta_{12}$
$\text{Im } P_{32}$	0

Table 6.3: Coefficients of P_{fg} in the slope of the Majorana phase difference for $\theta_{13} = 0$. The abbreviations \mathcal{S}_{ij} and \mathcal{Q}_{ij}^\pm depend on the mass eigenvalues and phases only, and enhance the running for a degenerate mass spectrum since they are of the form $f_{ij}(m_i, m_j, \varphi_1, \varphi_2)/(m_j^2 - m_i^2)$. They are listed in Tab. D.1.

case below the see-saw scales.

6.5 Evolution of the Masses

In the RGEs for the neutrino mass eigenvalues above the see-saw scales, the contributions proportional to P become important, if the neutrino Yukawa matrix Y_ν has entries of the order of one. In this case, the evolution of the masses depends on the mixing angles, even for small $\tan \beta$, because the contribution of $Y_\nu^\dagger Y_\nu$ is not suppressed then. This is in contrast to the evolution below the see-saw scales which is a simple rescaling in the SM and in the MSSM for small $\tan \beta$ [74–76]. The Majorana phases still influence the running only indirectly. The coefficients of P_{fg} in \dot{m}_i are given in Tab. 6.4.

In the case of $Y_\nu \sim Y_u$, the flavor-diagonal part in the β -function α is positive but small at the GUT scale, since the different terms cancel approximately. Therefore, the contribution of P can become dominant. The terms proportional to the diagonal entries in P enhance the running, while those involving the real parts of the off-diagonal entries can either enhance or damp it, depending on their signs.

On the other hand, some GUT models suggest $Y_\nu \sim Y_e$. This will result in small eigenvalues of $Y_\nu^\dagger Y_\nu$, if $\tan \beta$ is small. Therefore, α dominates the running, but the contribution of P is not negligible for large $\tan \beta$, as it is the case below the see-saw scales. Since α is negative at the GUT scale now, the contributions from the diagonal entries in P decrease the RG effects. The off-diagonal entries again can both increase and decrease them. As the terms in \dot{m}_i that involve the imaginary part of P are proportional to $\sin \theta_{13}$, they do not contribute in the approximation of vanishing θ_{13} .

The same considerations also apply for the mass squared differences. In the case of $Y_\nu \sim Y_u$, the diagonal entries of P enhance the running of Δm_{sol}^2 as long as $\tan \theta_{12} \geq \frac{m_1}{m_2}$. The evolution of Δm_{atm}^2 is usually enhanced by P_{22} and P_{33} , but damped by P_{11} . (For an inverted hierarchy, the term proportional to P_{11} also causes an enhancement.) The effect of the off-diagonal entries depends on their signs. In the case of $Y_\nu \sim Y_e$, the situation is just the other way around, since α is negative. The coefficients of P_{fg} in the slope of the mass squared differences are given in Tab. 6.5.

	$16\pi^2 \dot{m}_1/m_1$	$16\pi^2 \dot{m}_2/m_2$	$16\pi^2 \dot{m}_3/m_3$
α	1	1	1
P_{11}	$2c_{12}^2$	$2s_{12}^2$	0
P_{22}	$2s_{12}^2 c_{23}^2$	$2c_{12}^2 c_{23}^2$	$2s_{23}^2$
P_{33}	$2s_{12}^2 s_{23}^2$	$2c_{12}^2 s_{23}^2$	$2c_{23}^2$
$\text{Re } P_{21}$	$-2 \sin 2\theta_{12} c_{23}$	$2 \sin 2\theta_{12} c_{23}$	0
$\text{Re } P_{31}$	$2 \sin 2\theta_{12} s_{23}$	$-2 \sin 2\theta_{12} s_{23}$	0
$\text{Re } P_{32}$	$-2 \sin 2\theta_{23} s_{12}^2$	$-2 \sin 2\theta_{23} c_{12}^2$	$2 \sin 2\theta_{23}$
$\text{Im } P_{21}$	0	0	0
$\text{Im } P_{31}$	0	0	0
$\text{Im } P_{32}$	0	0	0

Table 6.4: Coefficients of P_{fg} in the slope of the mass eigenvalues for $\theta_{13} = 0$.

	$8\pi^2 \frac{d}{dt} \Delta m_{\text{sol}}^2$	$8\pi^2 \frac{d}{dt} \Delta m_{\text{atm}}^2$
α	Δm_{sol}^2	Δm_{atm}^2
P_{11}	$2s_{12}^2 m_2^2 - 2c_{12}^2 m_1^2$	$-2s_{12}^2 m_2^2$
P_{22}	$2c_{23}^2 [c_{12}^2 m_2^2 - s_{12}^2 m_1^2]$	$2s_{23}^2 m_3^2 - 2c_{12}^2 c_{23}^2 m_2^2$
P_{33}	$2s_{23}^2 [c_{12}^2 m_2^2 - s_{12}^2 m_1^2]$	$2c_{23}^2 m_3^2 - 2c_{12}^2 s_{23}^2 m_2^2$
$\text{Re } P_{21}$	$2 \sin 2\theta_{12} c_{23} [m_2^2 + m_1^2]$	$-2 \sin 2\theta_{12} c_{23} m_2^2$
$\text{Re } P_{31}$	$-2 \sin 2\theta_{12} s_{23} [m_2^2 + m_1^2]$	$2 \sin 2\theta_{12} s_{23} m_2^2$
$\text{Re } P_{32}$	$-2 \sin 2\theta_{23} [c_{12}^2 m_2^2 - s_{12}^2 m_1^2]$	$2 \sin 2\theta_{23} [m_3^2 + c_{12}^2 m_2^2]$
$\text{Im } P_{21}$	0	0
$\text{Im } P_{31}$	0	0
$\text{Im } P_{32}$	0	0

Table 6.5: Coefficients of P_{fg} in the slope of the mass squared differences for $\theta_{13} = 0$.

Chapter 7

Renormalization of SM extended by a Triplet Higgs

7.1 Definition of the additional Renormalization Factors

The same definitions are used as in Jörn Kerstens diploma thesis [59], where the renormalization constants for the SM extended by right-handed neutrinos have been calculated. Here, only the additional renormalization factors and a few others which show up in the calculation are given. The counterterms of the SM extended by right-handed neutrinos are given in Sec. 3.6 of Jörn Kerstens diploma thesis [59], as well as the Feynman rules which are given in the appendix. The Feynman rules for the additional terms in the Lagrangian are given in App. A.5.

The wave function of Δ is renormalized in the usual way by

$$\Delta_B = Z_{\Delta}^{\frac{1}{2}} \Delta . \quad (7.1)$$

The parameters in the Higgs potential have to be renormalized additively

$$Z_{\Delta} (M_{\Delta}^2)_B = M_{\Delta}^2 + \delta M_{\Delta}^2 \quad (7.2a)$$

$$Z_{\Delta}^2 (\Lambda_1)_B = \mu^{\epsilon} (\Lambda_1 + \delta \Lambda_1) \quad (7.2b)$$

$$Z_{\Delta}^2 (\Lambda_2)_B = \mu^{\epsilon} (\Lambda_2 + \delta \Lambda_2) \quad (7.2c)$$

$$Z_{\Delta} Z_{\phi} (\Lambda_4)_B = \mu^{\epsilon} (\Lambda_4 + \delta \Lambda_4) \quad (7.2d)$$

$$Z_{\Delta} Z_{\phi} (\Lambda_5)_B = \mu^{\epsilon} (\Lambda_5 + \delta \Lambda_5) \quad (7.2e)$$

$$\left(Z_{\Delta}^{\dagger} \right)^{\frac{1}{2}} \left(Z_{\phi}^T \right)^{\frac{1}{2}} (\Lambda_6)_B Z_{\phi}^{\frac{1}{2}} = \mu^{\frac{\epsilon}{2}} (\Lambda_6 + \delta \Lambda_6) \quad (7.2f)$$

and the Yukawa vertex is renormalized multiplicatively

$$\left(\left(Z_{\ell_L}^T \right)^{\frac{1}{2}} (Y_{\Delta})_B Z_{\ell_L}^{\frac{1}{2}} Z_{\Delta}^{\frac{1}{2}} \right)_{fg} = \mu^{\frac{\epsilon}{2}} (Y_{\Delta} Z_{Y_{\Delta}})_{fg} \quad (7.2g)$$

and $\delta Z_{Y_{\Delta}}$ is defined as $\delta Z_{Y_{\Delta}} = Z_{Y_{\Delta}} - 1$. The used renormalization factors from the renor-

malization of the SM extended by right-handed neutrinos [59] are given by

$$\phi_B = Z_\phi^{\frac{1}{2}} \phi \quad (7.3a)$$

$$(\ell_L)_B = Z_{\ell_L}^{\frac{1}{2}} \ell_L \quad (7.3b)$$

$$Z_\phi m_B^2 = m^2 + \delta m^2 \quad (7.3c)$$

$$\left(Z_{\nu_R}^{\frac{1}{2}} (Y_\nu)_B Z_\phi^{\frac{1}{2}} Z_{\ell_L}^{\frac{1}{2}} \right)_{fg} = \mu^{\frac{\epsilon}{2}} (Y_\nu Z_\nu)_{fg} . \quad (7.3d)$$

7.2 Counterterm Lagrangian

The insertion of the definitions of the renormalized quantities into the bare Lagrangian yields the counterterm part of the Lagrangian which is needed to cancel the divergencies. Thus the counterterm Lagrangian is given by

$$\begin{aligned} \mathcal{C}_{\Delta(\text{kin})} = & \delta Z_\Delta \text{tr} (D_\mu \Delta)^\dagger (D^\mu \Delta) - \delta M_\Delta^2 \text{tr} \Delta^\dagger \Delta \\ & \left[i \text{tr} (D_\mu \Delta)^\dagger \delta Z_{g_1 g_1} B^\mu \Delta + \delta Z_{g_2 g_2} \frac{\sigma_i}{2} [W^{i\mu}, \Delta] + \text{h.c.} \right] \end{aligned} \quad (7.4a)$$

$$\begin{aligned} \mathcal{C}_{\Delta(\text{int})} = & -\frac{\delta \Lambda_1}{2} \left(\text{tr} \Delta^\dagger \Delta \right)^2 - \frac{\delta \Lambda_2}{2} \left[\left(\text{tr} \Delta^\dagger \Delta \right)^2 - \text{tr} \left(\Delta^\dagger \Delta \Delta^\dagger \Delta \right) \right] \\ & - \delta \Lambda_4 \phi^\dagger \phi \text{tr} \Delta^\dagger \Delta - \delta \Lambda_5 \phi^\dagger [\Delta^\dagger, \Delta] \phi \\ & - \frac{\delta \Lambda_6}{\sqrt{2}} \phi^T (i\sigma_2) \Delta^\dagger \phi \end{aligned} \quad (7.4b)$$

$$\mathcal{C}_{Y_\Delta} = -\frac{Y_\Delta}{\sqrt{2}} \delta Y_\Delta \overline{\ell_L^C} (i\sigma_2) \Delta \ell_L . \quad (7.4c)$$

In addition, the used part of the remaining counterterm Lagrangian is stated:

$$\mathcal{C}_{\text{kin}} = \overline{\ell_L^g} (i\gamma^\mu D_\mu) (\delta Z_{\ell_L})_{gf} \ell_L^f \quad (7.5a)$$

$$\begin{aligned} \mathcal{C}_\phi = & \delta Z_\phi (D_\mu \phi)^\dagger (D^\mu \phi) - \delta m^2 \phi^\dagger \phi - \frac{1}{4} \delta Z_\lambda \lambda \left(\phi^\dagger \phi \right)^2 \\ & + \left[\frac{i}{2} (D_\mu \phi)^\dagger (\delta Z_{g_1 g_1} B^\mu + \delta Z_{g_2 g_2} \sigma_i W^{i\mu}) \phi + \text{h.c.} \right] . \end{aligned} \quad (7.5b)$$

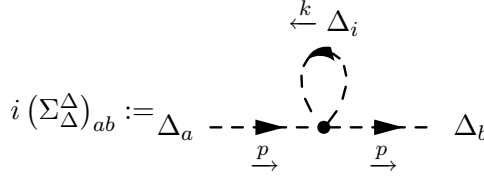
Next, the diagrams contributing to the renormalization constants have to be calculated. First the self-energy diagrams are calculated for the Higgs triplet and the additional contributions for the Higgs and lepton doublets. Then the vertex corrections are calculated.

7.3 Self Energy Diagrams

7.3.1 Self Energy of Higgs Triplet Σ_Δ

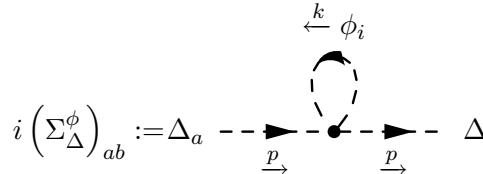
There are 3 different types of contributions to the self-energy of the Higgs triplet. At first, there are contributions from the Higgs sector by the Higgs triplet and the doublet. Moreover, there are contributions from the gauge bosons which the triplet is coupling to, and finally there is a contribution from the left-handed doublet in the loop.

Contributions from the Higgs Potential

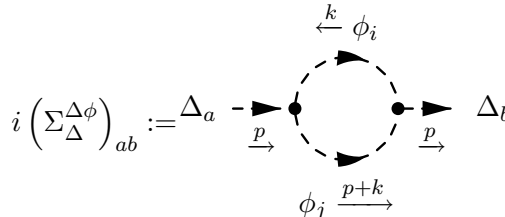


$$\begin{aligned}
i(\Sigma_{\Delta}^{\Delta})_{ab} &:= \Delta_a \text{ --- } \text{---} \text{---} \text{---} \Delta_b \\
&= \frac{1}{2} \sum_i \int \frac{d^d k}{(2\pi)^d} [-i\mu^\epsilon (\Lambda_1 (\delta_{ba}\delta_{ii} + \delta_{ia}\delta_{bi}) + \Lambda_2 \delta_{bi}\delta_{ia})] \frac{i}{k^2 - M_{\Delta}^2 + i\varepsilon} \\
&= \frac{1}{2} [4\Lambda_1 + \Lambda_2] \mu^\epsilon \int \frac{d^d k}{(2\pi)^d} \frac{1}{k^2 - M_{\Delta}^2 + i\varepsilon} \\
&= \frac{1}{2} [4\Lambda_1 + \Lambda_2] \frac{i\pi^2}{(2\pi)^4} A_0(M_{\Delta}^2) + \text{UV finite} \\
&= \frac{i}{16\pi^2\epsilon} M_{\Delta}^2 [4\Lambda_1 + \Lambda_2] \delta_{ab} + \text{UV finite}
\end{aligned} \tag{7.6}$$

The integrals in d dimensions showing up here can be solved by expressing them in Passarino-Veltman functions, whose divergent part is given in App. C.5. Another possibility to solve these integrals is sketched in Sec. 3.2.4. However, we use the Passarino-Veltman function, because it is more convenient. The calculation of the other diagrams is similar. Hence, only the ansatz and the result are given.

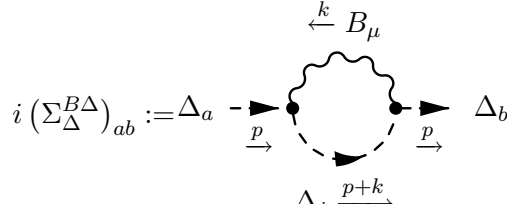


$$\begin{aligned}
i(\Sigma_{\Delta}^{\phi})_{ab} &:= \Delta_a \text{ --- } \text{---} \text{---} \text{---} \Delta_b \\
&= \sum_i \int \frac{d^d k}{(2\pi)^d} [-i\mu^\epsilon (\Lambda_4 \delta_{ii} \delta_{ba} + \Lambda_5 i\epsilon_{bam} (\sigma_m)_{ii})] \frac{i}{k^2 - m^2 + i\varepsilon} \\
&= \frac{i\Lambda_4}{4\pi^2\epsilon} m^2 \delta_{ab} + \text{UV finite}
\end{aligned} \tag{7.7}$$



$$\begin{aligned}
i(\Sigma_{\Delta}^{\Delta\phi})_{ab} &:= \Delta_a \text{ --- } \text{---} \text{---} \text{---} \Delta_b \\
&= \frac{1}{2} \sum_{i,j} \int \frac{d^d k}{(2\pi)^d} [\Lambda_4 \mu^{\frac{\epsilon}{2}} (\sigma_2 \sigma_b)_{ij}] \frac{i}{k^2 - m^2 + i\varepsilon} [-\Lambda_4^* \mu^{\frac{\epsilon}{2}} (\sigma_a \sigma_2)_{ji}] \\
&= \frac{i}{8\pi^2\epsilon} |\Lambda_4|^2 \delta_{ba} + \text{UV finite}
\end{aligned} \tag{7.8}$$

Contributions from Gauge Bosons

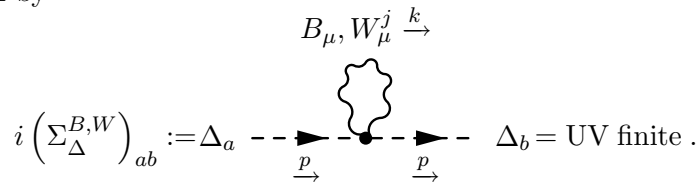


$$\begin{aligned}
 i(\Sigma_{\Delta}^{B\Delta})_{ab} &:= \Delta_a - \Delta_b \\
 &= \sum_i \int \frac{d^d k}{(2\pi)^d} \left[-i\sqrt{\frac{3}{5}} g_1 \mu^{\frac{\epsilon}{2}} (2p_\mu + k_\mu) \delta_{ai} \right] \\
 &\quad i \frac{-\eta^{\mu\nu} + (1 - \xi_1) \frac{k^\mu k^\nu}{k^2}}{k^2 + i\epsilon} \left[-i\sqrt{\frac{3}{5}} g_1 \mu^{\frac{\epsilon}{2}} (2p_\nu + k_\nu) \delta_{bi} \right] \frac{i}{(p+k)^2 - M_\Delta^2 + i\epsilon} \\
 &= -\frac{3}{5} \frac{ig_1^2}{8\pi^2 \epsilon} \delta_{ab} [(3 - \xi_1) p^2 + \xi_1 M_\Delta^2] + \text{UV finite}
 \end{aligned} \tag{7.9}$$

There is a graph with the same topology, but the B_μ boson is replaced by a W_μ boson. It only differs by the coupling constant, gauge fixing parameter and the $SU(2)_L$ structure, but the integral is the same. The $SU(2)_L$ structure changes from $\delta_{ai}\delta_{bi}$ to $i\epsilon_{bj i} i\epsilon_{ija} = 2\delta_{ba}$. Thus the graph for the W_μ boson results in

$$i(\Sigma_{\Delta}^{W\Delta})_{ab} = -\frac{ig_2^2}{4\pi^2 \epsilon} \delta_{ba} [(3 - \xi_2) p^2 + \xi_2 M_\Delta^2] + \text{UV finite} \tag{7.10}$$

The diagrams involving the gauge bosons depend on the corresponding gauge parameter ξ_i . This gives a good check for the β -function, because the β -function has to be independent of the gauge fixing parameter. Thus the gauge parameter has to cancel non-trivially. The other contribution from the gauge bosons is due to the coupling of two gauge bosons to two Higgs triplets. It is given by



$$i(\Sigma_{\Delta}^{B,W})_{ab} := \Delta_a - \Delta_b = \text{UV finite} . \tag{7.11}$$

This diagram is UV finite, since it is proportional to the one-point Passarino-Veltman function $A_0(0)$ with $m^2 = 0$. More precisely, it is a scale-less integral in d dimensions which has to vanish by the definition of dimensional regularization [35].

Contributions from Fermions

Finally, the fermion in the loop¹ yields

¹Note the minus sign from the closed loop of fermions.

$$\begin{aligned}
i \left(\Sigma_{\Delta}^{LL} \right)_{ab} &:= \Delta_a - \text{Diagram} \Delta_b \\
&= (-1) \frac{1}{2} \int \frac{d^d k}{(2\pi)^d} \text{tr} \left[(Y_{\Delta})_{fg} \mu^{\frac{\epsilon}{2}} (\sigma_2 \sigma_a)_{ji} P_L \right] \frac{i (\not{p} + \not{k})}{(p+k)^2 + i\epsilon} \\
&\quad \left[- (Y_{\Delta}^{\dagger})_{gf} \mu^{\frac{\epsilon}{2}} (\sigma_b \sigma_2)_{ij} P_R \right] \frac{-i \not{k}}{k^2 + i\epsilon} \\
&= - \frac{ip^2}{8\pi^2 \epsilon} \text{tr} \left(Y_{\Delta}^{\dagger} Y_{\Delta} \right) \delta_{ba} + \text{UV finite} .
\end{aligned}
\tag{7.12}$$

Wave Function Renormalization of Δ

The wave function renormalization is obtained from the condition, that the propagator is UV finite to one-loop order, i.e.

$$\begin{aligned}
\text{UV finite} \stackrel{!}{=} & - \text{Diagram 1} = \text{Diagram 2} + \text{Diagram 3} + \text{Diagram 4} + \text{Diagram 5} \\
& + \text{Diagram 6} + \sum_m \text{Diagram 7} + \text{Diagram 8} + \text{Diagram 9}
\end{aligned}
\tag{7.13}$$

As the result is required to be UV finite, the divergent part of this equation has to satisfy

$$\begin{aligned} & \frac{4\Lambda_1 + \Lambda_2}{16\pi^2\epsilon} M_\Delta^2 + \frac{\Lambda_4}{4\pi^2\epsilon} m^2 + \frac{|\Lambda_6|^2}{8\pi^2\epsilon} - \frac{3}{5} \frac{g_1^2}{8\pi^2\epsilon} [(3 - \xi_1)p^2 + \xi_1 M_\Delta^2] \\ & - \frac{g_2^2}{4\pi^2\epsilon} [(3 - \xi_2) + \xi_2 M_\Delta^2] - \frac{1}{8\pi^2\epsilon} \text{tr} \left(Y_\Delta^\dagger Y_\Delta \right) p^2 + p^2 \delta Z_\Delta - \delta M_\Delta^2 \stackrel{!}{=} 0. \quad (7.14) \end{aligned}$$

From this equation, the renormalization factor of the wave function is

$$\delta Z_{\Delta} = \frac{1}{16\pi^2\epsilon} \left[\frac{6}{5} (3 - \xi_1) g_1^2 + 4 (3 - \xi_2) g_2^2 + 2 \text{tr} \left(Y_{\Delta}^{\dagger} Y_{\Delta} \right) \right] \quad (7.15)$$

and the mass counterterm

$$\delta M_\Delta^2 = \frac{1}{16\pi^2\epsilon} \left[\left(4\Lambda_1 + \Lambda_2 - \frac{6}{5}\xi_1 g_1^2 - 4\xi_2 g_2^2 \right) M_\Delta^2 + \Lambda_4 m^2 + 2|\Lambda_6|^2 \right] \quad (7.16)$$

can be read off by requiring, that the counterterms are momentum-independent.

There are additional contributions to the self-energy of the Higgs doublet from the Higgs triplet through the vertices proportional to Λ_4 and Λ_6 in the Higgs potential.

[illegible]

$$\begin{aligned}
i \left(\Sigma_{\phi}^{\Delta\phi} \right)_{ab} &:= \phi_a - \text{Feynman diagram} \rightarrow \phi_b \\
&= \sum_{i,j} \int \frac{d^d k}{(2\pi)^d} \left[\Lambda_6 \mu^{\frac{\epsilon}{2}} (\sigma_2 \sigma_j)_{ai} \right] \frac{i}{(p+k)^2 - M_\Delta^2 + i\varepsilon} \left[-\Lambda_6^* \mu^{\frac{\epsilon}{2}} (\sigma_j \sigma_2)_{ib} \right] \\
&\quad \frac{i}{k^2 - m^2 + i\varepsilon} \\
&= \frac{3i|\Lambda_6|^2}{8\pi^2\epsilon} \delta_{ba} + \text{UV finite}
\end{aligned} \tag{7.18}$$

Calculation of the Wave Function Renormalization

The wave function renormalization is obtained from the condition, that the propagator is UV finite to one-loop order, i.e.

$$\text{UV finite} \stackrel{!}{=} - \text{triangle with shaded circle} = - \text{triangle with circle} + \text{triangle with self-energy loop } \phi + \text{triangle with bubble } \phi + \text{triangle with cross} \quad (7.19)$$

The divergent parts which have already been calculated [59] are summarized as

$$-\text{Feynman diagram with two fermion lines and a scalar loop} = -i(p^2 \delta Z_\phi^0 - \delta m_0^2) \quad (7.20)$$

Thus the new contribution due to the Higgs triplet just add to the other contributions. The wave function renormalization does not change [59], i.e.

$$\delta Z_\phi = -\frac{1}{16\pi^2\epsilon} \left[2 \operatorname{tr} \left(Y_\nu^\dagger Y_\nu + Y_e^\dagger Y_e + 3Y_u^\dagger Y_u + 3Y_d^\dagger Y_d \right) - \frac{3}{10} (3 - \xi_1) g_1^2 - \frac{3}{2} (3 - \xi_2) g_2^2 \right], \quad (7.21)$$

but the mass renormalization receives an additional contribution

$$\begin{aligned} \delta m^2 &= \delta m_0^2 + \frac{3\Lambda_4}{8\pi^2\epsilon} M_\Delta^2 + \frac{3|\Lambda_6|^2}{8\pi^2\epsilon} \\ &= \frac{1}{16\pi^2\epsilon} \left[\left(3\lambda - \frac{3}{10}\xi_1 g_1^2 - \frac{3}{2}\xi_2 g_2^2 \right) m^2 - 4 \operatorname{tr} \left(Y_\nu^\dagger M^2 Y_\nu \right) + 6\Lambda_4 M_\Delta^2 + 6|\Lambda_6|^2 \right]. \end{aligned} \quad (7.22)$$

Self Energy of left-handed Lepton Doublet

The Yukawa coupling of the left-handed lepton doublet to the Higgs triplet results in a contribution to the self-energy of the left-handed doublet yielding an additional term in the β function of all vertices involving the left-handed doublet in turn.

$$\begin{aligned} i(\Sigma_{\ell_L}^\Delta)_{ab} &:= \text{Diagram: } \ell_{La}^f \xrightarrow{p} \text{loop} \xrightarrow{p} \ell_{Lb}^g \text{ with } \ell_{Li}^h \text{ and } \Delta_j \text{ in the loop} \\ &= \int \frac{d^d k}{(2\pi)^d} \left[- \left(Y_\Delta^\dagger \right)_{gh} \mu^{\frac{\epsilon}{2}} (\sigma_j \sigma_2)_{bi} P_R \right] \frac{-i \not{k}}{k^2 + i\epsilon} \\ &\quad \left[(Y_\Delta)_{hf} \mu^{\frac{\epsilon}{2}} (\sigma_2 \sigma_j)_{ia} P_L \right] \frac{i}{(p+k)^2 - M_\Delta^2 + i\epsilon} \\ &= \frac{3i \not{p}}{16\pi^2\epsilon} \left(Y_\Delta^\dagger Y_\Delta \right)_{gf} \delta_{ba} P_L + \text{UV finite} \end{aligned} \quad (7.23)$$

Calculation of the Wave Function Renormalization

The condition determining the counterterm is given by

$$\text{UV finite} \stackrel{!}{=} \text{Diagram: } \ell_L \text{ with a shaded circle} = \text{Diagram: } \ell_L \text{ with an open circle} + \text{Diagram: } \ell_L \text{ with a loop } \ell_L \text{ and } \Delta + \text{Diagram: } \ell_L \text{ with a cross} \quad (7.24)$$

The already calculated terms are summarized as

$$\text{Diagram: } \ell_{La}^f \text{ with an open circle } \ell_{Lb}^g = i \not{p} (\delta Z_{\ell_L}^0)_{gf} P_L \delta_{ba}. \quad (7.25)$$

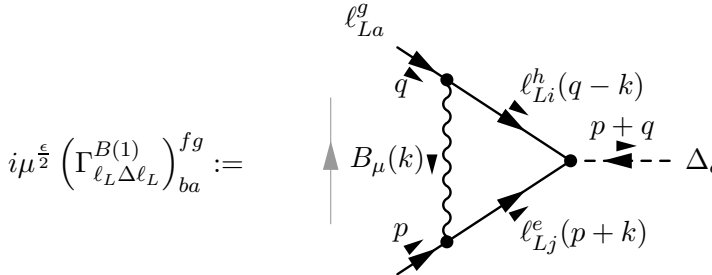
Hence, the wave function renormalization for the lepton doublet receives an additional contribution from a Higgs triplet in the loop.

$$\begin{aligned}\delta Z_{\ell_L} &= \delta Z_{\ell_L}^0 + \frac{3}{16\pi^2\epsilon} Y_\Delta^\dagger Y_\Delta \\ &= -\frac{1}{16\pi^2\epsilon} \left[Y_\nu^\dagger Y_\nu + Y_e^\dagger Y_e + \frac{3}{10} \xi_1 g_1^2 + \frac{3}{2} \xi_2 g_2^2 - 3 Y_\Delta^\dagger Y_\Delta \right]\end{aligned}\quad (7.26)$$

7.4 Vertex Corrections

7.4.1 Vertex Corrections to $\ell_L \Delta \ell_L$

There are only contributions from gauge bosons to the counterterm of Y_Δ , because all other possible diagrams are UV finite by power counting.



$$\begin{aligned}i\mu^{\frac{\epsilon}{2}} \left(\Gamma_{\ell_L \Delta \ell_L}^{B(1)} \right)_{ba}^{fg} &:= \\ &= \sum_{h,e,i,j} \int \frac{d^d k}{(2\pi)^d} \left[\frac{i}{2} \mu^{\frac{\epsilon}{2}} \sqrt{\frac{3}{5}} g_1 \delta_{ef} \delta_{bj} \gamma_\nu P_L \right] i \frac{-\eta^{\mu\nu} + (1 - \xi_1) \frac{k^\mu k^\nu}{k^2}}{k^2 + i\epsilon} \\ &\quad \left[-\frac{i}{2} \mu^{\frac{\epsilon}{2}} \sqrt{\frac{3}{5}} g_1 \delta_{gh} \delta_{ia} \gamma_\mu P_R \right] \frac{-i(q-k)}{(q-k)^2 + i\epsilon} \left[(Y_\Delta)_{hl} \mu^{\frac{\epsilon}{2}} (\sigma_2 \sigma_c)_{ij} P_L \right] \frac{i(p+k)}{(p+k)^2 + i\epsilon} \\ &= -\frac{3}{5} \frac{g_1^2}{32\pi^2\epsilon} (Y_\Delta)_{gf} \mu^{\frac{\epsilon}{2}} (\sigma_2 \sigma_c)_{ab} (3 + \xi_1) P_L + \text{UV finite}\end{aligned}\quad (7.27)$$

The graph with B_μ replaced by W_μ can be obtained by replacing ξ_1 with ξ_2 and $\frac{3}{5} g_1^2 (\sigma_2 \sigma_c)_{ab}$ by $g_2^2 \sum_m (\sigma_m^T \sigma_2 \sigma_c \sigma_m)_{ab}$. Using Eq. (C.28c), the $SU(2)_L$ -structure can be simplified and the contribution of the graph with W_μ is given by

$$i\mu^{\frac{\epsilon}{2}} \left(\Gamma_{\ell_L \Delta \ell_L}^{W(1)} \right)_{ba}^{fg} = -\frac{g_2^2}{32\pi^2\epsilon} (Y_\Delta)_{gf} \mu^{\frac{\epsilon}{2}} (\sigma_2 \sigma_c)_{ab} (3 + \xi_2) P_L + \text{UV finite} . \quad (7.28)$$

There is another graph with one end of the gauge boson line attached to the Higgs triplet,

namely

$$\begin{aligned}
i\mu^{\frac{\epsilon}{2}} \left(\Gamma_{\ell_L \Delta \ell_L}^{B(2)} \right)_{ba}^{fg} &:= \\
&= \sum_{i,h,d} \int \frac{d^d k}{(2\pi)^d} \left[-\frac{i}{2} \mu^{\frac{\epsilon}{2}} \sqrt{\frac{3}{5}} g_1 \delta_{gh} \delta_{ai} \gamma_\mu P_R \right] \frac{-i(q-k)}{(q-k)^2 + i\epsilon} \\
&\quad \left[(Y_\Delta)_{hf} \mu^{\frac{\epsilon}{2}} (\sigma_2 \sigma_d)_{ib} P_L \right] \frac{i}{(p+q-k)^2 - M_\Delta^2 + i\epsilon} \\
&\quad \left[-i \sqrt{\frac{3}{5}} g_1 \mu^{\frac{\epsilon}{2}} (k-2p-2q)_\nu \delta_{cd} \right] i \frac{-\eta^{\mu\nu} + (1-\xi_1) \frac{k^\mu k^\nu}{k^2}}{k^2 + i\epsilon} \\
&= \frac{3}{5} \frac{g_1^2}{16\pi^2 \epsilon} (Y_\Delta)_{gf} \mu^{\frac{\epsilon}{2}} (\sigma_2 \sigma_c)_{ba} \xi_1 + \text{UV finite} .
\end{aligned} \tag{7.29}$$

The graph with B_μ replaced by W_μ can be obtained by replacing ξ_1 with ξ_2 and $\frac{3}{5}g_1^2(\sigma_2\sigma_c)_{ab}$ by $-ig_2^2\sum_m(\sigma_m^T\sigma_2\sigma_d)_{ab}\epsilon_{dmc}$. Using Eq. (C.28c), the $SU(2)_L$ -structure can be simplified and the contribution of the graph with W_μ is given by

$$i \left(\Gamma_{\ell_L \Delta \ell_L}^{W(2)} \right)_{ba}^{fg} = \frac{g_2^2}{8\pi^2 \epsilon} (Y_\Delta)_{gf} \mu^{\frac{\epsilon}{2}} (\sigma_2 \sigma_c)_{ba} \xi_2 + \text{UV finite} \tag{7.30}$$

The same results apply for B_μ or W_μ , respectively, attached to the other fermion. The last diagram

$$i\mu^{\frac{\epsilon}{2}} \left(\Gamma_{\ell_L \Delta \ell_L}^P \right)_{ba}^{fg} := \tag{7.31}$$

is UV finite by power counting, because the vertex $\phi\Delta\phi$ has mass dimension 1. Hence, there is no contribution from the other Yukawa vertices and the counterterm is flavor-diagonal.

Vertex Counterterm

Finally, the counterterm for the $\ell_L \Delta \ell_L$ coupling is determined by

$$\begin{aligned}
 \text{UV finite} \stackrel{!}{=} & \text{Diagram 1} = \text{Diagram 2} + B_\mu \text{ Diagram 3} + \sum_m W_\mu^m \text{ Diagram 4} \\
 & + \ell_L \text{ Diagram 5} + \sum_m \ell_L \text{ Diagram 6} + \ell_L \text{ Diagram 7} \\
 & + \sum_m \ell_L \text{ Diagram 8} + \ell_L \text{ Diagram 9}
 \end{aligned} \tag{7.32}$$

The diagrams represent various Feynman diagrams for the vertex correction. Diagram 1 is a tree-level vertex with incoming ℓ_L^g and ℓ_L^f lines and an outgoing Δ line. Diagram 2 is a tree-level vertex with incoming ℓ_L and ℓ_L lines and an outgoing Δ line. Diagram 3 is a loop diagram with a B_μ boson exchange. Diagram 4 is a loop diagram with a W_μ^m boson exchange. Diagram 5 is a loop diagram with a B_μ boson exchange. Diagram 6 is a loop diagram with a W_μ^m boson exchange. Diagram 7 is a loop diagram with a B_μ boson exchange. Diagram 8 is a loop diagram with a W_μ^m boson exchange. Diagram 9 is a tree-level vertex with incoming ℓ_L and ℓ_L lines and an outgoing Δ line.

which leads to the counterterm of the vertex

$$\delta Z_{Y_\Delta} = \frac{1}{32\pi^2\epsilon} \left[\frac{9}{5} (1 - \xi_1) g_1^2 + (3 - 7\xi_2) g_2^2 \right]. \tag{7.33}$$

7.4.2 Vertex Corrections to $\nu_R \ell_L \phi$

The only graph which might contribute to the vertex correction of $\nu_R \ell_L \phi$

$$i\mu^{\frac{\epsilon}{2}} (\Gamma_{\nu_R \ell_L \phi})_{ba}^{fg} := \text{Diagram} \tag{7.34}$$

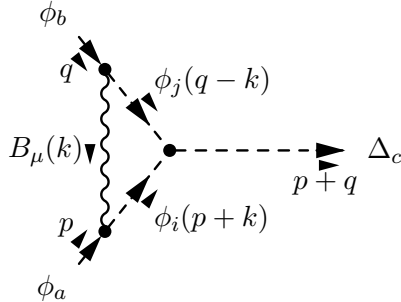
The diagram shows a vertex correction for the $\nu_R \ell_L \phi$ coupling. It features an incoming ν_R^g line, an incoming ℓ_L^f line, and an outgoing ϕ_a line. The loop consists of a ϕ boson and a Δ boson.

is convergent by power counting, since $D = 4 - (2 \cdot \frac{3}{2} + 1) - 1 \cdot 1 = -1$. Thus the counterterm for the neutrino Yukawa coupling does not receive an additional contribution.

7.4.3 Vertex Corrections to $\phi \Delta \phi$

There are 3 different types of graphs: vertex corrections from gauge bosons, the Higgs potential and fermion loops.

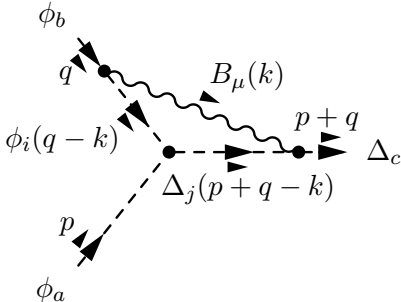
Contributions from Gauge Bosons



$$\begin{aligned}
i\mu^{\frac{\epsilon}{2}} \left(\Gamma_{\phi\Delta\phi}^{B(1)} \right)_{ba}^c &:= \\
&= \sum_{i,j} \int \frac{d^d k}{(2\pi)^d} \left[-\frac{i}{2} \mu^{\frac{\epsilon}{2}} \sqrt{\frac{3}{5}} g_1 (2q-k)_\mu \delta_{bi} \right] \frac{i}{(q-k)^2 - m^2 + i\epsilon} \left[\Lambda_6 \mu^{\frac{\epsilon}{2}} (\sigma_2 \sigma_c)_{ij} \right] \\
&\quad \frac{i}{(p+k)^2 - m^2 + i\epsilon} \left[-\frac{i}{2} \mu^{\frac{\epsilon}{2}} \sqrt{\frac{3}{5}} g_1 (2p+k)_\nu \delta_{ja} \right] i \frac{-\eta^{\mu\nu} + (1-\xi_1) \frac{k^\mu k^\nu}{k^2}}{k^2 + i\epsilon} \\
&= -\frac{3}{5} \frac{g_1^2 \Lambda_6}{32\pi^2 \epsilon} \xi_1 \mu^{\frac{\epsilon}{2}} (\sigma_2 \sigma_c)_{ba} + \text{UV finite}
\end{aligned} \tag{7.35}$$

The graph with B_μ exchanged by W_μ can be obtained by replacing $\sqrt{\frac{3}{5}}g_1$ by g_2 and ξ_1 by ξ_2 because of Eq. (C.28c). Thus the diagram with W_μ is given by

$$i\mu^{\frac{\epsilon}{2}} \left(\Gamma_{\phi\Delta\phi}^{W(1)} \right)_{ba}^c = -\frac{g_2^2 \Lambda_6}{32\pi^2 \epsilon} \xi_2 \mu^{\frac{\epsilon}{2}} (\sigma_2 \sigma_c)_{ba} . \tag{7.36}$$



$$\begin{aligned}
i\mu^{\frac{\epsilon}{2}} \left(\Gamma_{\phi\Delta\phi}^{B(2)} \right)_{ba}^c &:= \\
&= \sum_{i,j} \int \frac{d^d k}{(2\pi)^d} \left[-\frac{i}{2} \mu^{\frac{\epsilon}{2}} \sqrt{\frac{3}{5}} g_1 (2q-k)_\mu \delta_{bi} \right] \frac{i}{(q-k)^2 - m^2 + i\epsilon} \left[\Lambda_6 \mu^{\frac{\epsilon}{2}} (\sigma_2 \sigma_j)_{ia} \right] \\
&\quad \frac{i}{(p+q-k)^2 - M_\Delta^2 + i\epsilon} \left[-i\mu^{\frac{\epsilon}{2}} \sqrt{\frac{3}{5}} g_1 (2p+2q-k)_\nu \delta_{jc} \right] i \frac{-\eta^{\mu\nu} + (1-\xi_1) \frac{k^\mu k^\nu}{k^2}}{k^2 + i\epsilon} \\
&= \frac{3}{5} \frac{g_1^2 \Lambda_6}{16\pi^2 \epsilon} \xi_1 \mu^{\frac{\epsilon}{2}} (\sigma_2 \sigma_c)_{ba} + \text{UV finite}
\end{aligned} \tag{7.37}$$

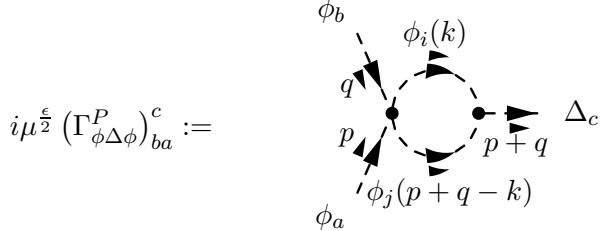
The graph with B_μ exchanged by W_μ can be obtained by replacing $\frac{3}{5}g_1^2$ by $2g_2^2$ and ξ_1 by ξ_2 because of Eq. (C.28d). Hence the contribution of W_μ yields

$$i\mu^{\frac{\epsilon}{2}} \left(\Gamma_{\phi\Delta\phi}^{W(2)} \right)_{ba}^c = \frac{g_2^2 \Lambda_6}{8\pi^2 \epsilon} \xi_2 \mu^{\frac{\epsilon}{2}} (\sigma_2 \sigma_c)_{ba} + \text{UV finite} . \tag{7.38}$$

The graph with the boson connected to the other Higgs doublet line yields the same result.

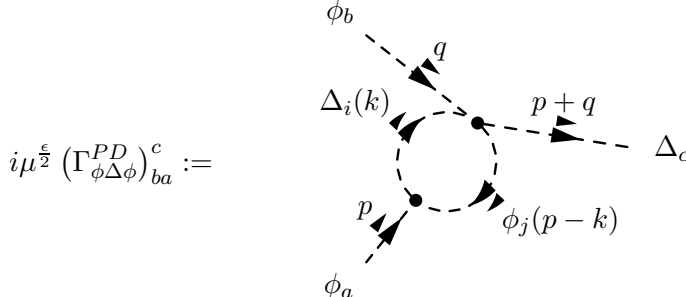
Contributions from the Higgs Potential

Moreover, there is one contribution from the quartic Higgs doublet coupling.



$$\begin{aligned}
 i\mu^{\frac{\epsilon}{2}} (\Gamma_{\phi\Delta\phi}^P)^c_{ba} &:= \\
 &= \frac{1}{2} \sum_{i,j} \int \frac{d^d k}{(2\pi)^d} \left[-\frac{i}{2} \mu^\epsilon \lambda (\delta_{ib} \delta_{ja} + \delta_{jb} \delta_{ia}) \right] \frac{i}{k^2 - m^2 + i\epsilon} \\
 &\quad \left[\Lambda_6 \mu^{\frac{\epsilon}{2}} (\sigma_2 \sigma_c)_{ij} \right] \frac{i}{(p+q-k)^2 - m^2 + i\epsilon} \\
 &= -\frac{\lambda \Lambda_6}{16\pi^2 \epsilon} \mu^{\frac{\epsilon}{2}} (\sigma_2 \sigma_c)_{ba} + \text{UV finite}
 \end{aligned} \tag{7.39}$$

Furthermore, there is a contribution from the coupling of two Higgs doublets to two Higgs triplets.



$$\begin{aligned}
 i\mu^{\frac{\epsilon}{2}} (\Gamma_{\phi\Delta\phi}^{PD})^c_{ba} &:= \\
 &= \sum_{i,j} \int \frac{d^d k}{(2\pi)^d} \left[-i\mu^\epsilon \left(\Lambda_4 \delta_{jb} \delta_{ci} + \Lambda_5 i\epsilon_{cim} (\sigma_m)_{jb} \right) \right] \frac{i}{k^2 - m^2 + i\epsilon} \\
 &\quad \left[\Lambda_6 \mu^{\frac{\epsilon}{2}} (\sigma_2 \sigma_i)_{ja} \right] \frac{i}{(p-k)^2 - m^2 + i\epsilon} \\
 &= \frac{i}{8\pi^2 \epsilon} \mu^{\frac{\epsilon}{2}} \Lambda_6 (\Lambda_4 - 2\Lambda_5) (\sigma_2 \sigma_c)_{ba} + \text{UV finite}
 \end{aligned} \tag{7.40}$$

The Higgs triplet attached to the other vertex yields the same result. Thus twice the contribution has to be added to the counterterm. Finally, there is the contribution from a loop of fermions.

Fig. 7.1.

$$\delta\Lambda_1 = \frac{1}{16\pi^2\epsilon} \left[\left(-\frac{12}{5}\xi_1 g_1^2 - 8g_2^2 \xi_2 \right) \Lambda_1 + \frac{36}{25}g_1^4 + 18g_2^4 + \frac{72}{5}g_1^2 g_2^2 + 8\Lambda_1^2 + \Lambda_2^2 + 2\Lambda_1 \Lambda_2 \right. \\ \left. + 4(\Lambda_4^2 + \Lambda_5^2) - 4 \text{tr} \left(Y_\Delta^\dagger Y_\Delta Y_\Delta^\dagger Y_\Delta \right) \right] \quad (7.44a)$$

$$\delta\Lambda_2 = \frac{1}{16\pi^2\epsilon} \left[\left(-\frac{12}{5}\xi_1 g_1^2 - 8g_2^2 \xi_2 \right) \Lambda_2 + 12g_2^4 - \frac{144}{5}g_1^2 g_2^2 + 3\Lambda_2^2 + 8\Lambda_1 \Lambda_2 - 8\Lambda_5^2 \right. \\ \left. + 4 \text{tr} \left(Y_\Delta^\dagger Y_\Delta Y_\Delta^\dagger Y_\Delta \right) \right] \quad (7.44b)$$

$$\delta\Lambda_4 = \frac{1}{32\pi^2\epsilon} \left[(-3\xi_1 g_1^2 - 11\xi_2 g_2^2) \Lambda_4 + \frac{54}{25}g_1^4 + 12g_2^4 + 2(8\Lambda_1 + 2\Lambda_2 + 3\lambda + 2\Lambda_4) \Lambda_4 \right. \\ \left. + 8\Lambda_5^2 - 8 \text{tr} \left(Y_\Delta^\dagger Y_\Delta Y_\nu^\dagger Y_\nu \right) \right] \quad (7.44c)$$

$$\delta\Lambda_5 = \frac{1}{32\pi^2\epsilon} \left[(-3\xi_1 g_1^2 - 11\xi_2 g_2^2) \Lambda_5 - \frac{36}{5}g_1^2 g_2^2 + 2(2\Lambda_1 - 2\Lambda_2 + \lambda + 4\Lambda_4 - 2\Lambda_5) \Lambda_5 \right. \\ \left. + 8 \text{tr} \left(Y_\Delta^\dagger Y_\Delta Y_\nu^\dagger Y_\nu \right) \right] \quad (7.44d)$$

Furthermore, there is an additional contribution to the renormalization of the quartic coupling of the Higgs doublet.

$$\delta\lambda = \delta\lambda^0 + \frac{3\Lambda_4^2 + 2\Lambda_5^2}{8\pi^2\epsilon}, \quad (7.45)$$

where λ_0 describes the contributions from other particles.

7.5 Calculation of the β -Functions

The counterterms of the vertices and the renormalization factors of the wave functions of the particles which are connected to the vertex, determine the β -function of the parameter describing the vertex. Here, the β -functions for the relevant parameters of the Higgs triplet contribution to the neutrino mass matrix (Y_Δ , Λ_6 and M_Δ^2) are calculated and the β -functions for the remaining parameters are stated. At first the relevant counterterms are summarized. The relevant wave function renormalizations are

$$\delta Z_\Delta = \frac{1}{16\pi^2\epsilon} \left[\frac{6}{5}(3 - \xi_1) g_1^2 + 4(3 - \xi_2) g_2^2 + 2 \text{tr} \left(Y_\Delta^\dagger Y_\Delta \right) \right] \quad (7.15)$$

$$\delta Z_\phi = -\frac{1}{16\pi^2\epsilon} \left[2 \text{tr} \left(Y_\nu^\dagger Y_\nu + Y_e^\dagger Y_e + 3Y_u^\dagger Y_u + 3Y_d^\dagger Y_d \right) - \frac{3}{10}(3 - \xi_1) g_1^2 - \frac{3}{2}(3 - \xi_2) g_2^2 \right] \quad (7.21)$$

$$\delta Z_{\ell_L} = -\frac{1}{16\pi^2\epsilon} \left[Y_\nu^\dagger Y_\nu + Y_e^\dagger Y_e + \frac{3}{10}\xi_1 g_1^2 + \frac{3}{2}\xi_2 g_2^2 - 3Y_\Delta^\dagger Y_\Delta \right] \quad (7.26)$$

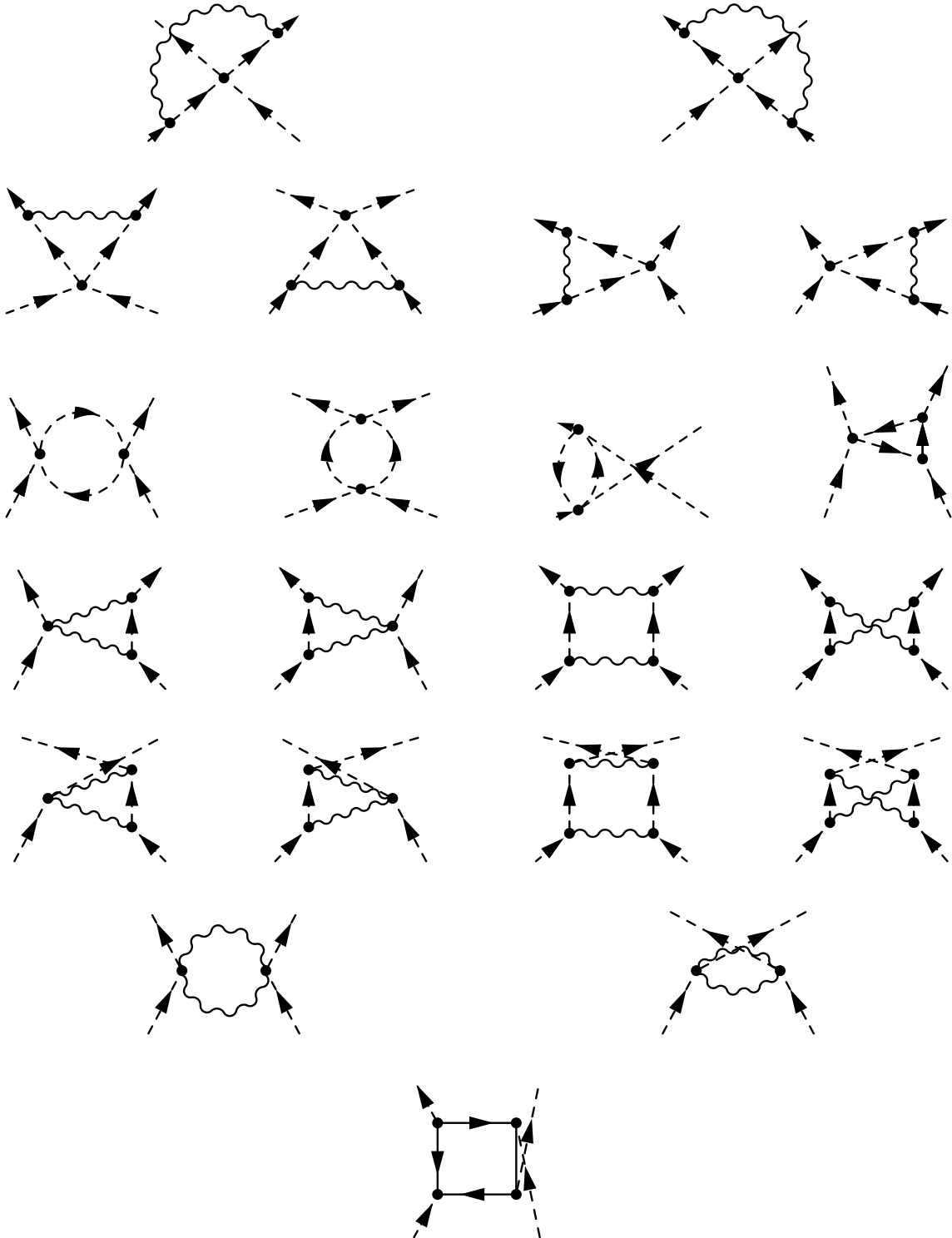


Figure 7.1: Different topologies of the vertices with 4 external lines in the Higgs sector

and the counterterms for the vertices are given by

$$\delta Z_{Y_\Delta} = \frac{1}{32\pi^2\epsilon} \left[\frac{9}{5} (1 - \xi_1) g_1^2 + (3 - 7\xi_2) g_2^2 \right] \quad (7.33)$$

$$\delta \Lambda_6 = - \frac{1}{32\pi^2\epsilon} \left[8 \operatorname{tr} \left(Y_\Delta^\dagger Y_\nu^T M Y_\nu \right) + \left(\frac{9}{5} g_1^2 \xi_1 + 7g_2^2 \xi_2 - 2\lambda + 8\Lambda_4 - 16\Lambda_5 \right) \Lambda_6 \right] \quad (7.43)$$

$$\delta M_\Delta^2 = \frac{1}{16\pi^2\epsilon} \left[\left(4\Lambda_1 + \Lambda_2 - \frac{6}{5} \xi_1 g_1^2 - 4\xi_2 g_2^2 \right) M_\Delta^2 + \Lambda_4 m^2 + 2|\Lambda_6|^2 \right]. \quad (7.16)$$

Note, that GUT charge normalization is used for the $U(1)_Y$ hypercharge. Thus the hypercharge q_Y^{SM} in the SM is related to the hypercharge in GUT normalization by $q_Y^{\text{GUT}} = \sqrt{\frac{3}{5}} q_Y^{\text{SM}}$ and the gauge coupling satisfies $(g_1^{\text{SM}})^2 = \frac{3}{5} (g_1^{\text{GUT}})^2$.

7.5.1 β -Function of Y_Δ

The renormalized Yukawa matrix Y_Δ is related to the bare one by

$$(Y_\Delta)_B = \left(Z_{\ell_L}^{-\frac{1}{2}} \right)^T Y_\Delta \mu^{\frac{\epsilon}{2}} Z_{Y_\Delta} Z_{\ell_L}^{-\frac{1}{2}} Z_\Delta^{-\frac{1}{2}}. \quad (7.46)$$

From this equation, the relevant parameters are determined which are defined in Eq. (B.1).

$$\begin{aligned} Z_{\phi_1} &= Z_{\ell_L}^T, & Z_{\phi_2} &= Z_{\ell_L}, & Z_{\phi_3} &= Z_\Delta, \\ Q &= Y_\Delta, & n_1 &= n_2 = n_3 = -\frac{1}{2}, & D_Q &= \frac{1}{2} \end{aligned} \quad (7.47)$$

Since Y_Δ is renormalized multiplicatively, Eq. (B.4) can be used to calculate the β -function of Y_Δ . The other parameters V_A which show up in Eq. (B.4) are the gauge couplings g_1 and g_2 , the Yukawa couplings Y_e and Y_ν , their complex conjugates or equivalently their hermitian conjugates and the gauge fixing parameters ξ_1 and ξ_2 . However, the gauge fixing parameters do not have to be included in the set of the V_A 's, because the gauge fixing parameters remain dimensionless in d dimensions, i.e. $D_{\xi_i} = 0$. The dimensions of the other parameters change. Thus they are multiplied by the renormalization scale to some power. In particular, the relevant parameters obey $D_{Y_e} = D_{Y_\nu} = D_{g_1} = D_{g_2} = \frac{1}{2}$. Inserting all definitions in Eq. (B.4) yields the β -function for Y_Δ

$$\begin{aligned} 32\pi^2 \beta_{Y_\Delta} &= \left[Y_\nu^\dagger Y_\nu + Y_e^\dagger Y_e - 3Y_\Delta^\dagger Y_\Delta \right]^T Y_\Delta + Y_\Delta \left[Y_\nu^\dagger Y_\nu + Y_e^\dagger Y_e - 3Y_\Delta^\dagger Y_\Delta \right] \\ &\quad + \left[-\frac{9}{5} g_1^2 - 9g_2^2 - 2 \operatorname{tr} \left(Y_\Delta^\dagger Y_\Delta \right) \right] Y_\Delta. \end{aligned} \quad (7.48)$$

Although the counterterm for the Yukawa vertex is flavor-diagonal, the β -function is not flavor-diagonal, because of the contributions from the wave function renormalization of the left-handed lepton doublet. The other contribution to the neutrino mass matrix is from the $\phi\Delta\phi$ interaction in the Higgs potential and M_Δ^2 .

7.5.2 β -Functions of Λ_6 and the Anomalous Dimension of M_Δ

The vertex $\phi\Delta\phi$ can not be renormalized multiplicatively, because there is a contribution from a fermion loop which is not proportional to Λ_6 . Hence, the formula Eq. (B.2) for the β -function of an additively renormalized quantity has to be used, but the procedure is the same. At first, the parameters are determined from the relation of the bare coupling to the renormalized one:

$$(\Lambda_6)_B = \left(Z_\phi^{-\frac{1}{2}} \right)^T Z_\Delta^{-\frac{1}{2}} \mu^\epsilon (\Lambda_6 + \delta\Lambda_6) Z_\phi^{-\frac{1}{2}}. \quad (7.49)$$

Thus it can be read off, that

$$\begin{aligned} Z_{\phi_1} &= Z_\phi^T, & Z_{\phi_2} &= Z_\Delta, & Z_{\phi_3} &= Z_\phi, \\ Q &= \Lambda_6, & n_1 &= n_2 = n_3 = -\frac{1}{2}, & D_Q &= 1 \end{aligned} \quad (7.50)$$

and the set of the other parameters is given by $g_1, g_2, \xi_1, \xi_2, Y_\nu, Y_e, Y_u, Y_d, Y_\Delta$ and their hermitian conjugates. The same considerations apply for the dimension of the parameters. Thus the Yukawa and the gauge couplings obey $D_{Y_j} = D_{g_i} = \frac{1}{2}$. Using Eq. (B.2), the β -function is determined to be

$$\begin{aligned} 32\pi^2\beta_{\Lambda_6} &= \left[2\lambda - 8\Lambda_4 + 16\Lambda_5 - \frac{27}{5}g_1^2 - 21g_2^2 \right. \\ &\quad \left. + 2\text{tr} \left(Y_\nu^\dagger Y_\nu + Y_e^\dagger Y_e + 3Y_u^\dagger Y_u + 3Y_d^\dagger Y_d + Y_\Delta^\dagger Y_\Delta \right) \right] \Lambda_6 - 8\text{tr} \left(Y_\Delta^\dagger Y_\nu^T M Y_\nu \right). \end{aligned} \quad (7.51)$$

Note, that Λ_6 receives contributions from the right-handed neutrinos. Thus it is natural to assume, that Λ_6 is of the order of the masses of the right-handed neutrinos. The anomalous dimension of M_Δ^2 can be calculated similarly. In Sec. 3.5.2, the anomalous dimension is expressed in terms of $\mu \frac{d}{d\mu} M_\Delta^2$ which can be calculated in the same way as for Λ_6 . The only difference for M_Δ^2 is, that M_Δ^2 does not change its mass dimension during the continuation to d dimensions. Hence, $D_{M_\Delta^2}$ vanishes and some terms drop out in Eq.(B.2). The derivative with respect to μ is given by

$$16\pi^2\mu \frac{d}{d\mu} M_\Delta^2 = \left[-\frac{18}{5}g_1^2 - 12g_2^2 + 4\Lambda_1 + \Lambda_2 - 2\text{tr} \left(Y_\Delta^\dagger Y_\Delta \right) \right] M_\Delta^2 + 4\Lambda_4 m^2 + |\Lambda_6|^2. \quad (7.52)$$

Therefore, the anomalous dimension of M_Δ results in

$$\begin{aligned} 16\pi^2\gamma_{M_\Delta} &= -\frac{1}{2M_\Delta^2} 16\pi^2\mu \frac{d}{d\mu} M_\Delta^2 \\ &= \frac{9}{5}g_1^2 + 6g_2^2 - 2\Lambda_1 - \frac{1}{2}\Lambda_2 + \text{tr} \left(Y_\Delta^\dagger Y_\Delta \right) - 2\Lambda_4 \frac{m^2}{M_\Delta^2} - \frac{1}{2} \frac{|\Lambda_6|^2}{M_\Delta^2}. \end{aligned} \quad (7.53)$$

7.5.3 β -Functions of the other Parameters in the Higgs Potential

The β functions of the other parameters in the Higgs potential can be calculated in the same way. Therefore the calculations are not shown, but only the results are stated.

$$16\pi^2\beta_{\Lambda_1} = -\frac{36}{5}g_1^2 - 24g_2^2 + \frac{36}{25}g_1^4 + 18g_2^4 + \frac{72}{5}g_1^2g_2^2 + 8\Lambda_1^2 + 2\Lambda_1\Lambda_2 \\ + \Lambda_2^2 + 4\Lambda_4^2 + 4\Lambda_5^2 - 4\text{tr}\left(Y_\Delta^\dagger Y_\Delta\right) - 4\text{tr}\left(Y_\Delta^\dagger Y_\Delta Y_\Delta^\dagger Y_\Delta\right) \quad (7.54a)$$

$$16\pi^2\beta_{\Lambda_2} = -\frac{36}{5}g_1^2 - 24g_2^2 + 12g_2^4 - \frac{144}{5}g_1^2g_2^2 + 3\Lambda_2^2 + 8\Lambda_1\Lambda_2 - 8\Lambda_5^2 \\ - 4\text{tr}\left(Y_\Delta^\dagger Y_\Delta\right) + 4\text{tr}\left(Y_\Delta^\dagger Y_\Delta Y_\Delta^\dagger Y_\Delta\right) \quad (7.54b)$$

$$32\pi^2\beta_{\Lambda_4} = -9g_1^2 - 33g_2^2 + \frac{54}{25}g_1^4 + 12g_2^4 + 2\left[8\Lambda_1 + 2\Lambda_2 + 3\lambda + 3\Lambda_4\right. \\ \left.+ 4\text{tr}\left(Y_e^\dagger Y_e + Y_\nu^\dagger Y_\nu + 3Y_u^\dagger Y_u + 3Y_d^\dagger Y_d - Y_\Delta^\dagger Y_\Delta\right)\right] \Lambda_4 + 8\Lambda_5^2 - 8\text{tr}\left(Y_\Delta^\dagger Y_\Delta Y_\nu^\dagger Y_\nu\right) \quad (7.54c)$$

$$32\pi^2\beta_{\Lambda_5} = -9g_1^2 - 33g_2^2 - \frac{36}{5}g_1^2g_2^2 + 2\left[2\Lambda_1 - 2\Lambda_2 + \lambda + 4\Lambda_4 - 3\Lambda_5\right. \\ \left.+ 4\text{tr}\left(Y_e^\dagger Y_e + Y_\nu^\dagger Y_\nu + 3Y_u^\dagger Y_u + 3Y_d^\dagger Y_d - Y_\Delta^\dagger Y_\Delta\right)\right] \Lambda_5 + 8\text{tr}\left(Y_\Delta^\dagger Y_\Delta Y_\nu^\dagger Y_\nu\right) \quad (7.54d)$$

7.5.4 Corrections to other β -Functions

Moreover, other β -functions receive additional contributions from the Higgs triplet. The anomalous dimension of the Higgs doublet mass [59] gets an additional contribution from the Higgs triplet and therefore it is given by

$$16\pi^2\gamma_m = \frac{9}{20}g_1^2 + \frac{9}{4}g_2^2 - \frac{3}{2}\lambda - \text{tr}\left(Y_e^\dagger Y_e + Y_\nu^\dagger Y_\nu + 3Y_u^\dagger Y_u + 3Y_d^\dagger Y_d\right) \\ + \frac{2}{m^2}\text{tr}\left(Y_\nu^\dagger M^2 Y_\nu\right) - 3\Lambda_4 \frac{M_\Delta^2}{m^2} - 3\frac{|\Lambda_6|^2}{m^2}. \quad (7.55)$$

Furthermore the quartic Higgs doublet coupling in the SM [59–61] receives an additional contribution resulting in

$$16\pi^2\beta_\lambda = 6\lambda^2 - 3\lambda\left(3g_2^2 + \frac{3}{5}g_1^2\right) + 3g_2^4 + \frac{3}{2}\left(\frac{3}{5}g_1^2 + g_2^2\right)^2 \\ + 4\lambda\text{tr}\left(Y_e^\dagger Y_e + Y_\nu^\dagger Y_\nu + 3Y_d^\dagger Y_d + 3Y_u^\dagger Y_u\right) \\ - 8\text{tr}\left(Y_e^\dagger Y_e Y_e^\dagger Y_e + Y_\nu^\dagger Y_\nu Y_\nu^\dagger Y_\nu + 3Y_u^\dagger Y_u Y_u^\dagger Y_u + 3Y_d^\dagger Y_d Y_d^\dagger Y_d\right) + 6\Lambda_4^2 + 4\Lambda_5^2 \quad (7.56)$$

As the wave function renormalization constant for the left-handed lepton doublets has an additional term, all vertices receive an additional contribution per left-handed lepton attached

to the vertex which is given by

$$-\frac{1}{16\pi^2} \frac{3}{2} Y_\Delta^\dagger Y_\Delta \quad (7.57)$$

multiplied by the matrix characterizing the vertex from the left or from the right, respectively. In particular, the β -functions for the lepton Yukawa couplings [59–61] change to

$$16\pi^2 \beta_{Y_\nu = Y_\nu} \left[\frac{3}{2} Y_\nu^\dagger Y_\nu - \frac{3}{2} Y_e^\dagger Y_e - \frac{3}{2} Y_\Delta^\dagger Y_\Delta \right] + Y_\nu \left[\text{tr} \left(Y_\nu^\dagger Y_\nu + Y_e^\dagger Y_e + 3Y_u^\dagger Y_u + 3Y_d^\dagger Y_d \right) - \frac{9}{20} g_1^2 - \frac{9}{4} g_2^2 \right] \quad (7.58a)$$

$$16\pi^2 \beta_{Y_e = Y_e} \left[\frac{3}{2} Y_\nu^\dagger Y_\nu - \frac{3}{2} Y_e^\dagger Y_e - \frac{3}{2} Y_\Delta^\dagger Y_\Delta \right] + Y_e \left[\text{tr} \left(Y_\nu^\dagger Y_\nu + Y_e^\dagger Y_e + 3Y_u^\dagger Y_u + 3Y_d^\dagger Y_d \right) - \frac{9}{4} g_1^2 - \frac{9}{4} g_2^2 \right] \quad (7.58b)$$

and the β -function of the effective neutrino mass operator κ function changes to

$$16\pi^2 \beta_\kappa = \left[\frac{1}{2} Y_\nu^\dagger Y_\nu - \frac{3}{2} Y_e^\dagger Y_e - \frac{3}{2} Y_\Delta^\dagger Y_\Delta \right]^T \kappa + \kappa \left[\frac{1}{2} Y_\nu^\dagger Y_\nu - \frac{3}{2} Y_e^\dagger Y_e - \frac{3}{2} Y_\Delta^\dagger Y_\Delta \right] + \left[2 \text{tr} \left(Y_\nu^\dagger Y_\nu + Y_e^\dagger Y_e + 3Y_u^\dagger Y_u + 3Y_d^\dagger Y_d \right) - 3g_2^2 + \lambda \right] \kappa. \quad (7.58c)$$

7.5.5 β -Function of the Neutrino Mass Matrix

The neutrino mass matrix will be given by the type-II see-saw formula above the thresholds

$$m_\nu = -\frac{v^2}{2} \left(Y_\nu^T M^{-1} Y_\nu - \frac{Y_\Delta \Lambda_6}{M_\Delta^2} \right), \quad (7.59)$$

if there are no other contributions to the dimension 5 operator, like from a coupling to gravity [26]. Thus the β -function of the neutrino mass is given by the sum of the β -function for the contribution from the right-handed neutrinos and the contribution from the Higgs triplet.

Contribution from the right-handed Neutrinos

The renormalization group equation for the contribution of the right-handed neutrinos has an additional term which is proportional to $Y_\Delta^\dagger Y_\Delta$. Hence, there is an additional contribution to the matrix P in comparison to the type-I see-saw case which changes the evolution of the mixing parameters. In case of large quasi-degenerate eigenvalues of Y_Δ to explain a quasi-degenerate spectrum for the neutrino masses (See Sec. 4.4.3) the contribution from the triplet can be approximated like the degenerate case in the type-I see-saw scenario. This results in the following formula for P

$$P = C_e y_\tau^2 \left[\text{diag}(0, 0, 1) + \text{diag} \left(\frac{y_e^2}{y_\tau^2}, \frac{y_\mu^2}{y_\tau^2}, 0 \right) \right] + C_\nu y_3^2 \left[(U_{Li3} U_{Lj3}^*)_{i,j=1,2,3} + U_L \text{diag} \left(\frac{y_1^2}{y_3^2}, \frac{y_2^2}{y_3^2}, 0 \right) U_L^\dagger \right] + C_\Delta z_3^2 \left[\mathbb{1} + U_L^\Delta \text{diag} \left(\frac{z_1^2 - z_3^2}{z_3^2}, \frac{z_2^2 - z_3^2}{z_3^2}, 0 \right) U_L^{\Delta\dagger} \right], \quad (7.60)$$

where C_Δ ($C_\Delta = -\frac{3}{2}$ in the SM) is the coefficient in front of $Y_\Delta^\dagger Y_\Delta$. Thus, the triplet mainly contributes to the running of the masses, but there are only small corrections to the evolution of the mixing parameters.

Contribution from the Higgs Triplet

The evolution of $\kappa_\Delta = -2\frac{Y_\Delta \Lambda_6}{M_\Delta^2}$ which is proportional to the contribution of the triplet to the neutrino mass matrix is given by

$$\begin{aligned}
 16\pi^2 \beta_{\kappa_\Delta} = & \left[\frac{1}{2} Y_\nu^\dagger Y_\nu + \frac{1}{2} Y_e^\dagger Y_e - \frac{3}{2} Y_\Delta^\dagger Y_\Delta \right]^T \kappa_\Delta + \kappa_\Delta \left[\frac{1}{2} Y_\nu^\dagger Y_\nu + \frac{1}{2} Y_e^\dagger Y_e - \frac{3}{2} Y_\Delta^\dagger Y_\Delta \right] \\
 & + \kappa_\Delta \left[-3g_2^2 + \lambda - 4\Lambda_1 - \Lambda_2 - 4\Lambda_4 + 8\Lambda_5 - 4 \frac{\text{tr}(Y_\Delta^\dagger Y_\nu^T M Y_\nu)}{\Lambda_6} - 4\Lambda_4 \frac{m^2}{M_\Delta^2} - \frac{|\Lambda_6|^2}{M_\Delta^2} \right. \\
 & \left. + \text{tr}(Y_e^\dagger Y_e + Y_\nu^\dagger Y_\nu + 3Y_u^\dagger Y_u + 3Y_d^\dagger Y_d + 2Y_\Delta^\dagger Y_\Delta) \right]. \quad (7.61)
 \end{aligned}$$

Hence, the evolution of the contribution from the Higgs triplet is analogous to the evolution of the contribution from the right-handed neutrinos. However, the coefficients in the matrix P and α are not the same, as it can be seen in Eq. (7.61). α strongly depends on the parameters in the Higgs potential. Note, that α depends on the masses of the Higgs doublet and triplet. As we assume, that the mass of the Higgs triplet is close to the GUT scale, the other dimensionful parameters, m and Λ_6 , should be assumed to be of the same order², because they receive contributions from the right-handed neutrinos and the Higgs triplet.

Hence, the ratios $\frac{m^2}{M_\Delta^2}$, $\frac{|\Lambda_6|^2}{M_\Delta^2}$ and $\frac{\text{tr}(Y_\Delta^\dagger Y_\nu^T M Y_\nu)}{\Lambda_6}$ are of the order of one. The matrix P for the term from the Higgs triplet is generally larger compared to P in the contribution of the right-handed neutrino sector. Thus a stronger running for the mixing parameters is expected from the contribution proportional to the diagonal terms P_{ii} . In the case of quasi-degenerate neutrinos, the contribution from the Higgs triplet dominates and the other part can be neglected. Then, the running above the threshold of the Higgs triplet is stronger compared to the evolution below the threshold where the evolution is described by the effective neutrino mass operator. If both terms contribute equally, both terms have to be considered and the sum of the two terms shows a more complicated behavior (See Sec. 5.2.). In this case, it is difficult to make predictions analytically and the evolution has to be calculated numerically. Anyway, the evolution of the neutrino masses in type-II see-saw scenarios has to be discussed further.

²The large mass of the Higgs doublet is called the gauge hierarchy problem which has been stated in Sec. 4.1. However, the mass of the Higgs doublet should be of the order of the weak scale to explain the masses of the SM fermions without fine-tuning in the Yukawa couplings.

Chapter 8

Numerical Code

One part of this diploma thesis was the development of a code to solve the renormalization group equations for the mass matrices numerically. The approximate analytical formulae and the numerical code have been checked against each other and they agree very well. The code is implemented as a Mathematica package in order to provide an interface which is comfortable to use. It considers the evolution of the right-handed neutrinos and threshold effects of the right-handed neutrinos can be treated by integrating out the right-handed neutrinos below its mass threshold. The threshold effects of the MSSM particles are not implemented, since they are numerically less relevant [84]. Moreover, the code can be easily extended by other models. For the extraction of the mixing parameters, it relies on the package `MixingParameterTools` [72].

The Mathematica package is called **R**enormalization group **E**volution of **A**ngles and **P**hases (**REAP**) [71].

8.1 `MixingParameterTools`

The package `MixingParameterTools` consists of a set of functions to extract mixing parameters from 3×3 matrices on the one hand and to construct orthogonal and unitary 3×3 matrices from a set of given mixing parameters in standard parameterization which is given in App. A.2, on the other hand. In the case of the extraction of mixing parameters, several special cases have to be considered, because some phases will be undefined, if angles vanish.

8.2 REAP

The package **REAP** is divided in three parts. The main part is `RGESolver` which provides a standard interface between the different models and the user. Thus the user does not have to know anything about the implementation details of the different models besides the parameters of the models. The second part are the different models, like `RGESM`, `RGEMSSM`, ... which contain the model specific parts of the package. So far 3 different models have been implemented: SM, MSSM and 2HDM. Every model has 3 different versions: without right-handed neutrinos (`*0N`), with right-handed Majorana neutrinos (`*`) and with right-handed Dirac neutrinos (`*Dirac`). The extension of the SM by a Higgs triplet will be implemented soon. The third part is formed by some utility packages (`RGEUtilities`, `RGEParameters`,

`RGEInitial`, `RGEFusaokaYukawa`, `RGESymbol`) which provide several useful functions to the different models. In principle, a user only needs a limited set of functions of `RGESolver`.

8.2.1 `RGESolver`

The package distinguishes between two different kind of functions. On the one hand, there are functions which directly work with the supplied models. They are named `RGE*Model*`. On the other hand, there are functions dealing with the models which are used as an EFT, i.e. have been added by `RGEAddEFT`. These functions are named `RGE*EFT*`.

At the beginning, all models have to be loaded by `RGERegisterModel` in order to make them accessible through `RGESolver`. `RGERegisterModel` takes as argument different functions to communicate with the model. After all models have been registered which is done by the packages, the models are contained in, the user has to specify, how his sequence of EFTs is made up. Different models can be added as EFT by `RGEAddEFT`. The cutoff is specified by the option `RGECutoff`. Next, the initial values have to be supplied by the function `RGESetInitial`. Then the renormalization group equations are solved by executing `RGESolve` which uses `NDSolve` to numerically integrate the differential equations. Finally, the parameters can be obtained through `RGEGetSolution` at any scale. In order to illustrate the use of `REAP`, a small example is given.

Example

The setup is the MSSM extended by 3 right-handed neutrinos at the GUT scale of $2 \cdot 10^{16}$ GeV and set the SUSY breaking scale to 1 TeV. The initial values are set to the suggested values which are specified in the documentation [71].

- At first, we define the model and set the initial values.

```
RGEAddModel["MSSM"];
RGEAddModel["SM",RGECutoff->1000];
RGESetInitial[2 10^16];
```

The execution of `RGESolve[91.19, 2 · 1016]` solves the RGE and finds the scales where the right-handed neutrinos are integrated out.

The algorithm works in the following way:

1. Solve the RGE for the MSSM with 3 right-handed neutrinos between the GUT scale and the SUSY breaking scale without considering any thresholds.
2. Find the heaviest right-handed neutrino with mass M_3 and add a new EFT by `RGEAddEFT["MSSM",RGECutoff-> M_3 , RGEIntegratedOut->1]`.
3. Calculate initial values for MSSM with 2 right-handed neutrinos by matching κ, Y_ν, M and the other parameters at the scale where the first right-handed neutrino is integrated out.
4. Solve the RGE for the MSSM with 2 right-handed neutrinos between M_3 and the SUSY breaking scale.
5. Find the second to heaviest right-handed neutrino with mass M_2 and add a new EFT by `RGEAddEFT["MSSM", RGECutoff-> M_2 , RGEIntegratedOut->2]`.

6. Calculate initial values for MSSM with 1 right-handed neutrino.
 7. Solve the RGE for the MSSM with 1 right-handed neutrinos between M_2 and the SUSY breaking scale.
 8. Find the lightest right-handed neutrino with mass M_1 and add a new EFT by `RGEAddEFT["MSSMON", RGEcutoff-> M_1]`.
 9. Calculate initial values for MSSM without right-handed neutrinos.
 10. Solve the RGE for the MSSM without right-handed neutrinos between M_1 and the SUSY breaking scale.
 11. Calculate initial values for the SM
 12. Since all right-handed neutrinos have been integrated out already, change SM to SMON.
 13. Solve the RGE for SMON between the SUSY breaking scale and the mass of Z^0 .
- Using `RGEGetSolution[scale, quantity]`, we can query the value of a parameter *quantity* at the energy *scale*. For example, this returns the mass matrix of the light neutrinos at 100 GeV:

```
MatrixForm[RGEGetSolution[100, RGE\ [Nu]]]
```

- To find the leptonic mass parameters, the function `MNSParameters[m_ν, Y_e]` (which also needs the Yukawa matrix of the charged leptons) can be used. The results are given in the order $\{\{\theta_{12}, \theta_{13}, \theta_{23}, \delta, \delta_e, \delta_\mu, \delta_\tau, \varphi_1, \varphi_2\}, \{m_1, m_2, m_3\}, \{y_e, y_\mu, y_\tau\}\}$.

```
MNSParameters[RGEGetSolution[100, RGE\ [Nu]], RGEGetSolution[100, RGEYe]]
```

- Finally, the running of the mixing angles can be plotted:

```
Needs["Graphics`Graphics`"]
mNu[x_] := RGEGetSolution[x, RGE\ [Nu]]
Ye[x_] := RGEGetSolution[x, RGEYe]
\ [Theta] 12[x_] := MNSParameters[mNu[x], Ye[x]] [[1, 1]]
\ [Theta] 13[x_] := MNSParameters[mNu[x], Ye[x]] [[1, 2]]
\ [Theta] 23[x_] := MNSParameters[mNu[x], Ye[x]] [[1, 3]]
LogLinearPlot[{ \ [Theta] 12[x], \ [Theta] 13[x], \ [Theta] 23[x] },
{x, 91.19, 2*10^16}]
```

To produce nicer plots, the notebook `RGEPlots.nb` which is included in the package, can be used. One example of a plot is shown in Fig. 8.1. The grayish regions correspond to the different EFTs. At each border between the regions, one right-handed neutrino is integrated out. The kink in the curve for the solar angle θ_{12} is due to the transition from the MSSM to the SM, because the evolution of θ_{12} is enhanced by $\tan^2 \beta$ in the MSSM.

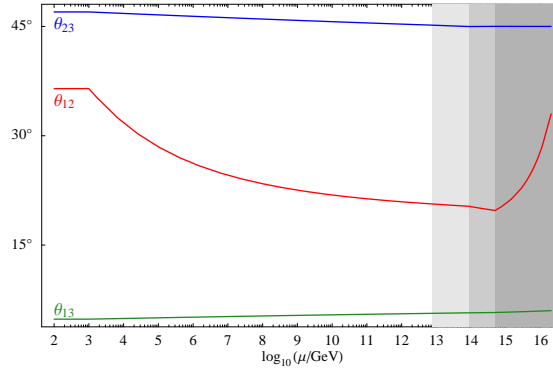


Figure 8.1: Example of a plot of the leptonic mixing angles

8.2.2 Implementation of RGESearchTransitions

The algorithm to find the scale where a right-handed neutrino is integrated out is a fixed-point iteration. It will be guaranteed to converge by the Banach fixed-point theorem, if the Lipschitz constant of the function $x \rightarrow \text{Max}(\text{Eigenvalues}(\text{Mass}(x)))$ is smaller than 1 for the relevant interval between the starting point and the fixed-point. Equivalently, the first derivative of the natural logarithm of this function has to be smaller than 1 in this interval. In order to decide, whether the fixed-point iteration converges, the RGE for the right-handed neutrino masses have to be observed. The running is small, as it can be seen in Sec. 5.5 which yields that it will be smaller than one, if the condition $\sum_j |(Y_\nu)_{ij}|^2 < \frac{8\pi^2}{C_r}$ is satisfied. Hence, the algorithm is convergent, since the Yukawa couplings are of the order of one.

8.2.3 Initial Values and Output Functions

The initial values are set via the function `RGESetInitial`. At first, this function determines the name of the model which is valid at this scale. Then it calls a function of the model which generates the initial values from the options which are passed to `RGESetInitial`. If an option is not set, the function will use default values which are provided by each model. All models have default values at the GUT scale and some have default values at the mass of the Z^0 boson.

The function `RGEGetSolution` is the standard interface to return the parameters of a given model. It hides the EFTs which are valid in the different energy ranges, by determining first the name of the valid model and then calling the function which has to be provided by the model, e.g. although all right-handed neutrinos are integrated out, `RGESMON` provides a function to determine the right-handed neutrino mass matrix and the user does not have to care about the different ranges of validity of the EFTs.

Chapter 9

Summary & Conclusions

In this thesis, the dependence of the low-energy leptonic mixing parameters on the renormalization scale μ in see-saw models has been investigated.

In the type-I see-saw scenario, the RGEs of the mixing parameters have been discussed. The equations show that, above and between the see-saw scales, the running differs from the evolution in the effective theory, because P is in general non-diagonal and therefore there are more contributions to the running. These additional contributions can suppress the RG effect by cancellations or enhance the effect. In addition, it is possible that the evolution above the see-saw scales is canceled by the RG change in the effective theory. Although the general form of the expressions is the same, namely

$$\mu \frac{d\theta_{ij}}{d\mu}, \mu \frac{d\delta}{d\mu}, \mu \frac{d\varphi_i}{d\mu} \propto \sum_k \frac{f_k(\text{masses}, \delta, \varphi_1, \varphi_2)}{m_j^2 - m_i^2} \times F_k^{(ij)}(\text{Yukawa couplings}, \theta_{12}, \theta_{13}, \theta_{23}), \quad (6.5)$$

above the see-saw scales, some of the statements which are valid in the effective theory do not hold above the lightest right-handed neutrino. Firstly, the mixing parameters can be generated radiatively and zero mixing is not a fixed point any longer. In addition, the solar angle θ_{12} can evolve towards smaller values for $\theta_{13} = 0$ when running down and the dependence on $\tan \beta$ in the MSSM is not as strong as below the see-saw scales, because the relation between the neutrino Yukawa couplings and the masses is almost independent of $\tan \beta$. However, the size of the RG effect is still governed by the mass squared difference in the denominator. Hence, the strongest running effects are in the case of a quasi-degenerate spectrum, too. In addition, the evolution is particularly important between the thresholds. Although the thresholds are close to each other compared to the large mass of the right-handed neutrinos, there are large RG effects which can be of the same order as the total effect in the effective theory. The two different contributions to the neutrino mass matrix from the effective neutrino mass operator and the see-saw mechanism are generally governed by a different dependence on the renormalization scale μ which leads to a particularly strong evolution of the angles and phases. Furthermore, the stability of the quark-lepton complementarity (QLC) relation against radiative corrections has been discussed. The strong dependence on the neutrino mass hierarchy, $\tan \beta$, the strength of the Yukawa couplings and the Majorana CP phase difference has been pointed out and illustrated in plots showing the region in parameter space compatible with QLC.

Moreover, it has been shown, that right-handed neutrinos will have an invertedly hierarchical spectrum, if they are degenerate at some high-energy scale and the neutrino Yukawa matrix

obeys a normal hierarchy. This is due to the proportionality of the RG effect of the right-handed neutrinos to the square of the corresponding Yukawa coupling. The generated splitting might be used in leptogenesis to enhance the lepton asymmetry resonantly. As the resonance condition is strongly dependent on the mass splitting, the RG evolution of the masses has to be taken into account in resonant leptogenesis.

Furthermore, the renormalization group equation of the type-II see-saw contribution in the SM has been calculated, as well as the RGEs of the parameters in the Higgs potential. These can be used to estimate the RG effects in type-II see-saw models. Besides the additional contribution to the neutrino mass, also the RGEs of the type-I contribution receive an additional term enhancing the RG effect. As the RGE of the type-II contribution differs from the RGE of the type-I contribution, the situation is the same as between the see-saw scales. Due to the interplay of both contributions, large RG effects of the mixing angles and phases can be expected. However, in the case of a quasi-degenerate spectrum, the neutrino mass is dominantly given by the triplet contribution and the part from the right-handed neutrinos can be neglected. Hence, the evolution of the neutrino mass matrix is approximately described by the β -function of the triplet contribution above the threshold of the triplet. Below the threshold, it is described by the evolution of the effective neutrino mass operator κ . As the RG evolution of the mixing angles is generally large in the MSSM, performing the same calculation in the MSSM would be interesting to estimate the RG effects in supersymmetric type-II see-saw models.

Finally, a code was developed to calculate the evolution of the mixing parameters numerically. The numerically calculated evolution of the mixing parameters has been compared to the approximate analytical formulae and the slopes of the mixing parameters agree well. As the RG effects are especially important in the case of quasi-degenerate neutrinos and the RGEs in the complete type-II scenario are difficult to solve analytically, the numerical code **REAP** will prove to be useful in the analysis of type-II see-saw models. In general, as soon as there are several contributions to the neutrino mass matrix of the same order it is difficult to solve the RGEs analytically and a numerical calculation is necessary. Furthermore, **REAP** can serve as a practical tool for model builders to check the consistency of their predictions at an high-energy scale with the experimental data in the low-energy regime.

Concluding, the renormalization group evolution is important in the lepton sector, because the mass squared differences are small and the angles are large in contrast to the quark sector. In the field of the renormalization group evolution in the lepton sector, it will be interesting to derive the RGEs for the type-II see-saw case in the MSSM to estimate the RG effects, but the application of the RG effects to specific models will be even more rewarding, in particular, to models which predict quasi-degenerate neutrinos. **REAP** can be used in this case to obtain the low-energy observables from high-energy predictions in order to compare them with the experiment.

Appendix A

Models

In this section, the SM model and two extensions are briefly reviewed and the Feynman rules for the extension of the SM by a Higgs triplet are presented. The main purpose is the definition of the Lagrangian and the terminology.

A.1 Standard Model (SM)

The SM gauge group is $G_{321} = \text{SU}(3)_C \times \text{SU}(2)_L \times \text{U}(1)_Y$ and the fermionic particle content is given by all combinations of the fundamental representations of the gauge groups, except for the total singlet corresponding to a right-handed neutrino. The particle content is given in Tab. A.1. There are 3 different flavors — families — of each particle. The gauge interactions are mediated by 12 gauge bosons, 8 gauge bosons of strong interactions and 4 gauge bosons of electroweak interactions. As the gauge group which is measured in the low-energy regime is not G_{321} but $\text{SU}(3)_C \times \text{U}(1)_{\text{em}}$, the gauge symmetry has to be broken. In the SM, this is done via the Higgs mechanism which is sketched in Sec. 2.1.3. Therefore, there is also a scalar $\text{SU}(2)_L$ -doublet. The Lagrangian is defined as

$$\mathcal{L} = \mathcal{L}_{\text{fermion}} + \mathcal{L}_{\text{Yukawa}} + \mathcal{L}_{\text{gauge}} + \mathcal{L}_{\text{gf}} + \mathcal{L}_{\text{ghost}} + \mathcal{L}_{\text{Higgs}} , \quad (\text{A.1})$$

where the terms are given by

$$\begin{aligned} \mathcal{L}_{\text{fermion}} = & \overline{Q}_L \not{D} Q_L + \overline{u}_R \not{D} u_R + \overline{d}_R \not{D} d_R \\ & + \overline{\ell}_L \not{D} \ell_L + \overline{e}_R \not{D} e_R \end{aligned} \quad (\text{A.2a})$$

$$\begin{aligned} \mathcal{L}_{\text{Yukawa}} = & - (Y_d)_{ij} \overline{d}_R^i Q_L^j \phi - (Y_u)_{ij} \overline{u}_R^i Q_L^j \phi^C \\ & - (Y_e)_{ij} \overline{e}_R^i \ell_L^j \phi + \text{h.c.} \end{aligned} \quad (\text{A.2b})$$

$$\mathcal{L}_{\text{Higgs}} = \overline{D}_\mu \phi D^\mu \phi - V(\phi^\dagger \phi) \quad (\text{A.2c})$$

$$\mathcal{L}_{\text{gauge}} = -\frac{1}{4} B_{\mu\nu} B^{\mu\nu} - \frac{1}{2} \text{tr} W_{\mu\nu} W^{\mu\nu} - \frac{1}{2} \text{tr} G_{\mu\nu} G^{\mu\nu} \quad (\text{A.2d})$$

$$\mathcal{L}_{\text{gauge fixing}} = -\frac{1}{2\xi_1} (\partial_\mu B^\mu)^2 - \sum_i \frac{1}{2\xi_2} (\partial_\mu W_i^\mu)^2 - \sum_i \frac{1}{2\xi_3} (\partial_\mu G_i^\mu)^2 \quad (\text{A.2e})$$

$$\mathcal{L}_{\text{ghost}} = (\partial_\mu c_2^i)^\dagger \left(\delta^{ij} \partial^\mu + g_2 \epsilon^{ijk} W^{k\mu} \right) c_2^j + (\partial_\mu c_3^A)^\dagger \left(\delta^{AB} \partial^\mu + g_3 f^{ABC} W^{C\mu} \right) c_3^B ,$$

	$SU(3)_C$	$SU(2)_L$	q_Y^{SM}	q_Y^{GUT}
quarks				
Q_L	3	2	$\frac{1}{6}$	$\sqrt{\frac{1}{60}}$
u_R	3	1	$\frac{2}{3}$	$\sqrt{\frac{4}{15}}$
d_R	3	1	$-\frac{1}{3}$	$-\sqrt{\frac{1}{15}}$
leptons				
L_L	1	2	$-\frac{1}{2}$	$-\sqrt{\frac{3}{20}}$
e_R	1	1	-1	$-\sqrt{\frac{3}{5}}$
ν_R	1	1	0	0
Higgs				
Higgs h	1	2	$\frac{1}{2}$	$\sqrt{\frac{3}{20}}$
gauge bosons				
gluon g	8	1	0	0
W boson W	1	3	0	0
B	1	1	0	0

Table A.1: Particle content of the SM extended by right-handed neutrinos. The electric charge is related to the $SU(2)_L \times U(1)_Y$ quantum numbers by $Q = T_3 + XSY$.

(A.2f)

where ϵ^{ijk} and f^{ABC} are the structure constants of $SU(2)_L$ and $SU(3)_C$, respectively. The Higgs potential is defined as

$$V(\phi^\dagger \phi) = \frac{\lambda}{2} \left(\phi^\dagger \phi - \frac{v^2}{2} \right) \quad (\text{A.3})$$

and the covariant derivative is given by

$$D_\mu = \partial_\mu + i\sqrt{\frac{3}{5}}g_1 Y B_\mu + ig_2 W_\mu + ig_3 G_\mu, \quad (\text{A.4})$$

where $W_\mu = \frac{\sigma_m}{2} W_\mu^m$, B_μ are the gauge fields of electroweak interactions ($SU(2)_L \times U(1)_Y$) and $G_\mu = \frac{\lambda_m}{2} G_\mu^{m1}$ is the gauge field of strong interactions ($SU(3)_C$). We use the GUT charge normalization throughout this thesis which is related to the charge normalization in the SM by

$$q_Y^{\text{GUT}} = \sqrt{\frac{3}{5}} q_Y^{\text{SM}}. \quad (\text{A.5})$$

¹The matrices λ_m are the Gell-Mann matrices.

Therefore the coupling constant satisfies

$$(g_1^{\text{SM}})^2 = \frac{3}{5} (g_1^{\text{GUT}})^2. \quad (\text{A.6})$$

The covariant derivative depends on the representation of the particle, e.g. for leptons, there is no $\text{SU}(3)_C$ -term. The field strengths are given by

$$B_{\mu\nu} = \partial_\mu B_\nu - \partial_\nu B_\mu \quad (\text{A.7a})$$

$$W_{\mu\nu}^i = \partial_\mu W_\nu^i - \partial_\nu W_\mu^i + ig_2 \epsilon^{ijk} W_\mu^j W_\nu^k \quad (\text{A.7b})$$

$$G_{\mu\nu}^A = \partial_\mu G_\nu^A - \partial_\nu G_\mu^A + ig_3 f^{ABC} G_\mu^B G_\nu^C. \quad (\text{A.7c})$$

The terms containing the Hodge dual field $\widetilde{G}_{\mu\nu} = \frac{1}{2} \epsilon_{\mu\nu\kappa\lambda} G^{\kappa\lambda}$ strength,

$$\mathcal{L}_{\text{dual}} = -\frac{1}{2} \text{tr} \widetilde{W}_{\mu\nu} W^{\mu\nu} - \frac{1}{2} \text{tr} \widetilde{G}_{\mu\nu} G^{\mu\nu} \quad (\text{A.8})$$

are omitted, since they have not been measured yet. The problem of the smallness of these terms is called the strong CP problem [85].

Besides the gauge couplings and the Higgs self-coupling, the parameters of the SM are the masses and the mixing angles and phases in the quark and lepton sector. The mixing matrix in the quark sector is called Cabbibo-Kobayashi-Maskawa (CKM) matrix and is described by 3 angles and 1 CP phase. In the lepton sector, there is no mixing matrix, as long as neutrinos are massless. However, if the neutrinos are massive and Majorana particles, the mixing matrix will be described by 3 angles and 3 phases. In the next section we give our parameterization of the MNS matrix.

A.2 Standard Parameterization

A unitary matrix can be described by 3 angles and 6 phases. Thus it can be written in the following way:

$$U = \text{diag}(e^{i\delta_e}, e^{i\delta_\mu}, e^{i\delta_\tau}) \cdot V(\theta_{12}, \theta_{13}, \theta_{23}) \cdot \text{diag}(e^{-i\varphi_1/2}, e^{-i\varphi_2/2}, 1) \quad (\text{A.9})$$

V is a special unitary matrix and is parameterized in standard parameterization like the CKM matrix in the quark sector with 3 angles (θ_{12} , θ_{13} , θ_{23}) and 1 CP phase (δ).

$$V(\theta_{12}, \theta_{13}, \theta_{23}) = \begin{pmatrix} c_{12}c_{13} & s_{12}c_{13} & s_{13}e^{-i\delta} \\ -c_{23}s_{12} - s_{23}s_{13}c_{12}e^{i\delta} & c_{23}c_{12} - s_{23}s_{13}s_{12}e^{i\delta} & s_{23}c_{13} \\ s_{23}s_{12} - c_{23}s_{13}c_{12}e^{i\delta} & -s_{23}c_{12} - c_{23}s_{13}s_{12}e^{i\delta} & c_{23}c_{13} \end{pmatrix} \quad (\text{A.10})$$

where s_{ij} and c_{ij} are defined as $s_{ij} = \sin \theta_{ij}$ and $c_{ij} = \cos \theta_{ij}$, respectively. In addition there are phase matrices multiplied from both sides. The matrix on the left-hand side is characterized by the unphysical phases δ_e , δ_μ and δ_τ which can be rotated away by a change of the phases in the charged left-handed leptons in the extended (MS)SM.

$$|\ell_L\rangle \rightarrow \text{diag}(e^{-i\delta_e}, e^{-i\delta_\mu}, e^{-i\delta_\tau}) |\ell_L\rangle \quad (\text{A.11})$$

The matrix on the right-hand side is described by the Majorana phases φ_1 and φ_2 . These can not be rotated away by a redefinition of fields, because the effective neutrino mass term is a Majorana mass term which is diagonalized by an unitary transformation and not by a biunitary transformation like the Yukawa matrix of the charged leptons.

A.3 \mathbb{Z}_2 -symmetric Two Higgs Doublet Model

The two Higgs doublet model (2HDM) contains a second Higgs particle in addition to the SM particles. In the \mathbb{Z}_2 -symmetric 2HDM all particles obey a \mathbb{Z}_2 symmetry. Depending on the representation $\mathbf{1}$ or $\mathbf{1}'$ of the particle, one of the 2 Higgs doublets couples to the particle. Concretely, the first Higgs is in the $\mathbf{1}$ representation and the second Higgs in the $\mathbf{1}'$ representation. Particles which are in the $\mathbf{1}$ representation, obtain their mass by the first Higgs and particles which are in the $\mathbf{1}'$ representation, receive their mass from the second Higgs.

$$\mathbf{1} \times \mathbf{1} = \mathbf{1} \quad (\text{A.12a})$$

$$\mathbf{1} \times \mathbf{1}' = \mathbf{1}' \quad (\text{A.12b})$$

$$\mathbf{1}' \times \mathbf{1}' = \mathbf{1} \quad (\text{A.12c})$$

There are 4 different types of \mathbb{Z}_2 -symmetric two Higgs doublet models which are shown in Tab. A.2 without right-handed neutrinos and 8 with right-handed neutrinos.

particle	(i)	(ii)	(iii)	(iv)
u	$\mathbf{1}$	$\mathbf{1}'$	$\mathbf{1}$	$\mathbf{1}'$
d	$\mathbf{1}$	$\mathbf{1}$	$\mathbf{1}'$	$\mathbf{1}'$

Table A.2: Different two Higgs doublet models without right-handed neutrinos. The charged leptons are always in the trivial representation $\mathbf{1}$

The Higgs potential of the \mathbb{Z}_2 -symmetric 2HDM depends on 5 parameters ($\lambda_1 \dots \lambda_5$).

$$\begin{aligned} \mathcal{L}_{\text{Higgs}} = & -\frac{\lambda_1}{4} \left(\phi_1^\dagger \phi_1 \right)^2 - \frac{\lambda_2}{4} \left(\phi_2^\dagger \phi_2 \right)^2 - \lambda_3 \left(\phi_1^\dagger \phi_1 \right) \left(\phi_2^\dagger \phi_2 \right) \\ & - \lambda_4 \left(\phi_1^\dagger \phi_2 \right) \left(\phi_2^\dagger \phi_1 \right) - \left[\frac{\lambda_5}{4} \left(\phi_1^\dagger \phi_2 \right)^2 + \text{h.c.} \right] \end{aligned} \quad (\text{A.13})$$

Without an imposed \mathbb{Z}_2 -symmetry, there are more terms in the Higgs potential allowed, like $\phi_1^\dagger \phi_1 \phi_1^\dagger \phi_2, \dots$. The main problem will be flavor changing neutral currents (FCNC), if there is no \mathbb{Z}_2 -symmetry or another symmetry ensuring that there are not two mass terms for one particle. As two mass terms for a fermion usually are not diagonal at the same time, but only the sum is diagonal in the mass basis, there are off-diagonal elements in the mass matrices inducing FCNC which already are strongly constrained by experimental upper bounds.

A.4 Minimal Supersymmetric Standard Model

The minimal supersymmetric standard model (MSSM) [86] extends the SM by another space-time symmetry. This new symmetry is called supersymmetry and transforms bosons into fermions and vice versa. All space-time symmetries form a super Lie algebra, i.e. a \mathbb{Z}_2 -graded Lie algebra. There is not any other extension of the Poincaré symmetry which is based on a Lie algebra and is compatible with the SM, as it is stated by the Coleman-Mandula theorem. In addition to the particles of the SM, the MSSM contains a superpartner of every particle and an additional Higgs particle to give mass to all chiral fermions, because the superpotential

is required to be analytic and therefore the charge conjugate of a Higgs doublet is forbidden. Moreover, the particles are arranged in supermultiplets which are the irreps of the super Lie algebra. Hence, the superpartner has the same quantum numbers as the corresponding particle. The interactions are described by the superpotential which is formed by products of supermultiplets. One of the main achievements of supersymmetry is the solution of the gauge hierarchy problem in the SM (See Sec. 4.1, since the contributions of the fermion in the multiplet exactly cancels the contributions of the scalars in the loop).

A.5 Feynman Rules for the new Vertices involving the Higgs Triplet

Feynman rules for theories, in which the fermion number is violated, have to be treated carefully to get the correct relative sign for the interfering vertices. This is the case in theories involving Majorana fermions, like the right-handed neutrinos. Therefore, the Feynman rules are derived according to the prescription given by Denner [87], who has replaced the fermion number flow by the fermion flow to accommodate for the correct sign between interfering Feynman diagrams. This fermion flow is of no importance for the additional Higgs triplet, since the Yukawa matrix Y_Δ of the $\ell_L \ell_L \Delta$ vertex is symmetric. Hence, the diagram of the reversed fermion flow gives the same result. However, the fermion flow is important for the other diagrams which are given in App. A.1 of Jörn Kerstens diploma thesis [59].

Propagator

$$\begin{array}{c} \text{---} \Delta_a \text{---} \longrightarrow \text{---} \Delta_b \text{---} \end{array} : \quad iS_\Delta(p) = \frac{i}{p^2 - M_\Delta^2 + i\varepsilon} \delta_{ba} \quad (\text{A.14})$$

Higgs - Higgs Interactions

$$\begin{array}{c} \begin{array}{ccc} & \nearrow & \nwarrow \\ \Delta_b & \bullet & \Delta_d \\ & \nwarrow & \nearrow \\ \Delta_a & \bullet & \Delta_c \end{array} \end{array} : \quad -i\mu^\epsilon (\Lambda_1 (\delta_{ba}\delta_{dc} + \delta_{da}\delta_{bc}) + \Lambda_2 \delta_{bd}\delta_{ca}) \quad (\text{A.15a})$$

$$\begin{array}{c} \begin{array}{ccc} & \nearrow & \nwarrow \\ \Delta_b & \bullet & \phi_d \\ & \nwarrow & \nearrow \\ \Delta_a & \bullet & \phi_c \end{array} \end{array} : \quad -i\mu^\epsilon (\Lambda_4 \delta_{dc}\delta_{ba} + \Lambda_5 i\epsilon_{bam} (\sigma_m)_{dc}) \quad (\text{A.15b})$$

$$: \Lambda_6 \mu^{\frac{\epsilon}{2}} (\sigma_2 \sigma_c)_{ba} \quad (\text{A.15c})$$

$$: -\Lambda_6^* \mu^{\frac{\epsilon}{2}} (\sigma_c \sigma_2)_{ab} \quad (\text{A.15d})$$

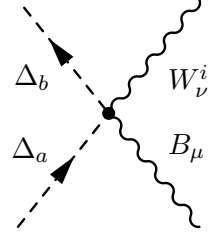
Gauge Boson - Higgs Interactions

$$: -i\sqrt{\frac{3}{5}} g_1 \mu^{\frac{\epsilon}{2}} (p_\mu + q_\mu) \delta_{ba} \quad (\text{A.16a})$$

$$: -ig_2 \mu^{\frac{\epsilon}{2}} (p_\mu + q_\mu) (i\epsilon_{bia}) \quad (\text{A.16b})$$

$$: i\frac{6}{5} g_1^2 \mu^\epsilon \eta_{\mu\nu} \delta_{ba} \quad (\text{A.16c})$$

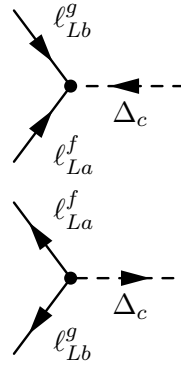
$$: -ig_2^2 \mu^\epsilon \eta_{\mu\nu} (\delta_{bi} \delta_{ja} + \delta_{bj} \delta_{ia} - 2\delta_{ij} \delta_{ba}) \quad (\text{A.16d})$$



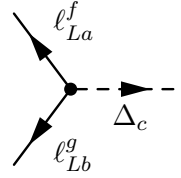
$$: -2\sqrt{\frac{3}{5}}g_1g_2\mu^\epsilon\eta_{\mu\nu}\epsilon_{bia} \quad (\text{A.16e})$$

Note, that GUT charge normalization is used for the $U(1)_Y$ hypercharge, i.e. the charge q_Y is related to the charge in GUT normalization by $q_Y^U = \sqrt{\frac{3}{5}}q_Y$ and the gauge coupling satisfies $g_1^2 = \frac{3}{5}(g_1^U)^2$. Furthermore, the convention is used, that ∂_μ in position space corresponds to $-ip_\mu$ in momentum space.

Lepton - Higgs Interactions

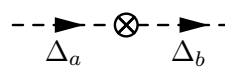


$$: (Y_\Delta)_{gf} \mu^{\frac{\epsilon}{2}} (\sigma_2 \sigma_c)_{ba} P_L \quad (\text{A.17a})$$



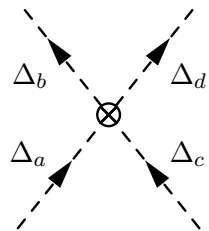
$$: -\left(Y_\Delta^\dagger\right)_{fg} \mu^{\frac{\epsilon}{2}} (\sigma_c \sigma_2)_{ab} P_R \quad (\text{A.17b})$$

Counterterms for 2-Point Functions

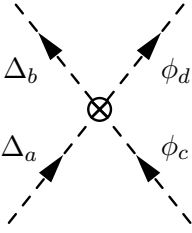


$$: i(p^2 \delta Z_\Delta - \delta M_\Delta^2) \delta_{ba} \quad (\text{A.18})$$

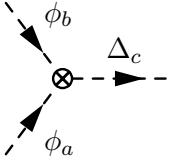
Counterterms for Higgs - Higgs Vertices



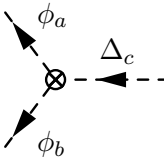
$$: -i\mu^\epsilon [\delta\Lambda_1 (\delta_{ba}\delta_{dc} + \delta_{da}\delta_{bc}) + \delta\Lambda_2 \delta_{bd}\delta_{ac}] \quad (\text{A.19a})$$



$$: -i\mu^\epsilon [\delta\Lambda_4\delta_{ab}\delta_{cd} + \delta\Lambda_5 i\epsilon_{bam} (\sigma_m)_{dc}] \quad (\text{A.19b})$$

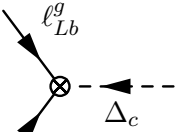


$$: \delta\Lambda_6\mu^{\frac{\epsilon}{2}} (\sigma_2\sigma_c)_{ba} \quad (\text{A.19c})$$

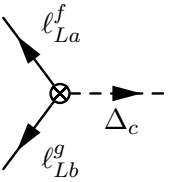


$$: -\delta\Lambda_6^*\mu^{\frac{\epsilon}{2}} (\sigma_c\sigma_2)_{ab} \quad (\text{A.19d})$$

Counterterms for Yukawa Vertices



$$: (Y_\Delta\delta Z_{Y_\Delta})_{gf}\mu^{\frac{\epsilon}{2}} (\sigma_2\sigma_c)_{ba} P_L \quad (\text{A.20a})$$



$$: -\left(\delta Z_{Y_\Delta}^\dagger Y_\Delta^\dagger\right)_{fg}\mu^{\frac{\epsilon}{2}} (\sigma_c\sigma_2)_{ab} P_R \quad (\text{A.20b})$$

Appendix B

β -Function of a tensorial Quantity

In this section, the formula for the β -function of a tensorial quantity is stated [59]. The β function of an arbitrary quantity Q , which is defined as

$$Q_B = \left(\prod_{i=1}^M Z_{\phi_i}^{n_i} \right) [Q + \delta Q] \mu^{D_Q \epsilon} \left(\prod_{j=M+1}^{M+N} Z_{\phi_j}^{n_j} \right), \quad (\text{B.1})$$

is given by

$$\begin{aligned} \beta_Q^{(0)} = & D_Q \left\langle \frac{d\delta Q_{,1}}{dQ} | Q \right\rangle + \sum_A D_{V_A} \left\langle \frac{d\delta Q_{,1}}{dV_A} | V_A \right\rangle - D_Q \delta Q_{,1} \\ & + \sum_{i=1}^M n_i \left[D_Q \left\langle \frac{d\delta Z_{\phi_i,1}}{dQ} | Q \right\rangle + \sum_A D_{V_A} \left\langle \frac{d\delta Z_{\phi_i,1}}{dV_A} | V_A \right\rangle \right] Q \\ & + Q \sum_{j=M+1}^{M+N} n_j \left[D_Q \left\langle \frac{d\delta Z_{\phi_j,1}}{dQ} | Q \right\rangle + \sum_A D_{V_A} \left\langle \frac{d\delta Z_{\phi_j,1}}{dV_A} | V_A \right\rangle \right], \end{aligned} \quad (\text{B.2})$$

where V_A are other independent parameters¹ and D_{V_A} are like D_Q the exponents of the renormalization scale. The other used definitions are the expansions of all quantities in Eq. (B.1)

$$\beta_Q = \beta_Q^{(0)} + \beta_Q^{(1)} \epsilon + \dots \quad (\text{B.3a})$$

$$Z_{\phi_i}^{n_i} = 1 + n_i \delta Z_{\phi_i,1} \frac{1}{\epsilon} + \dots \quad (\text{B.3b})$$

$$\delta Q = \delta Q_{,1} \frac{1}{\epsilon} + \dots \quad (\text{B.3c})$$

and the definition of the abbreviation

$$\left\langle \frac{dF}{dx} | y \right\rangle := \begin{cases} \frac{dF}{dx} y & \text{for scalars } x, y \\ \frac{dF}{dx_n} y_n & \text{for vectors } x, y \\ \frac{dF}{dx_{mn}} y_{mn} & \text{for matrices } x, y \\ \dots & \end{cases}. \quad (\text{B.3d})$$

¹Note, that complex conjugates are independent parameters.

Note, that parameters V_B obeying $D_{V_B} = 0$ do not have to be included in the set of the parameters V_A . These are for example, the masses of scalar particles and the gauge fixing parameters. In the case of multiplicative renormalization, i.e. $\delta Q = Q\delta Z_Q$, the formula simplifies to

$$\begin{aligned}
\beta_Q^{(0)} = & Q \left[D_Q \left\langle \frac{d\delta Z_{Q,1}}{dQ} | Q \right\rangle + \sum_A D_{V_A} \left\langle \frac{d\delta Z_{Q,1}}{dV_A} | V_A \right\rangle \right] \\
& + \sum_{i=1}^M n_i \left[D_Q \left\langle \frac{d\delta Z_{\phi_{i,1}}}{dQ} | Q \right\rangle + \sum_A D_{V_A} \left\langle \frac{d\delta Z_{\phi_{i,1}}}{dV_A} | V_A \right\rangle \right] Q \\
& + Q \sum_{j=M}^{M+N} n_j \left[D_Q \left\langle \frac{d\delta Z_{\phi_{j,1}}}{dQ} | Q \right\rangle + \sum_A D_{V_A} \left\langle \frac{d\delta Z_{\phi_{j,1}}}{dV_A} | V_A \right\rangle \right] .
\end{aligned} \tag{B.4}$$

Appendix C

Mathematics

This chapter is a compilation of useful formulae and theorems which are often needed in the renormalization group analysis of chiral gauge theories.

C.1 Diagonalization of Matrices

Here, 3 theorems about matrix diagonalization are given [72] which are often used for mass matrices.

C.1.1 Diagonalization of Hermitian Matrices

Hermitian matrices H have non-negative real eigenvalues μ_i .

$$Hu_i = \mu_i u_i \quad (\text{C.1})$$

The eigenvectors u_i form a unitary matrix $U = [u_1, \dots, u_n]$ which can be used to diagonalize

$$H = UDU^\dagger, \quad (\text{C.2})$$

where $D = \text{diag}(\mu_1, \dots, \mu_n)$ is a diagonal matrix. The proof for the eigenvalue decomposition of hermitian matrices can be found in any linear algebra book.

C.1.2 Singular Value Decomposition (SVD)

The singular values of a complex $m \times n$ matrix A are non-negative real numbers μ satisfying

$$Au = \mu v \quad (\text{C.3a})$$

$$A^\dagger v = \mu u, \quad (\text{C.3b})$$

where u, v are the singular vectors. These singular values and vectors induce a decomposition of the matrix A in 3 matrices,

$$A = VSU^\dagger, \quad (\text{C.4})$$

where $U = [u_1, \dots, u_n]$, $V = [v_1, \dots, v_m]$ are 2 unitary matrices made up of the singular vectors and S consists of the corresponding singular values on the first $\min(m, n)$ entries of the form $S_{i,i}$. This decomposition is unique (up to reordering). In order to prove this

theorem, assume that $n > m$. Otherwise look at A^\dagger . If no eigenvalue of AA^\dagger is zero, define the hermitian matrix

$$H^2 := AA^\dagger \quad (\text{C.5})$$

and diagonalize H^2 by

$$V^\dagger H^2 V = S^2 = \text{diag} . \quad (\text{C.6})$$

Then $H = VSV^\dagger$. Since no eigenvalue equals zero, H is invertible. Define the matrix

$$\tilde{U} := H^{-1}A \quad (\text{C.7})$$

which is unitary, because

$$\tilde{U}^\dagger \tilde{U} \stackrel{H^\dagger=H}{=} A^\dagger H^{-1} H^{-1} A = A^\dagger (AA^\dagger)^{-1} A = \mathbb{1} . \quad (\text{C.8})$$

Thus the matrix A can be written as

$$A = H\tilde{U} = VSV^\dagger\tilde{U} =: VSU^\dagger . \quad (\text{C.9})$$

This decomposition is unique up to reordering by the uniqueness of the eigenvalue decomposition.

C.1.3 Diagonalization of Symmetric Matrices

Complex symmetric matrices $A = A^T$ can also be diagonalized. this can be easily seen by looking at the SVD

$$VSU^\dagger = A = A^T = U^*SV^T \quad (\text{C.10})$$

By the uniqueness of the SVD for quadratic matrices

$$U^* = V \quad (\text{C.11})$$

Therefore the symmetric matrix A can be decomposed in

$$A = VSV^T , \quad (\text{C.12})$$

where S contains the singular values of A on the diagonal.

C.2 Group Theory of $\text{SL}(2, \mathbb{C})$

C.2.1 Lorentz Group

The Lorentz group $L \cong \mathcal{O}(3, 1)$ is the group of rotations in Minkowski space leaving the scalar product

$$x_\mu x^\mu = t^2 - \vec{x}^2 \quad (\text{C.13})$$

invariant. $L_+^\uparrow \cong \text{SO}(3, 1)$ is the connected component of the Lorentz group containing the identity transformation. This subgroup is not simply connected and the same applies for the Lorentz group L . Thus there is a double cover of L_+^\uparrow which is simply connected:

$$\text{SL}(2, \mathbb{C}) \xrightarrow{\sigma} L_+^\uparrow . \quad (\text{C.14})$$

	$\text{sign } \Lambda_0^0$	$\det \Lambda$	
L_+^\uparrow	1	1	proper orthochronous
$L_-^\uparrow = \mathcal{P}L_+^\uparrow$	1	-1	improper orthochronous
$L_-^\downarrow = \mathcal{T}L_+^\uparrow$	-1	-1	
$L_+^\downarrow = \mathcal{PT}L_+^\uparrow$	-1	1	

Table C.1: Connected components of the Lorentz group L . $\Lambda \in L$

Topology of the Lorentz Group

The Lorentz group L has 4 connected components which are characterized by the sign of the determinant and the 00-element of the representation on Minkowski space.

The different connected components are related by two discrete Lorentz transformations:

- space-inversion or parity \mathcal{P}

$$\vec{x} \xrightarrow{\mathcal{P}} -\vec{x}, \quad t \xrightarrow{\mathcal{P}} t \quad (\text{C.15})$$

- time-reversal \mathcal{T}

$$\vec{x} \xrightarrow{\mathcal{T}} \vec{x}, \quad t \xrightarrow{\mathcal{T}} -t \quad (\text{C.16})$$

Therefore, L_+^\uparrow , $L_+^\uparrow \cup L_-^\uparrow$, $L_+^\uparrow \cup L_-^\downarrow$ and $L_+^\uparrow \cup L_+^\downarrow$ are normal subgroups with the factor groups given by $\{\mathcal{E}, \mathcal{P}\}$, $\{\mathcal{E}, \mathcal{T}\}$ and $\{\mathcal{E}, \mathcal{P}, \mathcal{T}, \mathcal{PT}\}$, respectively.

Representations

The irreps of $SL(2, \mathbb{C})$ can be classified by 2 half-integers (A, B) corresponding to the relation of $SL(2, \mathbb{C})$ to $SU(2) \times SU(2)$. If $A + B$ is an integer, the irrep $V_{(A,B)}$ will be a vector representation which is also a representation of $SO(3, 1)$, i.e. the diagram

$$\begin{array}{ccc} SL(2, \mathbb{C}) & \xrightarrow{D} & GL(V_{(A,B)}) \\ \downarrow \sigma & \nearrow D' & \\ SO(3, 1) & & \end{array} \quad (\text{C.17})$$

commutes. Otherwise $A + B$ is an odd half-integer and the representation is called a spinor representation which is a double-valued representation of $SO(3, 1)$. In particular $(\frac{1}{2}, 0)$ and $(0, \frac{1}{2})$ are the smallest irreps corresponding to Majorana particles. They are represented by the transformations

$$e^{\pm i\sigma_\mu x^\mu} \quad (\text{C.18})$$

on a 2 dimensional complex vector space ($\sigma^\mu = (1, \vec{\sigma})$). These irreps as well as all irreps with $A \neq B$ are not invariant under parity \mathcal{P} and time-reversal \mathcal{T} , i.e. they are not irreps of the full Lorentz group $L \cong O(3, 1)$, but only of the proper orthochronous Lorentz group $L_+^\uparrow \cong SO(3, 1)$. However, it is easy to construct an irrep of L out of an irrep of L_+^\uparrow . If (A, B) is an irrep of L_+^\uparrow , then $(A, B) \oplus (B, A)$ is an irrep of the full Lorentz group. In particular, $(\frac{1}{2}, 0) \oplus (0, \frac{1}{2})$ is an irrep of L corresponding to a Dirac particle. A scalar particle is described by the trivial irrep $(0, 0)$ and a vector particle by $(\frac{1}{2}, \frac{1}{2})$.

$\mathcal{C}, \mathcal{P}, \mathcal{T}$ in different Representations

The transformation properties of vectors under \mathcal{P} and \mathcal{T} are the defining relations of the transformations and they are given in Eqs. (C.15, C.16). Dirac spinors, i.e. states in the $(\frac{1}{2}, 0) \oplus (0, \frac{1}{2})$ transform under \mathcal{P} and \mathcal{T} as follows¹

$$\psi(x) \xrightarrow{\mathcal{P}} \gamma^0 \psi(\mathcal{P}x) \quad (\text{C.19a})$$

$$\psi(x) \xrightarrow{\mathcal{T}} i\gamma^1 \gamma^3 \psi(\mathcal{T}x) . \quad (\text{C.19b})$$

In addition to the discrete transformations, there is charge conjugation \mathcal{C} transforming particles into antiparticles and vice versa. All additive quantum numbers change their sign. Dirac spinors transform under \mathcal{C} like

$$\psi \xrightarrow{\mathcal{C}} C \bar{\psi}^T = i\gamma^2 \psi^* . \quad (\text{C.19c})$$

The handedness changes under charge conjugation \mathcal{C} :

$$(\psi_{L/R})^{\mathcal{C}} = C \overline{(\mathbf{P}_{L/R} \psi)}^T = i\gamma^2 \mathbf{P}_{L/R} \psi^* = \mathbf{P}_{R/L} i\gamma^2 \psi^* = \mathbf{P}_{R/L} \psi^{\mathcal{C}} = (\psi^{\mathcal{C}})_{R/L} . \quad (\text{C.20})$$

Spinors which are invariant under charge conjugation \mathcal{C} , i.e. $\mathcal{C}\psi = \psi$, are their own antiparticles. Thus they are Majorana spinors and are in the $(\frac{1}{2}, 0)$ or $(0, \frac{1}{2})$ representation. Complex scalars are changed to their complex conjugate under charge conjugation

$$\phi \xrightarrow{\mathcal{C}} \phi^* , \quad (\text{C.21})$$

but they are invariant under parity \mathcal{P} and time-reversal \mathcal{T} . The charge conjugation induces a transformation in the internal symmetry space as well, e.g. a complex scalar $\text{SU}(2)_L$ doublet, like the SM Higgs particle transforms under charge conjugation non-trivially

$$\phi \xrightarrow{\mathcal{C}} i\sigma_2 \phi^* . \quad (\text{C.22})$$

C.2.2 Poincaré Group

The Poincaré group K is the group of space-time transformations leaving the scalar product invariant. These are rotations in Minkowski space and translations in space-time. Thus the Poincaré group can be written as the semi-direct product of the Lorentz-group L with the group of space-time translations $T \cong \mathbb{R}^4$.

$$K = L \rtimes T \cong \text{SO}(3, 1) \rtimes \mathbb{R}^4 \quad (\text{C.23})$$

The multiplication in the Poincaré group is given by

$$(\Lambda, a)(\Lambda', a') = (\Lambda\Lambda', a + \Lambda a') , \quad (\text{C.24})$$

i.e. the application of two successive Poincaré transformations on a vector yields

$$(\Lambda, a)(\Lambda', a')x = (\Lambda, a)(\Lambda'x + a') = \Lambda\Lambda'x + \Lambda a' + a = (\Lambda\Lambda', a + \Lambda a')x , \quad (\text{C.25})$$

where Λ and Λ' are Lorentz transformations and a, a' are translations in Minkowski-space.

¹In general, every discrete transformation is accompanied by the multiplication of an arbitrary phase. Here, the phases are set to zero.

C.3 Useful Formulae in Group Theory

C.3.1 Pauli Spin Matrices

The Pauli spin matrices are defined as

$$\sigma_1 := \begin{pmatrix} 0 & 1 \\ 1 & 0 \end{pmatrix}, \quad \sigma_2 := \begin{pmatrix} 0 & -i \\ i & 0 \end{pmatrix}, \quad \sigma_3 := \begin{pmatrix} 1 & 0 \\ 0 & -1 \end{pmatrix}. \quad (\text{C.26})$$

They are proportional to the generators of $\mathfrak{su}(2)$ which is the Lie algebra of $\text{SU}(2)$ and thus they satisfy the commutation relations

$$\left[\frac{\sigma_i}{2}, \frac{\sigma_j}{2} \right] = i\epsilon_{ijk} \frac{\sigma_k}{2} \quad (\text{C.27a})$$

$$\left\{ \frac{\sigma_i}{2}, \frac{\sigma_j}{2} \right\} = \frac{\delta_{ij}}{2} \mathbb{1}. \quad (\text{C.27b})$$

Some useful identities are the following products and traces of σ -matrices:

$$\sigma_b \sigma_a = i\epsilon_{bac} \sigma_c + \delta_{ba} \mathbb{1} \quad (\text{C.28a})$$

$$\sigma_b \sigma_i \sigma_a = \delta_{bi} \sigma_a + \delta_{ia} \sigma_b - \delta_{ba} \sigma_i + i\epsilon_{bia} \quad (\text{C.28b})$$

$$\sigma_m^T \sigma_2 \sigma_c \sigma_m = \sigma_2 \sigma_c \quad (\text{C.28c})$$

$$\sigma_m^T \sigma_2 \sigma_d \epsilon_{dmc} = 2i \sigma_2 \sigma_c \quad (\text{C.28d})$$

$$\sigma_m [\sigma_2, \sigma_m] \sigma_c = -4 \sigma_2 \sigma_c \quad (\text{C.28e})$$

$$\frac{1}{2} \text{tr} \sigma_b = 0 \quad (\text{C.28f})$$

$$\frac{1}{2} \text{tr} \sigma_b \sigma_a = \delta_{ba} \quad (\text{C.28g})$$

$$\frac{1}{2} \text{tr} \sigma_b \sigma_i \sigma_a = i\epsilon_{bia} \quad (\text{C.28h})$$

$$\frac{1}{2} \text{tr} \sigma_j \sigma_b \sigma_i \sigma_a = \delta_{jb} \delta_{ia} + \delta_{ja} \delta_{ib} - \delta_{ba} \delta_{ji} \quad (\text{C.28i})$$

$$\sigma_{ab}^i \sigma_{cd}^i = 2\delta_{ad} \delta_{bc} - \delta_{ab} \delta_{cd}. \quad (\text{C.28j})$$

The last relation is a special version of the general group theoretical relation which is valid for the generators of $\text{SU}(N)$

$$t_{ab}^A t_{cd}^A = \frac{1}{2} \left(\delta_{ad} \delta_{bc} - \frac{1}{N} \delta_{ab} \delta_{cd} \right). \quad (\text{C.29})$$

Furthermore it is useful to define the creator and annihilator

$$\sigma^\pm = \sigma_1 \pm i\sigma_2, \quad (\text{C.30})$$

which form a basis of the adjoint representation together with σ_3 . Another useful identity is the product of two ϵ symbols

$$\epsilon_{abc} \epsilon_{cde} = \delta_{ad} \delta_{be} - \delta_{ae} \delta_{bd}. \quad (\text{C.31})$$

C.3.2 Dirac Matrices

The Dirac matrices γ^μ are given in the Dirac representation by

$$\gamma^i := \begin{pmatrix} 0 & \sigma_i \\ -\sigma_i & 0 \end{pmatrix}, \quad \gamma^0 := \begin{pmatrix} 1 & 0 \\ 0 & -1 \end{pmatrix}, \quad (\text{C.32})$$

where the entries are 2×2 matrices. They form the representation $(\frac{1}{2}, 0) \oplus (0, \frac{1}{2})$ of the Clifford algebra $\text{SL}(2, \mathbb{C})$. Thus they satisfy the anticommutation relations

$$\{\gamma_\mu, \gamma_\nu\} = 2\eta_{\mu\nu} \quad (\text{C.33})$$

Furthermore, γ_5 is defined as the product of the matrices γ^μ , i.e.

$$\gamma^5 = i\gamma^0\gamma^1\gamma^2\gamma^3 = \frac{i}{4!}\epsilon_{\mu\nu\rho\sigma}\gamma^\mu\gamma^\nu\gamma^\rho\gamma^\sigma. \quad (\text{C.34})$$

In the Dirac representation, γ_5 is given by

$$\gamma_5 = \begin{pmatrix} 0 & 1 \\ 1 & 0 \end{pmatrix}. \quad (\text{C.35})$$

It satisfies the following relations

$$\{\gamma_5, \gamma^\mu\} = 0 \quad (\text{C.36a})$$

$$P_{L/R}\gamma^\mu = \gamma^\mu P_{R/L} \quad (\text{C.36b})$$

Traces of γ matrices often appear in the evaluation of Feynman diagrams. The traces can be evaluated by applying Eq. (C.33) successively and using the anticommutation relation of γ_5 .

$$\text{tr } 1 = 4 \quad (\text{C.37a})$$

$$\text{tr } \gamma_5 = 0 \quad (\text{C.37b})$$

$$\text{tr odd number of } \gamma \text{ matrices} = 0 \quad (\text{C.37c})$$

$$\text{tr } \gamma^\mu\gamma^\nu = 4\eta^{\mu\nu} \quad (\text{C.37d})$$

$$\text{tr } \gamma^\mu\gamma^\nu\gamma^\rho\gamma^\sigma = 4(\eta^{\mu\nu}\eta^{\rho\sigma} + \eta^{\mu\sigma}\eta^{\nu\rho} - \eta^{\mu\rho}\eta^{\nu\sigma}) \quad (\text{C.37e})$$

C.3.3 γ -Algebra in d Dimensions

In d dimensions, the products of γ matrices change because of $\eta_\mu^\mu = d$. Here, some useful identities are given which can be easily derived from the defining relation of the Clifford algebra $\text{SL}(2, \mathbb{C})$:

$$\gamma_\mu\gamma^\mu = d \quad (\text{C.38a})$$

$$\gamma_\lambda\gamma^\mu\gamma^\lambda = (2-d)\gamma^\mu \quad (\text{C.38b})$$

$$\gamma_\lambda\gamma^\mu\gamma^\nu\gamma^\lambda = 4\eta^{\mu\nu} - (4-d)\gamma^\mu\gamma^\nu \quad (\text{C.38c})$$

$$\gamma_\lambda\gamma^\mu\gamma^\nu\gamma^\kappa\gamma^\lambda = -2\gamma^\kappa\gamma^\nu\gamma^\mu + (4-d)\gamma^\mu\gamma^\nu\gamma^\kappa. \quad (\text{C.38d})$$

However, there is a problem involving terms like $\text{tr } (\gamma_5\gamma^\mu\gamma^\nu\gamma^\xi\gamma^\eta)$, because it is not possible to assign a unique value to this expression using the usual anticommutation relations. One

consistent definition which reduces to the usual definition of γ_5 and $\epsilon_{\mu\nu\kappa\lambda}$ can be obtained by treating the first 4 dimensions differently from the other dimensions [42]. Hence, the indices $\mu = 0, 1, 2, 3$ are treated in the usual way, but the remaining indices are treated differently:

$$\epsilon_{\mu\nu\kappa\lambda} = \begin{cases} 1 & \text{if } (\mu\nu\kappa\lambda) \text{ is an even permutation of } (0123) \\ -1 & \text{if } (\mu\nu\kappa\lambda) \text{ is an odd permutation of } (0123) \\ 0 & \text{otherwise} \end{cases} . \quad (\text{C.39})$$

This definition leads to the following commutation relations for γ_5

$$\{\gamma_5, \gamma^\mu\} = 0, \quad \text{if } \mu = 0, 1, 2, 3 \quad (\text{C.40a})$$

$$[\gamma_5, \gamma^\mu] = 0, \quad \text{otherwise} \quad (\text{C.40b})$$

$$(\gamma_5)^2 = 1 \quad (\text{C.40c})$$

$$\gamma_5^\dagger = \gamma_5 \quad (\text{C.40d})$$

Apparently, this violates Lorentz symmetry in d dimensions. Thus Lorentz symmetry is a good symmetry only in the first 4 dimensions. However, as long as $\text{tr}(\gamma_5 \gamma^\mu \gamma^\nu \gamma^\xi \gamma^\eta)$ does not show up in the calculations, naive dimensional regularization can be used, i.e.

$$\{\gamma_5, \gamma^\mu\} = 0 \quad (\text{C.41a})$$

$$\text{tr } \gamma_5 = 0 \quad (\text{C.41b})$$

$$\text{tr}(\gamma_5 \gamma^\mu \gamma^\nu) = 0 \quad (\text{C.41c})$$

C.4 Special Functions

In the calculation of d -dimensional integrals, there often show up Gamma functions and the related Beta function.

C.4.1 Gamma Function

The Gamma function is the natural continuation of the factorial from integers to complex numbers. It is defined as

$$\Gamma(z) := \int_0^\infty e^{-t} t^{z-1} dt \quad \forall z \in \mathbb{C}, \text{Re } z > 0 . \quad (\text{C.42})$$

It clearly satisfies the recursive definition of factorial

$$\Gamma(z+1) = z\Gamma(z), \quad \Gamma(1) = 1 . \quad (\text{C.43})$$

Furthermore, the Gamma function has first order singularities for all $x = 0, -1, -2, \dots$. At these poles the Gamma function can be expanded to

$$\Gamma(-n + \epsilon) = \frac{(-1)^n}{n!} \left[\frac{1}{\epsilon} + \psi_1(n+1) + \mathcal{O}(\epsilon) \right] , \quad (\text{C.44})$$

where $\psi_1(n+1) = \sum_{k=1}^n \frac{1}{k} - \gamma_E = \frac{\Gamma'(x)}{\Gamma(x)}$ and $\gamma_E = 0.57721\dots$ is the Euler Mascheroni constant. Some useful identities are

$$\Gamma\left(\frac{1}{2}\right) = \sqrt{\pi} \quad (\text{C.45})$$

$$\Gamma\left(-\frac{1}{2}\right) = -2\sqrt{\pi} \quad (\text{C.46})$$

$$\Gamma(z)\Gamma(1-z) = \frac{\pi}{\sin \pi z} \quad \forall z \in \mathbb{C} \setminus \mathbb{Z} \quad (\text{C.47})$$

$$\Gamma(z)\Gamma(-z) = -\frac{\pi}{z \sin \pi z} \quad \forall z \in \mathbb{C} \setminus \mathbb{Z} . \quad (\text{C.48})$$

C.4.2 Beta Function

The Beta function is related to the Gamma function by

$$B(x, y) := \frac{\Gamma(x)\Gamma(y)}{\Gamma(x+y)} \quad x, y \in \mathbb{C}, x, y, x+y \neq 0, -1, -2, \dots \quad (\text{C.49})$$

Moreover, some representations are given by

$$B(x, y) = \int_0^1 t^{x-1} (1-t)^{y-1} dt \quad x > 0, y > 0 \quad (\text{C.50})$$

$$B(x, y) = 2 \int_0^\infty t^{2x-1} (1+t^2)^{-x-y} . \quad (\text{C.51})$$

C.5 Passarino-Veltman Functions

The Passarino-Veltman functions [88, 89] often appear in loop calculations. Thus they are summarized in this section. The arguments of the functions are omitted in the list, but they are given before each list. The integrals with a tensor structure can be decomposed in tensors formed from the momenta in the arguments and $\eta_{\mu\nu}$. Here, only the divergent parts are given.

C.5.1 The One-Point Function A_0

$$A_0(m^2) := \frac{\mu^\epsilon}{i\pi^2} \int d^d k \frac{1}{k^2 - m^2} \quad (\text{C.52})$$

The divergent part is

$$A_0(m^2) = \frac{2}{\epsilon} m^2 + \text{UV finite} . \quad (\text{C.53})$$

C.5.2 The Two-Point Functions B

The three-point functions C are functions of $B = B(p^2, m_1^2, m_2^2)$:

$$B_0 := \frac{\mu^\epsilon}{i\pi^2} \int d^d k \frac{1}{(k^2 - m_1^2) [(k+p)^2 - m_2^2]} \quad (\text{C.54a})$$

$$B_\mu := \frac{\mu^\epsilon}{i\pi^2} \int d^d k \frac{k_\mu}{(k^2 - m_1^2) [(k+p)^2 - m_2^2]} \quad (\text{C.54b})$$

$$B_{\mu\nu} := \frac{\mu^\epsilon}{i\pi^2} \int d^d k \frac{k_\mu k_\nu}{(k^2 - m_1^2) [(k+p)^2 - m_2^2]} . \quad (\text{C.54c})$$

The divergent parts are

$$B_0 = \frac{2}{\epsilon} + \text{UV finite} \quad (\text{C.55a})$$

$$B_\mu = -\frac{1}{\epsilon} p_\mu + \text{UV finite} \quad (\text{C.55b})$$

$$B_{\mu\nu} = -\frac{1}{6\epsilon} (p^2 - 3m_1^2 - 3m_2^2) \eta_{\mu\nu} + \frac{2}{3\epsilon} p_\mu p_\nu + \text{UV finite} . \quad (\text{C.55c})$$

C.5.3 The Three-Point Functions C

The three-point functions C are functions of $C = C(p^2, (p-q)^2, q^2, m_1^2, m_2^2, m_3^2)$:

$$C_0 := \frac{\mu^\epsilon}{i\pi^2} \int d^d k \frac{1}{(k^2 - m_1^2) [(k+p)^2 - m_2^2] [(k+q)^2 - m_3^2]} \quad (\text{C.56a})$$

$$C_\mu := \frac{\mu^\epsilon}{i\pi^2} \int d^d k \frac{k_\mu}{(k^2 - m_1^2) [(k+p)^2 - m_2^2] [(k+q)^2 - m_3^2]} \quad (\text{C.56b})$$

$$C_{\mu\nu} := \frac{\mu^\epsilon}{i\pi^2} \int d^d k \frac{k_\mu k_\nu}{(k^2 - m_1^2) [(k+p)^2 - m_2^2] [(k+q)^2 - m_3^2]} \quad (\text{C.56c})$$

$$C_{\mu\nu\rho} := \frac{\mu^\epsilon}{i\pi^2} \int d^d k \frac{k_\mu k_\nu k_\rho}{(k^2 - m_1^2) [(k+p)^2 - m_2^2] [(k+q)^2 - m_3^2]} . \quad (\text{C.56d})$$

The divergent parts are

$$C_{\mu\nu} = \frac{1}{2\epsilon} \eta_{\mu\nu} + \text{UV finite} \quad (\text{C.57a})$$

$$C_{\mu\nu\rho} = -\frac{1}{6\epsilon} [(\eta_{\mu\nu} p_\rho + \text{cyclic}) + (p \rightarrow q)] + \text{UV finite} . \quad (\text{C.57b})$$

C.5.4 The Four-Point Functions D

The four-point functions D are functions of

$$D = D(p^2, (p-q)^2, (q-l)^2, q^2, l^2, m_1^2, m_2^2, m_3^2, m_4^2) :$$

$$D_0 := \frac{\mu^\epsilon}{i\pi^2} \int d^d k \frac{1}{(k^2 - m_1^2) [(k+p)^2 - m_2^2] [(k+q)^2 - m_3^2] [(k+l)^2 - m_4^2]} \quad (\text{C.58a})$$

$$D_\mu := \frac{\mu^\epsilon}{i\pi^2} \int d^d k \frac{k_\mu}{(k^2 - m_1^2) [(k+p)^2 - m_2^2] [(k+q)^2 - m_3^2] [(k+l)^2 - m_4^2]} \quad (\text{C.58b})$$

$$D_{\mu\nu} := \frac{\mu^\epsilon}{i\pi^2} \int d^d k \frac{k_\mu k_\nu}{(k^2 - m_1^2) [(k+p)^2 - m_2^2] [(k+q)^2 - m_3^2] [(k+l)^2 - m_4^2]} \quad (\text{C.58c})$$

$$D_{\mu\nu\rho} := \frac{\mu^\epsilon}{i\pi^2} \int d^d k \frac{k_\mu k_\nu k_\rho}{(k^2 - m_1^2) [(k+p)^2 - m_2^2] [(k+q)^2 - m_3^2] [(k+l)^2 - m_4^2]} \quad (\text{C.58d})$$

$$D_{\mu\nu\rho\sigma} := \frac{\mu^\epsilon}{i\pi^2} \int d^d k \frac{k_\mu k_\nu k_\rho k_\sigma}{(k^2 - m_1^2) [(k+p)^2 - m_2^2] [(k+q)^2 - m_3^2] [(k+l)^2 - m_4^2]} . \quad (\text{C.58e})$$

The only divergent function is $D_{\mu\nu\rho\sigma}$ which is given by

$$D_{\mu\nu\rho\sigma} = \frac{1}{12\epsilon} (\eta_{\mu\nu}\eta_{\rho\sigma} + \eta_{\mu\rho}\eta_{\nu\sigma} + \eta_{\mu\sigma}\eta_{\nu\rho}) + \text{UV finite} . \quad (\text{C.59})$$

Appendix D

Tables

$\mathcal{Q}_{13}^{\pm} = \frac{ m_3 \pm m_1 e^{i\varphi_1} ^2}{\Delta m_{\text{atm}}^2 (1+\zeta)}$ $\mathcal{Q}_{23}^{\pm} = \frac{ m_3 \pm m_2 e^{i\varphi_2} ^2}{\Delta m_{\text{atm}}^2}$ $\mathcal{Q}_{12}^{\pm} = \frac{ m_2 e^{i\varphi_2} \pm m_1 e^{i\varphi_1} ^2}{\Delta m_{\text{sol}}^2}$	$\mathcal{S}_{13} = \frac{m_1 m_3 \sin \varphi_1}{\Delta m_{\text{atm}}^2 (1+\zeta)}$ $\mathcal{S}_{23} = \frac{m_2 m_3 \sin \varphi_2}{\Delta m_{\text{atm}}^2}$ $\mathcal{S}_{12} = \frac{m_1 m_2 \sin(\varphi_1 - \varphi_2)}{\Delta m_{\text{sol}}^2}$
$\mathcal{A}_{13}^{\pm} = \frac{(m_1^2 + m_3^2) \cos \delta \pm 2m_1 m_3 \cos(\delta - \varphi_1)}{\Delta m_{\text{atm}}^2 (1+\zeta)}$ $\mathcal{A}_{23}^{\pm} = \frac{(m_2^2 + m_3^2) \cos \delta \pm 2m_2 m_3 \cos(\delta - \varphi_2)}{\Delta m_{\text{atm}}^2}$	$\mathcal{B}_{13}^{\pm} = \frac{(m_1^2 + m_3^2) \sin \delta \pm 2m_1 m_3 \sin(\delta - \varphi_1)}{\Delta m_{\text{atm}}^2 (1+\zeta)}$ $\mathcal{B}_{23}^{\pm} = \frac{(m_2^2 + m_3^2) \sin \delta \pm 2m_2 m_3 \sin(\delta - \varphi_2)}{\Delta m_{\text{atm}}^2}$
$\mathcal{C}_{13}^{12} = \frac{m_1}{\Delta m_{\text{sol}}^2 (1+\zeta)} [(1+\zeta) m_2 \sin(\varphi_1 - \varphi_2) - \zeta m_3 \sin(2\delta - \varphi_1)]$ $\mathcal{C}_{13}^{23} = \frac{m_3}{\Delta m_{\text{atm}}^2 (1+\zeta)} [m_1 \sin(2\delta - \varphi_1) + (1+\zeta) m_2 \sin \varphi_2]$ $\mathcal{C}_{23}^{12} = \frac{m_2}{\Delta m_{\text{sol}}^2} [m_1 \sin(\varphi_1 - \varphi_2) - \zeta m_3 \sin(2\delta - \varphi_2)]$ $\mathcal{C}_{23}^{13} = \frac{m_3}{\Delta m_{\text{atm}}^2 (1+\zeta)} [m_1 \sin \varphi_1 + (1+\zeta) m_2 \sin(2\delta - \varphi_2)]$	
$\mathcal{D}_1 = \frac{m_3}{\Delta m_{\text{atm}}^2 (1+\zeta)} [m_1 \cos(\delta - \varphi_1) - (1+\zeta) m_2 \cos(\delta - \varphi_2)] \sin \delta$ $\mathcal{D}_2 = \frac{m_3}{\Delta m_{\text{atm}}^2 (1+\zeta)} [m_1 \cos(2\delta - \varphi_1) - (1+\zeta) m_2 \cos(2\delta - \varphi_2) + \zeta m_3]$	

Table D.1: Definition of the abbreviations used in Tabs. D.2,D.4,D.3 and 6.3

	$64\pi^2 \dot{\theta}_{12}$	$64\pi^2 \dot{\theta}_{13}$	$64\pi^2 \dot{\theta}_{23}$
P_{11}	$2\mathcal{Q}_{12}^+ \sin 2\theta_{12}$	0	0
P_{22}	$-2\mathcal{Q}_{12}^+ \sin 2\theta_{12} c_{23}^2$	$(\mathcal{A}_{23}^+ - \mathcal{A}_{13}^+) \sin 2\theta_{12} \sin 2\theta_{23}$	$2(\mathcal{Q}_{23}^+ c_{12}^2 + \mathcal{Q}_{13}^+ s_{12}^2) \sin 2\theta_{23}$
P_{33}	$-2\mathcal{Q}_{12}^+ \sin 2\theta_{12} s_{23}^2$	$-(\mathcal{A}_{23}^+ - \mathcal{A}_{13}^+) \sin 2\theta_{12} \sin 2\theta_{23}$	$-2(\mathcal{Q}_{23}^+ c_{12}^2 + \mathcal{Q}_{13}^+ s_{12}^2) \sin 2\theta_{23}$
$\text{Re } P_{21}$	$4\mathcal{Q}_{12}^+ \cos 2\theta_{12} c_{23}$	$4(\mathcal{A}_{13}^+ c_{12}^2 + \mathcal{A}_{23}^+ s_{12}^2) s_{23}$	$2(\mathcal{Q}_{23}^+ - \mathcal{Q}_{13}^+) \sin 2\theta_{12} s_{23}$
$\text{Re } P_{31}$	$-4\mathcal{Q}_{12}^+ \cos 2\theta_{12} s_{23}$	$4(\mathcal{A}_{13}^+ c_{12}^2 + \mathcal{A}_{23}^+ s_{12}^2) c_{23}$	$2(\mathcal{Q}_{23}^+ - \mathcal{Q}_{13}^+) \sin 2\theta_{12} c_{23}$
$\text{Re } P_{32}$	$2\mathcal{Q}_{12}^+ \sin 2\theta_{12} \sin 2\theta_{23}$	$2(\mathcal{A}_{23}^+ - \mathcal{A}_{13}^+) \sin 2\theta_{12} \cos 2\theta_{23}$	$4(\mathcal{Q}_{23}^+ c_{12}^2 + \mathcal{Q}_{13}^+ s_{12}^2) \cos 2\theta_{23}$
$\text{Im } P_{21}$	$8\mathcal{S}_{12} c_{23}$	$4(\mathcal{B}_{13}^- c_{12}^2 + \mathcal{B}_{23}^- s_{12}^2) s_{23}$	$4(\mathcal{S}_{23} - \mathcal{S}_{13}) \sin 2\theta_{12} s_{23}$
$\text{Im } P_{31}$	$-8\mathcal{S}_{12} s_{23}$	$4(\mathcal{B}_{13}^- c_{12}^2 + \mathcal{B}_{23}^- s_{12}^2) c_{23}$	$4(\mathcal{S}_{23} - \mathcal{S}_{13}) \sin 2\theta_{12} c_{23}$
$\text{Im } P_{32}$	0	$2(\mathcal{B}_{23}^- - \mathcal{B}_{13}^-) \sin 2\theta_{12}$	$8(\mathcal{S}_{23} c_{12}^2 + \mathcal{S}_{13} s_{12}^2)$

Table D.2: Coefficients of P_{fg} in the slope of the mixing parameters, θ_{ij} in the limit $\theta_{13} \rightarrow 0$. The abbreviations \mathcal{A}_{ij}^\pm , \mathcal{B}_{ij}^\pm , \mathcal{S}_{ij} and \mathcal{Q}_{ij}^\pm depend on the mass eigenvalues and phases only, and enhance the running for a degenerate mass spectrum since they are of the form $f_{ij}(m_i, m_j, \text{phases})/(m_j^2 - m_i^2)$. They are listed in Tab. D.1.

	$64\pi^2 \dot{\delta}^{(-1)}$
P_{11}	0
P_{22}	$-(\mathcal{B}_{23}^+ - \mathcal{B}_{13}^+) \sin 2\theta_{12} \sin 2\theta_{23}$
P_{33}	$(\mathcal{B}_{23}^+ - \mathcal{B}_{13}^+) \sin 2\theta_{12} \sin 2\theta_{23}$
$\text{Re } P_{21}$	$-4(\mathcal{B}_{13}^+ c_{12}^2 + \mathcal{B}_{23}^+ s_{12}^2) s_{23}$
$\text{Re } P_{31}$	$-4(\mathcal{B}_{13}^+ c_{12}^2 + \mathcal{B}_{23}^+ s_{12}^2) c_{23}$
$\text{Re } P_{32}$	$-2(\mathcal{B}_{23}^+ - \mathcal{B}_{13}^+) \sin 2\theta_{12} \cos 2\theta_{23}$
$\text{Im } P_{21}$	$4(\mathcal{A}_{13}^- c_{12}^2 + \mathcal{A}_{23}^- s_{12}^2) s_{23}$
$\text{Im } P_{31}$	$4(\mathcal{A}_{13}^- c_{12}^2 + \mathcal{A}_{23}^- s_{12}^2) c_{23}$
$\text{Im } P_{32}$	$2(\mathcal{A}_{23}^- - \mathcal{A}_{13}^-) \sin 2\theta_{12}$

	$64\pi^2 \dot{\delta}^{(0)}$
P_{11}	$-8((\mathcal{C}_{13}^{23} + \mathcal{S}_{12} - \mathcal{S}_{23}) c_{12}^2 + (\mathcal{C}_{23}^{13} + \mathcal{S}_{12} - \mathcal{S}_{13}) s_{12}^2)$
P_{22}	$8((\mathcal{S}_{12} - \mathcal{S}_{23}) c_{23}^2 + \mathcal{C}_{13}^{23} s_{23}^2) c_{12}^2 + ((\mathcal{S}_{12} - \mathcal{S}_{13}) c_{23}^2 + \mathcal{C}_{23}^{13} s_{23}^2) s_{12}^2$
P_{33}	$8((\mathcal{C}_{13}^{23} c_{23}^2 + (\mathcal{S}_{12} - \mathcal{S}_{23}) s_{23}^2) c_{12}^2 + (\mathcal{C}_{23}^{13} c_{23}^2 + (\mathcal{S}_{12} - \mathcal{S}_{13}) s_{23}^2) s_{12}^2)$
$\text{Re } P_{21}$	$-16\mathcal{S}_{12} c_{23} \cot 2\theta_{12} + 4(2\mathcal{D}_1 c_{23} + (\mathcal{S}_{23} - \mathcal{S}_{13}) s_{23} \tan \theta_{23}) \sin 2\theta_{12}$
$\text{Re } P_{31}$	$16\mathcal{S}_{12} s_{23} \cot 2\theta_{12} - 4(2\mathcal{D}_1 s_{23} + (\mathcal{S}_{23} - \mathcal{S}_{13}) c_{23} \cot \theta_{23}) \sin 2\theta_{12}$
$\text{Re } P_{32}$	$-16(\mathcal{S}_{23} c_{12}^2 + \mathcal{S}_{13} s_{12}^2) \cos 2\theta_{23} \cot 2\theta_{23} - 8(\mathcal{C}_{13}^{12} c_{12}^2 + \mathcal{C}_{23}^{12} s_{12}^2) \sin 2\theta_{23}$
$\text{Im } P_{21}$	$-8\mathcal{Q}_{12}^- c_{23} \csc 2\theta_{12} - 2(2\mathcal{D}_2 c_{23} + (\mathcal{Q}_{23}^- - \mathcal{Q}_{13}^-) \cos 2\theta_{23} \sec \theta_{23}) \sin 2\theta_{12}$
$\text{Im } P_{31}$	$8\mathcal{Q}_{12}^- s_{23} \csc 2\theta_{12} + 2(2\mathcal{D}_2 s_{23} - (\mathcal{Q}_{23}^- - \mathcal{Q}_{13}^-) \cos 2\theta_{23} \csc \theta_{23}) \sin 2\theta_{12}$
$\text{Im } P_{32}$	$-8(\mathcal{Q}_{23}^- c_{12}^2 + \mathcal{Q}_{13}^- s_{12}^2) \cot 2\theta_{23}$

Table D.3: Coefficients of P_{fg} in the slope of the Dirac CP phase for $\theta_{13} = 0$. The abbreviations \mathcal{A}_{ij}^\pm , \mathcal{B}_{ij}^\pm , \mathcal{Q}_{ij}^\pm , \mathcal{C}_{ij}^{kl} and \mathcal{D}_i depend on the mass eigenvalues and phases only, and enhance the running for a degenerate mass spectrum since they are of the form $f_{ij}(\text{masses, phases})/(m_j^2 - m_i^2)$. They are listed in Tab. D.1

	$16\pi^2\dot{\varphi}_1$
P_{11}	$-4\mathcal{S}_{12}c_{12}^2$
P_{22}	$4\mathcal{S}_{12}c_{12}^2c_{23}^2 - 4(\mathcal{S}_{23}c_{12}^2 + \mathcal{S}_{13}s_{12}^2)\cos 2\theta_{23}$
P_{33}	$4\mathcal{S}_{12}c_{12}^2s_{23}^2 + 4(\mathcal{S}_{23}c_{12}^2 + \mathcal{S}_{13}s_{12}^2)\cos 2\theta_{23}$
$\text{Re } P_{21}$	$-4\mathcal{S}_{12}c_{23}\cos 2\theta_{12}\cot \theta_{12} - 2(\mathcal{S}_{23} - \mathcal{S}_{13})\cos 2\theta_{23}\sec \theta_{23}\sin 2\theta_{12}$
$\text{Re } P_{31}$	$4\mathcal{S}_{12}s_{23}\cos 2\theta_{12}\cot \theta_{12} - 2(\mathcal{S}_{23} - \mathcal{S}_{13})\cos 2\theta_{23}\csc \theta_{23}\sin 2\theta_{12}$
$\text{Re } P_{32}$	$-8(\mathcal{S}_{23}c_{12}^2 + \mathcal{S}_{13}s_{12}^2)\cos 2\theta_{23}\cot 2\theta_{23} - 4\mathcal{S}_{12}c_{12}^2\sin 2\theta_{23}$
$\text{Im } P_{21}$	$-2\mathcal{Q}_{12}^-c_{23}\cot \theta_{12} - (\mathcal{Q}_{23}^- - \mathcal{Q}_{13}^-)\cos 2\theta_{23}\sec \theta_{23}\sin 2\theta_{12}$
$\text{Im } P_{31}$	$2\mathcal{Q}_{12}^-s_{23}\cot \theta_{12} - (\mathcal{Q}_{23}^- - \mathcal{Q}_{13}^-)\cos 2\theta_{23}\csc \theta_{23}\sin 2\theta_{12}$
$\text{Im } P_{32}$	$-4(\mathcal{Q}_{23}^-c_{12}^2 + \mathcal{Q}_{13}^-s_{12}^2)\cot 2\theta_{23}$
	$16\pi^2\dot{\varphi}_2$
P_{11}	$-4\mathcal{S}_{12}s_{12}^2$
P_{22}	$4\mathcal{S}_{12}c_{23}^2s_{12}^2 - 4(\mathcal{S}_{23}c_{12}^2 + \mathcal{S}_{13}s_{12}^2)\cos 2\theta_{23}$
P_{33}	$4\mathcal{S}_{12}s_{23}^2s_{12}^2 + 4(\mathcal{S}_{23}c_{12}^2 + \mathcal{S}_{13}s_{12}^2)\cos 2\theta_{23}$
$\text{Re } P_{21}$	$-4\mathcal{S}_{12}c_{23}\cos 2\theta_{12}\tan \theta_{12} - 2(\mathcal{S}_{23} - \mathcal{S}_{13})\cos 2\theta_{23}\sec \theta_{23}\sin 2\theta_{12}$
$\text{Re } P_{31}$	$4\mathcal{S}_{12}s_{23}\cos 2\theta_{12}\tan \theta_{12} - 2(\mathcal{S}_{23} - \mathcal{S}_{13})\cos 2\theta_{23}\csc \theta_{23}\sin 2\theta_{12}$
$\text{Re } P_{32}$	$-8(\mathcal{S}_{23}c_{12}^2 + \mathcal{S}_{13}s_{12}^2)\cos 2\theta_{23}\cot 2\theta_{23} - 4\mathcal{S}_{12}s_{12}^2\sin 2\theta_{23}$
$\text{Im } P_{21}$	$-2\mathcal{Q}_{12}^-c_{23}\tan \theta_{12} - (\mathcal{Q}_{23}^- - \mathcal{Q}_{13}^-)\cos 2\theta_{23}\sec \theta_{23}\sin 2\theta_{12}$
$\text{Im } P_{31}$	$2\mathcal{Q}_{12}^-s_{23}\tan \theta_{12} - (\mathcal{Q}_{23}^- - \mathcal{Q}_{13}^-)\cos 2\theta_{23}\csc \theta_{23}\sin 2\theta_{12}$
$\text{Im } P_{32}$	$-4(\mathcal{Q}_{23}^-c_{12}^2 + \mathcal{Q}_{13}^-s_{12}^2)\cot 2\theta_{23}$

Table D.4: Coefficients of P_{fg} in the slope of the Majorana phases for $\theta_{13} = 0$. The abbreviations \mathcal{S}_{ij} and \mathcal{Q}_{ij}^\pm depend on the mass eigenvalues and phases only, and enhance the running for a degenerate mass spectrum since they are of the form $f_{ij}(m_i, m_j, \text{phases})/(m_j^2 - m_i^2)$. They are listed in Tab. D.1.

Acknowledgments

I would like to thank everybody who supported this work in his way. In particular, I want to thank

- my supervisor Manfred Lindner for always having time for my questions, the excellent working environment and, in particular, for the possibility to go to the summer school in Italy and the workshop on neutrino physics in Trento.
- my office mate Ralph Bundschuh for the nice atmosphere in our office.
- especially Werner Rodejohann for proofreading the whole manuscript and giving useful comments.
- Jörn Kersten, Michael Ratz and Stefan Antusch for being great colleagues and especially Jörn and Michael for explaining me a lot of details.
- Mark Rolinec for explaining me the neutrino oscillation experiments.
- Claudia Hagedorn and Mathias Garny for useful discussions.
- Markus “MMM” Müller for keeping the computers running, especially for the fast exchange of my graphics card when the fan went noisy.
- Marc-Thomas “Mato” Eisele for driving to Trento.
- Mattias Andersson, Florian Bauer, Andreas Hohenegger, Patrick Huber, Florian Plentinger, Joe Sato, Thomas Schwetz and Walter Winter for contributing to the nice atmosphere of T30d and the interesting discussions during coffee break.
- our secretary Karin Ramm for a friendly smile in the morning.
- my brother Johannes for proofreading parts of the thesis.
- Christian Gohlke for the hospitality on Friday evenings and his efforts to make physicists interested in classical music and literature.
- Frank Straub for many interesting discussions about physics.
- Mrs. Dobler for supplying me with tickets.

Last, but not least, very special thanks to my family: Martin, Johannes and my parents for supporting me in every possible way during my studies and before.

Nomenclature

$\tilde{\alpha}$	Flavor-diagonal part of the β -function of $Y_e^\dagger Y_e$, page 39
α	Flavor-diagonal part of the β -function of m_ν , page 39
β	β -function of the gauge coupling, page 24
β	β -function of the coupling, page 24
B_μ	Gauge boson of $U(1)_Y$, page 79
c_i	Ghost field corresponding to gauge group i , page 79
θ_c	Cabbibo angle, page 46
D	Superficial degree of divergence, page 15
d	Number of space-time dimensions, page 15
Δ	Higgs triplet, page 30
Δ_B	Bare wave function of the Higgs triplet, page 53
δ	Dirac CP phase in the leptonic sector, page 81
$\delta\Lambda_1$	Counterterm for the divergencies in Λ_1 , page 53
$\delta\Lambda_2$	Counterterm for the divergencies in Λ_2 , page 53
$\delta\Lambda_3$	Counterterm for the divergencies in Λ_3 , page 53
$\delta\Lambda_4$	Counterterm for the divergencies in Λ_4 , page 53
$\delta\Lambda_5$	Counterterm for the divergencies in Λ_5 , page 53
$\delta\Lambda_6$	Counterterm for the divergencies in Λ_6 , page 53
d_i	Number of derivatives at a vertex of type i , page 16
δ_ξ	Anomalous dimension of the gauge parameter, page 24
d_R	Right-handed down-type quark, page 79
E_f	Number of external lines of particle species f , page 16
ℓ_L	Left-handed lepton doublet, page 79

ϵ	Dimensional expansion parameter $\epsilon = 4 - d$, page 20
e_R	Right-handed charged lepton, page 79
F	Off-diagonal part of the β -function of $Y_e^\dagger Y_e$, page 39
$G^{(n)}$	Renormalized n-point Green's function, page 24
g_1	Gauge coupling of $U(1)_Y$, page 79
g_2	Gauge coupling of $SU(2)_L$, page 79
g_3	Gauge coupling of $SU(3)_C$, page 79
γ	Anomalous dimension of the wave function, page 24
$\Gamma_{\ell_L \Delta \ell_L}$	Vertex correction to the vertex $\ell_L \Delta \ell_L$, page 60
$\Gamma_{\phi \Delta \phi}$	Vertex correction to the vertex $\phi \Delta \phi$, page 62
γ_m	Anomalous dimension of the mass, page 24
$\Gamma_{\nu_R \ell_L \phi}$	Vertex correction to $\nu_R \ell_L \phi$, page 62
$G_B^{(n)}$	Bare n-point Green's function, page 24
G_μ	Gauge boson of $SU(3)_C$, page 79
Z_ϕ	Wave function renormalization of the field ϕ , page 21
I_f	Number of internal lines of particle species f , page 15
κ	Effective neutrino mass operator, page 29
Λ_1	First term in the quartic coupling of the triplet Higgs, page 30
Λ_2	Second term in the quartic coupling of the triplet Higgs, page 30
Λ_3	Third term in the quartic coupling of the triplet Higgs, page 30
Λ_4	First term of the coupling of 2 Higgs doublet to 2 Higgs triplets, page 30
Λ_5	Second term of the coupling of 2 Higgs doublet to 2 Higgs triplets, page 30
Λ_6	Coupling constant of the coupling of 2 Higgs doublets to a Higgs triplet, page 30
M	Majorana mass term of the right-handed neutrino, page 30
m_ν	Mass matrix of the left-handed neutrinos, page 39
m^2	Mass squared of the Higgs doublet, page 79
μ	Renormalization scale, page 18
M_W	Mass of the W boson, page 11

M_Z	Mass of the Z boson, page 11
N_i	Number of vertices of type i , page 16
ν_R	Right-handed neutrino, page 30
P	Off-diagonal part of the β -function of m_ν , page 39
ϕ_1	Majorana CP phase in the leptonic sector, page 81
ϕ_2	Majorana CP phase in the leptonic sector, page 81
Q_L	Left-handed quark doublet, page 79
ρ	ρ parameter: $\rho = \frac{M_W^2}{M_Z^2 \cos^2 \theta_W}$, page 11
s_f	Number characterizing the nature (scalar, fermion, ...) of a particle species f , page 15
Σ_Δ	Self-energy of the Higgs triplet, page 55
Σ_{ℓ_L}	Self-energy of the left-handed lepton doublet, page 59
Σ_ϕ	Self-energy of the Higgs doublet, page 58
s_{ij}, c_{ij}	$\sin \theta_{ij}, \cos \theta_{ij}$, page 81
θ_{ij}	Mixing angles of the MNS matrix, page 81
u_R	Right-handed up-type quark, page 79
V	special unitary matrix in standard parameterization, page 81
W_μ	Gauge boson of $SU(2)_L$, page 79
ξ	Gauge fixing parameter, page 24
ξ_i	Gauge parameter of gauge group i , page 79
Y_d	Yukawa coupling of the down-type quarks, page 79
Y_Δ	Yukawa coupling of the left-handed lepton doublet to the Higgs triplet, page 30
Y_e	Yukawa coupling of the charged leptons, page 79
Y_ν	Yukawa coupling of the neutrinos, page 30
Y_u	Yukawa coupling of the up-type quarks, page 79
Z_Δ	Wave function renormalization factor of the Higgs triplet, page 53
Z_{ℓ_L}	Wave function renormalization factor of the left-handed lepton doublet, page 53
ζ	$\zeta = \frac{\Delta m_{\text{atm}}^2}{\Delta m_{\text{sol}}^2}$, page 46
Z_ϕ	Wave function renormalization factor of the Higgs doublet, page 53

Z_λ Gauge coupling renormalization factor of λ , page 21

Z_{Y_Δ} Vertex renormalization factor of the triplet Yukawa interaction, page 53

Bibliography

- [1] Super-Kamiokande Collaboration, Y. Fukuda et al., *Evidence for oscillation of atmospheric neutrinos*, Phys. Rev. Lett. **81** (1998), 1562–1567, [hep-ex/9807003](#).
- [2] K2K, M. H. Ahn et al., *Indications of neutrino oscillation in a 250-km long- baseline experiment*, Phys. Rev. Lett. **90** (2003), 041801, [hep-ex/0212007](#).
- [3] SNO Collaboration, Q. R. Ahmad et al., *Direct evidence for neutrino flavor transformation from neutral-current interactions in the Sudbury Neutrino Observatory*, Phys. Rev. Lett. **89** (2002), 011301, [nucl-ex/0204008](#).
- [4] J. Davis, Raymond, D. S. Harmer, and K. C. Hoffman, *Search for neutrinos from the sun*, Phys. Rev. Lett. **20** (1968), 1205–1209.
- [5] KamLAND Collaboration, K. Eguchi et al., *First results from KamLAND: Evidence for reactor anti- neutrino disappearance*, Phys. Rev. Lett. **90** (2003), 021802, [hep-ex/0212021](#).
- [6] P. Huber, M. Lindner, M. Rolinec, T. Schwetz, and W. Winter, *Prospects of accelerator and reactor neutrino oscillation experiments for the coming ten years*, (2004), [hep-ph/0403068](#).
- [7] LSND, C. Athanassopoulos et al., *Evidence for $\nu/\mu \rightarrow \nu/e$ neutrino oscillations from lsnd*, Phys. Rev. Lett. **81** (1998), 1774–1777, [nucl-ex/9709006](#).
- [8] H. V. Klapdor-Kleingrothaus, A. Dietz, H. L. Harney, and I. V. Krivosheina, *Evidence for neutrinoless double beta decay*, Mod. Phys. Lett. **A16** (2001), 2409–2420, [hep-ph/0201231](#).
- [9] J. Bonn et al., *The mainz neutrino mass experiment*, Nucl. Phys. Proc. Suppl. **91** (2001), 273–279.
- [10] J. Bonn and C. Weinheimer, *Neutrino mass from tritium beta decay: Present limits and perspectives*, Acta Phys. Polon. **B31** (2000), 1209–1220.
- [11] P. Minkowski, *$\mu \rightarrow e$ gamma at a rate of one out of 1-billion muon decays?*, Phys. Lett. **B67** (1977), 421.
- [12] T. Yanagida, in *Proceedings of the Workshop on the Unified Theory and the Baryon Number in the Universe* (O. Sawada and A. Sugamoto, eds.), KEK, Tsukuba, Japan, 1979, p. 95.

- [13] S. L. Glashow, *The future of elementary particle physics*, in *Proceedings of the 1979 Cargèse Summer Institute on Quarks and Leptons* (M. Lévy, J.-L. Basdevant, D. Speiser, J. Weyers, R. Gastmans, and M. Jacob, eds.), Plenum Press, New York, 1980, pp. 687–713.
- [14] M. Gell-Mann, P. Ramond, and R. Slansky, *Complex spinors and unified theories*, in *Supergravity* (P. van Nieuwenhuizen and D. Z. Freedman, eds.), North Holland, Amsterdam, 1979, p. 315.
- [15] R. N. Mohapatra and G. Senjanović, *Neutrino mass and spontaneous parity violation*, Phys. Rev. Lett. **44** (1980), 912.
- [16] S. Antusch, J. Kersten, M. Lindner, M. Ratz, and M. Schmidt, *work in preparation*.
- [17] T.-P. Cheng and L.-F. Li, *Gauge theory of elementary particle physics*, Oxford University Press, Oxford, UK, 1984.
- [18] Particle Data Group, S. Eidelman et al., *Review of particle physics*, Phys. Lett. **B592** (2004), 1.
- [19] A. Zee, *A theory of lepton number violation, neutrino Majorana mass, and oscillation*, Phys. Lett. **B93** (1980), 389.
- [20] K. S. Babu, *Model of 'calculable' Majorana neutrino masses*, Phys. Lett. **B203** (1988), 132.
- [21] R. N. Mohapatra and J. W. F. Valle, *Neutrino mass and baryon-number nonconservation in superstring models*, Phys. Rev. **D34** (1986), 1642.
- [22] J. C. Pati and A. Salam, *Unified lepton - hadron symmetry and a gauge theory of the basic interactions*, Phys. Rev. **D8** (1973), 1240.
- [23] M. Magg and C. Wetterich, *Neutrino mass problem and gauge hierarchy*, Phys. Lett. **B94** (1980), 61.
- [24] G. Lazarides, Q. Shafi, and C. Wetterich, *Proton lifetime and fermion masses in an $SO(10)$ model*, Nucl. Phys. **B181** (1981), 287.
- [25] R. N. Mohapatra and G. Senjanović, *Neutrino masses and mixings in gauge models with spontaneous parity violation*, Phys. Rev. **D23** (1981), 165.
- [26] C. Wetterich, *Neutrino masses and the scale of $B-L$ violation*, Nucl. Phys. **B187** (1981), 343.
- [27] N. Arkani-Hamed, L. J. Hall, H. Murayama, D. R. Smith, and N. Weiner, *Small neutrino masses from supersymmetry breaking*, Phys. Rev. **D64** (2001), 115011, hep-ph/0006312.
- [28] F. Borzumati and Y. Nomura, *Low-scale see-saw mechanisms for light neutrinos*, Phys. Rev. **D64** (2001), 053005, hep-ph/0007018.
- [29] R. Kitano, *Small Dirac neutrino masses in supersymmetric grand unified theories*, Phys. Lett. **B539** (2002), 102–106, hep-ph/0204164.

-
- [30] N. Arkani-Hamed, S. Dimopoulos, G. R. Dvali, and J. March-Russell, *Neutrino masses from large extra dimensions*, Phys. Rev. **D65** (2002), 024032, [hep-ph/9811448](#).
- [31] F. Bloch and A. Nordsieck, *Note on the radiation field of the electron*, Phys. Rev. **52** (1937), 54–59.
- [32] D. R. Yennie, S. C. Frautschi, and H. Suura, *The infrared divergence phenomena and high-energy processes*, Ann. Phys. **13** (1961), 379–452.
- [33] S. Weinberg, *High-energy behavior in quantum field theory*, Phys. Rev. **118** (1960), 838–849.
- [34] Y. Hahn and W. Zimmermann, Commun. Math. Phys. **10** (1968), 330.
- [35] J. C. Collins, *Renormalization*, Cambridge University Press, Cambridge, UK, 1984.
- [36] S. Weinberg, *The quantum theory of fields. vol. 1: Foundations*, Cambridge University Press, Cambridge, UK, 1995.
- [37] S. Weinberg, *The quantum theory of fields. vol. 2: Modern applications*, Cambridge University Press, Cambridge, UK, 1996.
- [38] F. J. Dyson, *The radiation theories of tomonaga, schwinger, and feynman*, Phys. Rev. **75** (1949), 486–502.
- [39] J. Gomis and S. Weinberg, *Are nonrenormalizable gauge theories renormalizable?*, Nucl. Phys. **B469** (1996), 473–487, [hep-th/9510087](#).
- [40] G. 't Hooft, *Renormalization of massless Yang-Mills fields*, Nucl. Phys. **B33** (1971), 173–199.
- [41] G. 't Hooft, *Renormalizable Lagrangians for massive Yang-Mills fields*, Nucl. Phys. **B35** (1971), 167–188.
- [42] G. 't Hooft and M. J. G. Veltman, *Regularization and renormalization of gauge fields*, Nucl. Phys. **B44** (1972), 189–213.
- [43] N. N. Bogoliubov and O. S. Parasiuk, *On the multiplication of the causal function in the quantum theory of fields*, Acta Math. **97** (1957), 227–266.
- [44] K. Hepp, Comm Math Phys. **2** (1966), 301–326.
- [45] W. Zimmermann, Comm Math Phys. **15** (1969), 208–234.
- [46] W. Zimmermann, Ann. Phys. (N.Y.) **77** (1973), 536.
- [47] W. Zimmermann, Ann. Phys. (N.Y.) **77** (1973), 570.
- [48] D. Kreimer, *On the hopf algebra structure of perturbative quantum field theories*, Adv. Theor. Math. Phys. **2** (1998), 303–334, [q-alg/9707029](#).
- [49] C. Becchi, A. Rouet, and R. Stora, *Renormalization of the abelian higgs-kibble model*, Commun. Math. Phys. **42** (1975), 127–162.

- [50] J. Taylor, Nucl. Phys. B **33** (1971), 436.
- [51] A. Slavnov, Theor. Math. Phys. **10** (1972), 152.
- [52] B. W. Lee and J. Zinn-Justin, *Spontaneously broken gauge symmetries. i. preliminaries*, Phys. Rev. **D5** (1972), 3121–3137.
- [53] B. W. Lee and J. Zinn-Justin, *Spontaneously broken gauge symmetries ii. perturbation theory and renormalization*, Phys. Rev. **D5** (1972), 3137–3155.
- [54] G. 't Hooft and M. J. G. Veltman, *Combinatorics of gauge fields*, Nucl. Phys. **B50** (1972), 318–353.
- [55] The OPAL Collaboration, G. Abbiendi et al., *Tests of the Standard Model and constraints on new physics from measurements of fermion pair production at 189 GeV at LEP*, Eur. Phys. J. **C13** (2000), 553–572, [hep-ex/9908008](#).
- [56] J. Callan, Curtis G., *Broken scale invariance in scalar field theory*, Phys. Rev. **D2** (1970), 1541–1547.
- [57] K. Symanzik, *Small distance behavior in field theory and power counting*, Commun. Math. Phys. **18** (1970), 227–246.
- [58] *Nobel laureates in physics 2004*, <http://nobelprize.org/physics/laureates/2004/index.html>.
- [59] J. Kersten, *Renormalization group evolution of neutrino masses*, 2001.
- [60] S. Antusch, *The running of neutrino masses, lepton mixings and CP phases*, Ph.D. thesis, TU München, 2003.
- [61] M. Ratz, *Running neutrino masses*, Ph.D. thesis, TU München, 2002.
- [62] K. Symanzik, *Infrared singularities and small distance behavior analysis*, Commun. Math. Phys. **34** (1973), 7–36.
- [63] T. Appelquist and J. Carazzone, *Infrared singularities and massive fields*, Phys. Rev. **D11** (1975), 2856.
- [64] M. Maltoni, T. Schwetz, M. A. Tortola, and J. W. F. Valle, *Status of global fits to neutrino oscillations*, (2004), [hep-ph/0405172](#).
- [65] S. Weinberg, *Phenomenological lagrangians*, Physica **A96** (1979), 327.
- [66] M. Fukugita and T. Yanagida, *Baryogenesis without grand unification*, Phys. Lett. **174B** (1986), 45.
- [67] W. Buchmüller, P. Di Bari, and M. Plümacher, *Leptogenesis for pedestrians*, (2004), [hep-ph/0401240](#).
- [68] G. C. Branco, L. Lavoura, and M. N. Rebelo, *Majorana neutrinos and cp violation in the leptonic sector*, Phys. Lett. **B180** (1986), 264.
- [69] A. Santamaria, *Masses, mixings, yukawa couplings and their symmetries*, Phys. Lett. **B305** (1993), 90–97, [hep-ph/9302301](#).

- [70] S. Davidson, *Parametrizations of the seesaw, or, can the seesaw be tested?*, (2004), [hep-ph/0409339](#).
- [71] S. Antusch, J. Kersten, M. Lindner, M. Ratz, and M. Schmidt, *Documentation of the mathematica package reap*, (2004).
- [72] S. Antusch, J. Kersten, M. Lindner, M. Ratz, and M. Schmidt, *Documentation of the mathematica package mixingparametertools*, (2004).
- [73] K. S. Babu, *Renormalization-Group analysis of the Kobayashi-Maskawa matrix*, Z. Phys. **C35** (1987), 69.
- [74] J. A. Casas, J. R. Espinosa, A. Ibarra, and I. Navarro, *General RG equations for physical neutrino parameters and their phenomenological implications*, Nucl. Phys. **B573** (2000), 652, [hep-ph/9910420](#).
- [75] S. Antusch, J. Kersten, M. Lindner, and M. Ratz, *Running neutrino masses, mixings and CP phases: Analytical results and phenomenological consequences*, Nucl. Phys. **B674** (2003), 401–433, [hep-ph/0305273](#).
- [76] P. H. Chankowski, W. Krolikowski, and S. Pokorski, *Fixed points in the evolution of neutrino mixings*, Phys. Lett. **B473** (2000), 109, [hep-ph/9910231](#).
- [77] P. H. Chankowski and S. Pokorski, *Quantum corrections to neutrino masses and mixing angles*, Int. J. Mod. Phys. **A17** (2002), 575–614, [hep-ph/0110249](#).
- [78] S. Antusch, J. Kersten, M. Lindner, and M. Ratz, *The LMA solution from bimaximal lepton mixing at the GUT scale by renormalization group running*, Phys. Lett. **B544** (2002), 1–10, [hep-ph/0206078](#).
- [79] A. Pilaftsis and T. E. J. Underwood, *Resonant leptogenesis*, Nucl. Phys. **B692** (2004), 303–345, [hep-ph/0309342](#).
- [80] W. Rodejohann, *A parametrization for the neutrino mixing matrix*, Phys. Rev. **D69** (2004), 033005, [hep-ph/0309249](#).
- [81] M. Raidal, *Prediction $\theta(c) + \theta(sol) = \pi/4$ from flavor physics: A new evidence for grand unification?*, (2004), [hep-ph/0404046](#).
- [82] H. Minakata and A. Y. Smirnov, *Neutrino mixing and quark lepton complementarity*, (2004), [hep-ph/0405088](#).
- [83] P. H. Frampton and R. N. Mohapatra, *Possible gauge theoretic origin for quark-lepton complementarity*, (2004), [hep-ph/0407139](#).
- [84] P. H. Chankowski and P. Wasowicz, *Low energy threshold corrections to neutrino masses and mixing angles*, [hep-ph/0110237](#) (2001).
- [85] R. D. Peccei, *Reflections on the strong cp problem*, (1998), [hep-ph/9807514](#).
- [86] S. P. Martin, *A supersymmetry primer*, (1997), [hep-ph/9709356](#).

- [87] A. Denner, H. Eck, O. Hahn, and J. Küblbeck, *Feynman rules for fermion number violating interactions*, Nucl. Phys. **B387** (1992), 467–484.
- [88] G. Passarino and M. Veltman, *One loop corrections for e^+e^- annihilation into $\mu^+\mu^-$ in the Weinberg model*, Nucl. Phys. **B160** (1979), 151.
- [89] A. Denner, *Techniques for calculation of electroweak radiative corrections at the one loop level and results for W physics at LEP200*, Fortschr. Phys. **41** (1993), 307–420.